ACCUMULATION AND BIOAVAILABILITY OF METALS IN MUDFLATS AND MANGROVES ALONG THE SOUTH KARNATAKA COAST

THESIS

SUBMITTED TO GOA UNIVERSITY FOR THE AWARD OF THE DEGREE OF

DOCTOR OF PHILOSOPHY

IN

MARINE SCIENCE

BY

MARIA C. FERNANDES
M.Sc

Department of Marine Sciences,
Goa University,
Taleigao, Goa – 403206

DECEMBER, 2015

ACCUMULATION AND BIOAVAILABILITY OF METALS IN MUDFLATS AND MANGROVES ALONG THE SOUTH KARNATAKA COAST

THESIS

SUBMITTED TO GOA UNIVERSITY FOR THE AWARD OF THE DEGREE OF

DOCTOR OF PHILOSOPHY

IN

MARINE SCIENCE

BY

MARIA C. FERNANDES
M.Sc

UNDER THE GUIDANCE OF

PROF. G. N. NAYAK

Department of Marine Sciences,
Goa University,
Taleigao, Goa – 403206

DECEMBER, 2015

DEDICATED

TO MY

FAMILY

STATEMENT

As required under the University ordinance OB.9.9 (iv), I state that the present thesis entitled "**ACCUMULATION AND BIOAVAILABILITY OF METALS IN MUDFLATS AND MANGROVES ALONG THE SOUTH KARNATAKA COAST**", is my original contribution and the same has not been submitted for any other previous occasion. To the best of my knowledge, the present study is the first comprehensive work of its kind from the area mentioned.

The literature related to the problem investigated has been cited. Due acknowledgements have been made wherever facilities and suggestions have been availed of.

Place: Goa University
Date: 24.12.2015

Ms. Maria C. Fernandes

CERTIFICATE

This is to certify that the thesis entitled, "**ACCUMULATION AND BIOAVAILABILITY OF METALS IN MUDFLATS AND MANGROVES ALONG THE SOUTH KARNATAKA COAST**", submitted by Ms. Maria C. Fernandes for the award of the Degree of Doctor of Philosophy in Marine Science is based on her original studies carried out by her under my supervision. The thesis or any part thereof has not been previously submitted for any other degree or diploma in any universities or institutions.

Place: Goa University
Date: 24.12.2015

Prof. G. N. Nayak

Research Guide
Department of Marine Sciences
Goa University, Goa

Acknowledgements

I consider myself extremely fortunate for having been surrounded by helpful, kind and knowledgeable people throughout this study. Many people have supported me and together we have made this thesis into what it is now. I am indebted to all of them but I want to thank a number of people in particular.

Foremost, I wish to thank my research guide and advisor Prof. G. N. Nayak, for suggesting this topic and granting me the opportunity to research on it. I thank him for his scientific advice and knowledge and many insightful discussions and suggestions. He patiently guided me through the process, without which, it would not be possible to carry out my research work.

I would like to express my gratitude to the FRC committee, comprising of the Dean of the faculty, Head of the Department, Vice chancellor's nominees viz. Prof. V. M. Matta and Dr. Hema Naik, and Research Guide Prof. G. N. Nayak, for their suggestions and encouragements during the course of my research leading to Ph.D. degree.

This research was supported by grants under the UGC scheme "Maulana Azad National Fellowship" for the period of five years. I am thankful to them.

I am grateful to Dr. SWA Naqvi, Director, National Institute of Oceanography (NIO), Goa, India, for allowing me to utilize the required facilities at the Institute. Special thanks to Dr. Pratima Kessarkar and Dr. Lina Fernandes, Scientists from NIO, Goa for their cooperation and technical support.

My profound gratitude to all my teachers of Department of Marine Sciences, Goa University, Prof. V. M. Matta, Prof. H.B.Menon, Dr. S. Upadhyay, Dr. Aftab Can and Prof. C. U. Rivonkar, for their encouragements and support. I thank the Head of Department (HOD) of Marine Sciences for providing the required laboratory facilities for carrying out the research work.

Furthermore, I thank all my colleagues at the Marine Science Department of Goa University, who were not only directly or indirectly involved in the science of this thesis, but who made my stay at the department and the conferences visited into unforgettable

events. I especially thank Deepti, Cheryl, Purnima, Shabnam, Shilpa, Soniya, Ratnaprabha, Samida, Anant, Cynthia, Kalpana, Vijaylaxmi, Maheshwar, Mahabaleshwar, Shrivardan, Dinesh, Abhilash, Vinay, Neha, Samiksha, Sahita, Arjun, Satyam, Renosh, Nutan, Lilian, Sweety, Vineel, Veloisa, Nila, Tanu and Vineet. I thank them all for their support.

I am thankful to the non-teaching staff of the Department of Marine Science, Goa University, viz, Mr. Rosario, Mr. Yashwant, Mr. Ashok, Mr. Narayan, Mr. Shatrugan, Mr. Achut, Mr. Samrat, for their kind help, required during the course. Also my thanks go to Mr. Serrao, Mr. Martin and Mr. Ulhas for rendering the required help during the course.

My sincere thanks to, The director, National Centre for Antarctic and Oceanic Research (NCAOR), Goa for giving me an opportunity to participate in the 6th Indian Southern Ocean Expedition during my research period. I express my thanks to Dr. Anil Kumar, Scientist, NCAOR, Goa and other colleagues for their constant support and motivation during the expedition and making it an unforgettable experience.

I would also like to thank Macloyd Francis, Akshay Parab, Gautam Loleinkar, Vanisha Sequeira, Janica, Ignacine Fernandes, Uday Gaonkar, Sangeeta, Joshua, Irfan Banglekar, Kingsly Lionel, Joyce Diniz, Mackelroy Noronha, Tracy Fernandes, Morishca Noronha, Meagan, Ruchita, Jesley, Dr. Shital, Dr. Ravi Naik, Juliana Francis, Stella Francis, Elton Fernandes, Maria Pereira, Mervyn Pereira, Christopher Fernandes, Cheryl George, Juliet George, Aparna Chopdekar, Swati Parwar and Pooja Palyekar for their help and support during the analyses.

Lastly and most importantly, I would like to say a big thank you to my family and friends for their endless support and encouragement over the past few years and for just being there. I miss my Grandfather (Appa) at this moment of achievement, the one who encouraged me for further studies. I feel a deep sense of gratitude for my parents who formed part of my vision, taught me the good things that really matter in life and made me what I am today.

Ms. Maria C. Fernandes

Table of Contents

List of Tables

List of Figures

Preface

Estuaries are a transition zone wherein there is mixing of fresh and marine water that enhances the rate of sedimentation. Vast amount of organic matter and metals enter into the estuarine waters through river run off, in-situ primary productivity, atmospheric deposition, diagenetic remobilization and anthropogenic inputs. Various sources of anthropogenic material supply significant loads of toxic metals are added to the estuaries. The material entered into the estuaries slowly gets deposited in quiet environment of deposition in mudflats and mangroves. Thus, mudflats and mangrove sediments are considered as potential reservoir of metals. Within these environments remobilization of trace metals are regulated by redox sensitive elements and are recycled with changing physicochemical conditions through the sediment–water interface. Therefore metals may get released into the water column of the estuary even after effluent discharge is ceased.

Along the coast of southern Karnataka, Sharavati is the large estuary while Chakra Nadi, Haladi, Sita Nadi, Swarna, Udyavara, Pavanje and Gurpur are smaller estuaries. The rivers travel through migmatite, granodiorite, granitic gneisses, charnockites, amphibolites and laterite rock types in the catchment area. The area receives an average rainfall of 3500 mm during June to September. Material from the catchment area is brought to estuaries during these monsoon months. Along this coast tidal range is less than 2 m. Estuaries in Karnataka are continuously influenced by geological processes like erosion, deposition, periodic storms and floods and changing sea level. Increasing population, industrial establishments and developments are common near the river banks along this coast. Coastal Karnataka is emerging as an urbanized region with industrial growth. Soil erosion is the biggest problem along river banks and coasts, and agro-ecosystem with the growing pollution, which poses greater threats to natural habitats. Life in the rivers, estuaries and the coastal seas is therefore under greater stress. Estuaries act as a sink to many types of pollutants received from effluent discharge by industries of different kind, port activities and dumping of fish and organic wastes. Industrial effluents with toxic chemicals enhance the level of bioavailability of metals which can pose a risk to biota. Estuaries in Karnataka have also been affected greatly due to construction of dams on rivers. This has led to change in deposition

pattern of sediments, organic matter and metals over a period of time. Therefore, it has become a necessity to understand the level of metal pollution in the estuaries along Karnataka coast.

Chapter 1 includes introduction, wherein detailed information on estuaries is provided. It covers definition and classification of estuaries and their sub-environments with main focus on mudflats and mangrove sedimentary environments. Information on the catchment area, factors controlling distribution of sediment components, organic matter and metal distribution within sediments are given in detail. Literature on role of sediment components in distribution of metals, speciation of metals is also presented. The description of the study area and objectives of the present study are detailed at the end of this chapter.

Chapter 2 provides detailed information on materials and methods adopted in order to fulfil the objectives of the present study. Fourteen sediment cores collected representing mudflat and mangrove sedimentary environments within estuaries from south Karnataka coast, were analysed for various sedimentological and geochemical parameters which include analysis of sediment components, organic matter, metals in bulk as well as in sand, silt and clay sediment fractions, metal speciation analyses are presented in this chapter.

Chapter 3 describes the results of various sedimentological and geochemical analysis carried out on sediment sub-samples and discusses the inference drawn. It is divided into four sections. Section I describes the distribution pattern of sediment components (sand, silt and clay), organic carbon, and metals in bulk sediments of large estuary. Similar description for smaller estuaries has been presented in section II. In section III, metals in each of the sediment size fractions have been discussed in detail. In order to understand the level of metal enrichment within sediments, Enrichment Factor (EF) and Index of geoaccumulation (I_{geo}) are computed. Isocon plots have also been used to compare different environments and regions. The results of speciation analysis are presented in section IV.

Chapter 4 provides summary of the results and discussions. The references are listed in alphabetical order at the end of the thesis.

Chapter 1

Introduction

1.1 Introduction

Estuaries are transition zones between land and sea wherein fresh water mixes with sea water thereby alters the salinity and pH of resulting water and favours high rate of sedimentation. Distribution of sediments within estuaries is often classified on the basis of grain size which in turn helps in understanding the hydrodynamic energy conditions prevailing in the area. Estuarine sediments retain large quantity of finer sediments and organic matter and act as sink for a wide range of metals which show high affinity for fine grained sediments. These metals get adsorbed onto the suspended particulate matter and are transported through the water column which finally gets incorporated into the sediments.

The word estuary is derived from Latin word, aestus, meaning the tide. There are more than 40 definitions of an estuary (Mikhailov and Gorin 2012). The most popular of which is given by Pritchard (1967), which is defined as “an estuary is a semi-enclosed coastal body of water, which has free connection with open sea, and within which sea water is measurably diluted with fresh water derived from land drainage.” According to Fairbridge (1980), an estuary is “an inlet of sea reaching into a river valley as far as the upper limit of tidal rise”, usually being divisible into three sectors (Fig. 1.1): a) a marine or lower estuary, which has free connections with open sea; b) a middle estuary subjected to strong salt and freshwater mixing; c) fluvial or an upper estuary, characterized by freshwater but subjected to tidal action. However, the boundaries or the transition zones between these sectors shift according to constantly changing tides and river discharge.

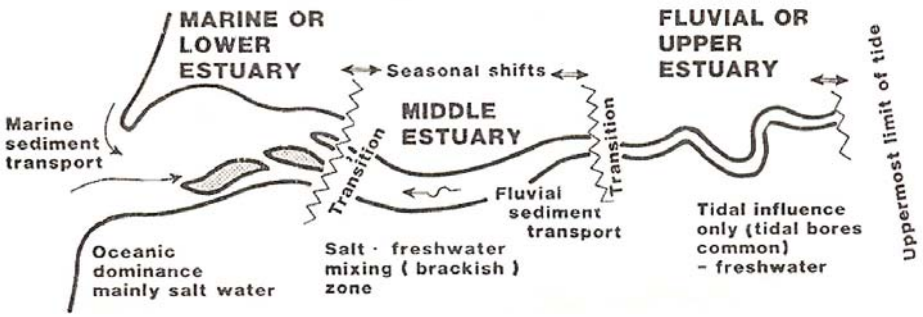

Fig. 1.1 Estuary showing three divisions – Lower, middle and upper estuary: The boundaries are the transition zones that shift according to season, weather and tides (After, Fairbridge 1980).

There are several different approaches to classify estuaries. One is to consider the geomorphological origin (Pritchard 1967) and geological formation for a classification primarily based on topographical features. Another approach is to investigate the salinity structure and thereby the stratification characteristics of an estuary, giving a classification based on internal circulation patterns (Pritchard 1955). Based on geomorphology estuaries are divided into five types: a) Drowned river valleys (coastal plain estuaries) b) Rias c) Fjord type estuaries d) Bar-built estuaries and e) Estuaries formed due to tectonic processes. Drowned river valleys are formed as a result of sub aerial weathering and/or sea level rise. Rias are special type of drowned river valley estuaries which have dissected mouth. Fjords are estuaries that have been formed by glacial erosion which generally occur at high latitudes, are relatively long and deep. Bar-built estuaries are formed similar to drowned river valleys but in this case the sedimentation rate is in pace with the inundation, creating a more mature estuarine type. Across the mouth of the estuary is a bar where waves break and that is formed by deposited sediments. While estuaries formed due to tectonic processes are created due to faulting, folding, earthquake, volcanoes or other diastrophic movements.

Based on salinity stratification, estuary can be classified as: a) Salt wedge estuary b) Partially mixed estuary and c) Well mixed or fully mixed estuaries. Salt wedge estuaries are highly stratified and river dominated which exist where the tidal range is small. Partially mixed estuaries exist where the tidal range is sufficiently large to produce turbulent mixing between the two layers in the estuary. The tidal current that is oscillating back and forth along the estuary will produce eddies in the interface between the layers. These eddies mix the water, raising the salinity in the upper layer, and lowering in the bottom layer. Thus, the salinity gradient is less steep than in the highly stratified estuary but due to the salt balance there still has to exist a two-layer flow in the estuary with seaward flowing top layer and a landward bottom current of sea water. Vertically homogeneous (fully mixed) estuaries form when the tidal currents are so strong that they completely mix the water along the whole water column. Therefore the vertical salinity differences become negligible. However, a longitudinal salinity gradient exists from head to mouth of the estuary.

Estuaries are also classified based on tidal range as microtidal, mesotidal and macrotidal estuaries. Microtidal estuaries are formed when the tidal range is less than 2 m and are generally dominated by fresh water discharge. Those estuaries which have tidal range between 2 to 4 m are classified as mesotidal estuaries and macrotidal estuaries are formed where the tidal range is more than 4 m.

The sediments brought to the estuaries may settle either within the channel or along the bank as intertidal flats. Intertidal flats within the estuaries vary from sandflat in the lower estuary to mudflat in the middle estuary. Reineek (1972) defined tidal flats as “sandy to muddy or marshy flats that are emerging during low tide and submerging during high tide”. According to Bates and Jackson (1987), these are sandy to muddy depositional systems along estuarine shores that are submerged and exposed in the course of the rise and fall of the tide at regular intervals. These are the sites of sediment deposition where silts and other finer sediments accumulate in the shallow water in quieter areas within estuaries. So, tidal flats are formed out of sand, silt and clay built up through the action of ocean tides and river waters and subjected to repeated changes of water level due to the ebb and flood tides. They are formed where there is abundant sediment deposition which later develops ability to prevent erosion. Mud deposition takes place in sheltered and protected low energy environments such as middle estuaries which are termed as “mudflats” and generally occur in intertidal regions. Due to regular and increased depth of flooding, mudflats prevents growing of salt tolerant plants and due to the lack of a solid substrate; seaweeds are unable to grow in these areas. It is difficult to predict development of an estuarine mudflat because they form due to the combined effect of physical, chemical and biological properties of the sediment (Patersion et al. 1990; Yallop et al. 1994). Macrotidal estuaries are known to have largest mudflats (greater than 4 m) and represent large surface areas at low tide. Intertidal estuarine mudflats are known for accumulation of fine grained sediments, organic matter and metals, originated from numerous marine and terrestrial sources including those of anthropogenic origin despite presence of strong hydrodynamic energy conditions.

The changing physicochemical properties of water are responsible for binding clay particles together in estuaries. These clay grains aggregate and form large particles

that sink through the water column. Therefore clay deposition is more in estuaries where there is mixing of seawater and freshwater, in the presence of organic matter having strong chemical binding properties. Fine grained mud, due to its stickiness can resist being re-suspended and transported by moving water which is capable of transporting larger, uncohesive sands and gravels.

A tidal flat can be classified into sand flat and mud flat depending on the components of sediments. The average width of sand flat is 1 km, and they generally form where there is rapid inflow of seawater and here the organic matter is only 1 to 2 %. However, a mud flat is formed where there is gentle flow of seawater and its width is over 5 km and is composed of particles having average diameter 0.031 mm. Due to its less porosity, seawater with oxygen and food do not penetrate the flat.

Intertidal mudflats can be separated into three distinct zones (Klein 1985): the lower tidal flats, middle flats and upper flats depending on spring and neap tides. The upper flats lie between the mean high water neap and mean high water springs while the middle flats are located between mean low water neaps and mean high water neaps and the lower tidal flats lie between mean low water neap and mean low water spring tide levels and are often subjected to strong tidal currents; The upper flats are the least affected part of the mudflat by wave action and are only submerged at high water by spring tides.

Mangroves begin to grow as far seaward as mean high water neaps while mudflats often continue to form below the level of low water spring tides, (McCann 1980). Generally, fine grained sediments get deposited in the upper flats, the fine silts in middle flats and sandy mud in the lower flats (Shi and Chen 1996). Sea-level changes and effects of anthropogenic input are very well recorded over mudflat and mangrove sedimentary environment. Mangrove environments are generally found in tropical coastal areas and also in sub-tropical region. Mangroves act as buffer zone between land and sea and serve as a habitat for various organisms. Further, mangroves are one of the productive ecosystems (Kathiresan 2003) and cover a large area on a global scale (Spalding et al. 1997).

The present study includes the detailed investigations on which covers mudflat and mangrove sedimentary environments within estuaries along southern part of Karnataka coast. Along this coast mangroves are well grown on fine sediments and are well maintained. Fourteen mangrove species belonging to 7 families (Table 1.1) are identified and recorded.

The important estuaries within which mangroves are present along Karnataka coast from North to South in Uttara Kannda District are Kali, Aghanashini, Sharavati, Ganagavali and Venkatapur and in Dakshina Kannada, Shiroor hole, Baindur hole, Swarna-Sita-Kodi, Chakra-Haladi-Kollur, Mulki-Pavanje, Udayavara-Pangala, Netravathi and Gurupur.

Table 1.1 Mangrove species available in Karnataka

Srl. No	Family	Species
1	Acanthaceae	*Acanthus ilicifolius*
2	Avicenniaceae	*Avicennia marina Avicennia officinalis*
3	Combretaceae	*Lumnitzera racemosa*
4	Euphorbiaceae	*Excoecaria agallocha*
5	Myrsinaceae	*Aegiceras corniculatum*
6	Rhizophoraceae	*Bruguiera cylindrica*
		Bruguiera gymnorrhiza
		Kandelia candel
		Rhizophora apiculata
		Rhizophora mucronata
		Ceriops decandra
7	Sonneratiaceae	*Sonneratia alba*
		Sonneratia caseolaris

Mudflats and mangroves are a place of high nutrient source, and also a sink. Mangroves are known for being highly productive. Compared with most other habitats, mudflats and mangroves are not much explored and the processes occurring on them are yet to be researched. Many of the researchers have noted that mudflats and mangroves are long term storage areas for a range of contaminants (Williams et al. 1994; Lee and Cundy 2001). Both mangrove and mudflat environments have tendency to release heavy metals to water column even after effluent discharge has -stopped. This is mainly due to variety of physical, chemical and biological processes which may mix, change the redox conditions, remobilise and finally release the metals into the

overlying water column through the processes of bioturbation, early diagenesis, dredging, and erosion (Pande and Nayak 2013; Filho et al. 2011; Deng et al. 2010).

Investigations on metals within sediments have increased many folds in recent years (Nguyen et al. 2009). When the abundance of metals is considered, major concentrations (99%) of metals are stored in sediments whereas a minor fraction (about 1%) is available in the dissolved form. Therefore, sediments are considered as the major sinks for metals. Further, within the water column the metals get recycled through biological and chemical processes (Nemati et al. 2011; Vink 2009; Bartoli et al. 2011) and transferred finally to the sediments. Therefore metals pollution in sediments is of major concern. Further, as they involve in persistence, bioavailability, metal toxicity, bio-accumulation and may get transferred to the overlying water column thereby entering into the food chain (Nemati et al. 2011; Díaz-de Alba et al. 2011). In general the trace metals that are mainy associated with silicates and primary minerals are less mobile than those which are of anthropogenic origin as they are mainly associated with carbonates, oxides, hydroxides and sulfides (Passos et al. 2010; Heltai et al. 2005). Metals enter into aquatic systems mainly by rock weathering and various anthropogenic activities like atmospheric inputs, industrial wastewater, soil erosion, drainage of land, urban wastes and biological activities (Díaz-de Alba et al. 2011; Carman et al. 2007). Determination of the total metal concentrations in sediments does not directly help in providing their mobility (Tüzen 2003) as the bioavailability and toxicity of the metals to the biota largely depends on their chemical forms (Ahlf et al. 2009). Therefore, it is essential to determine the metals with different geochemical phases. Sequential extraction provides adequate information related to the occurrence, origin, transport of metals, biological/physicochemical aspects, and their mobilization, though the procedure it is complicated and lengthy (Passos et al. 2010). Further, it provides information on role of degradation of organic matter, redox potential and pH on the mobilization and retention of the metals in the aquatic ecosystems (Saleem et al. 2015; Tessier et al. 1979). The change in salinity and pH occur when there is fresh-marine water interaction.

1.2 Literature review

To understand the area and depth of investigations and possible gaps in research a detailed literature review on the topic of research was carried out and is presented in table 1.2.

Table 1.2 Literature surveys of the studies carried out in the recent past in India and other parts of the world.

Authors	Parameters analysed	Observations
Volvoikar and Nayak (2015)	Metal speciation	Three sediment cores of the Dudh creek, west coast of India, were investigated for metal speciation. Higher concentration of metals in the bioavailable fraction were reported towards the surface of the cores, which the authors have interpreted as an increase in anthropogenic metal input in recent years as compared to the past. Authors further stated that metals in the Dudh creek posed a risk of toxicity to sediment associated biota as they were largely associated with the bioavailable fractions.
Fernandes and Nayak (2015)	Sediment grain size, TOC, metals and speciation	One core each collected from mudflat sedimentary environment from Gurpur and Swarna estuary were analysed for bioavailability of metals and their toxicity. High sand content was noted in Gurpur estuary. Metals studied, were found to be of lithogenic source. Authors reported high Co concentration in bioavailable phases in Swarna estuary which posed a high risk of toxicity to organisms associated with the sediments.
Volvoikar and Nayak (2014)	Sediment grain size, TOC and metals	Two cores collected from mangrove sedimentary environment of Vaitarna estuary were analysed for sediment components, organic carbon and selected metals. In both the cores, gradual decrease in sand and increase in clay from bottom to surface was noticed thereby indicating change in hydrodynamic conditions. Metals were mostly

		associated with sand, silt and clay while Fe-Mn oxides and organic carbon played a minor role. Enrichment Factor indicated increase of some metals towards the surface indicating an anthropogenic input in recent years.
Fernandes et al. (2014)	Sediment grain size, TOC and metals	Four sediment cores representing adjacent mangrove and mudflat environments of Middle Estuary (Shastri) were analysed for sand, silt, clay and organic carbon. Total metal concentration and chemical speciation on selected samples was also carried out on mudflat cores. The sediments in the upper middle estuary were found to be deposited under highly varying hydrodynamic energy conditions; whereas lower middle estuary experienced relatively stable hydrodynamic energy conditions with time. The tributary joining the river near the upper middle estuary is found to be responsible for the addition of enhanced organic carbon and metal concentrations. Speciation study indicated Fe and Co are from natural lithogenic origin while Mn is derived from anthropogenic sources. Higher Mn and Co than Apparent Effects Threshold (AET) can pose a high risk of toxicity to organisms associated with these sediments.
Pande and Nayak (2013a)	Sediment grain size, TOC and metals	Two cores collected from mudflat sedimentary environment of Dharamtar creek, out of which one was near mouth and other from middle region of Amba river were analysed for sediment components, organic carbon and selected metals. Both the cores were largely composed of silt and clay indicating calm conditions during deposition of sediments. EF and Igeo indicated different level of metal pollution in Dharamtar creek.
Volvoikar and Nayak	Sediment grain size, TOC,	Sediment cores collected from Vaitarna estuary representing mudflat sedimentary environment

(2013b)	metals in bulk sediments, metals in clay-sized fraction and metal speciation	were investigated for distributions of various parameters like sediment components, organic carbon and metals in bulk and in clay sized fraction (>2μm). Geoaccumulation Index computed by the authors indicated different level of pollution at the three locations. Large association of Pb and Zn with the clay fraction was observed which the authors reported as of lithogenic origin, while other metals originated from an anthropogenic source.
Law et al. (2012)	Grain size and porosity	Bottom sediment of muddy tidal flat in Willapa Bay were analysed for grain size by the authors. The disaggregated inorganic grain size (DIGS) distributions obtained from the sediment were analysed using various conventional methods. Authors reported more precipitation in the winter months caused increase in suspended-sediment concentrations. During the summer dry season, lower suspended-sediment concentrations lead to reduced floc fractions in the channels.
Leorri et al. (2013)	grain size, benthic foraminifera, sediment geochemistry,137Cs and 210Pb geochronology	Short sediment cores taken from (i) a recently regenerated salt marsh (Plentzia estuary), (ii) an incipient marsh and (iii) a pristine marsh (Urdaibai estuary), was studied for evidence of environmental impacts and sea-level change on the basis of micro faunal and geochemical determinations and historical land management data. The studies showed that with the current relative sea-level rise scenario, the salt marsh ecosystems might lose their ability to keep up with tidal flooding and drown following a transgressional pattern where marsh vegetation replaces woody plant species and this would lead to the development of a mudflat when sea level rises beyond low marsh accretion rates.
Luo et al.	Grain size	Analysis of sediment grain size along the middle

(2012)		and lower Yangtze River, downstream of the Three Gorges Dam (TGD) and along the major sediment dispersal pathway into the East China Sea, was carried out in this study. Authors reported the impact of the TGD on the relationship between median grain size and distance along the sandy bed of the middle and lower Yangtze.
Singh et al. (2013a)	Grain size, radionuclide analysis, magnetic susceptibility	Geochemical, magnetic related parameters and radionuclide analyses were carried out on sediment cores collected from mudflat regions of, Tadri creek (Gokarn), Mandovi estuary (Panaji) and Kolamb creek (Malvan). The rate of sedimentation in the study area varied from 0.13 to 2 cm per year. The rate varied from lower half of the cores to the near surface. Authors reported higher rate of sedimentation in the upper portions of the cores that indicated increased deposition of finer sediment components, magnetic minerals and metals.
Singh et al. (2013b)	Grain size, organic carbon, metals	Sediment components, organic carbon along with selected metals were determined in three sediment cores, collected from intertidal regions of the Zuari estuary and Cumbharjua canal. The cores collected from the upper middle estuarine environment, showed higher values of finer fractions and total organic carbon as well as metals than from the lower estuarine environment. Impact of mining has been discussed. Enrichment factor computed in all the cores was found to be above 2 for most of the studied metals which suggest a high degree of metal contamination. Authors reported influence of anthropogenic activities in recent years.
Volvoikar and Nayak	Sediment component	Two cores collected, near the mouth and other in the inner part of the Dudh creek were analysed for

(2013a)	analysis, TOC, metals	Sediment component, organic carbon and metal. The variation in the distribution of sediment components with depth suggests the changes in hydrodynamic condition in the creek over the years. Increase in concentration of most of the metals in the surface layers of the cores indicates additional input in recent years. The core collected in the inner part of the creek showed higher metal and organic carbon concentration as compared to the core collected towards mouth of the creek.
Anithamary et al. (2012)	Grain size, organic carbon, metals	Ten surface sediment samples were collected from Coleroon estuary and were analysed for sediment grain size, organic carbon and metals. The sediments were largely of sandy silt in nature. The surroundings of the coastal areas largely contributed to the organic carbon. Fine sediments and organic carbon played a vital role in metal distribution.
Idriss and Ahmad (2012)	pH, organic carbon, metals, speciation of metals	Sediment samples collected from Juru river, Malaysia were analysed for total metals, pH, organic carbon and metal speciation. The effect of pH and organic matter on metal concentration was studied. The concentration of Cu, Pb and Cd was found to be high in residual fraction.
Mohamed (2012)	Total metals and metal speciation	Heavy metals were analysed for the surface sediments to understand its mobility and availability. Most of the studied metals were available in organic and Fe-Mn oxide phase and Co in active phase. High metals were noted in the Lagoon side where as decrease in concentration was noted in the lake sediments.
Qiao et al. (2012)	Total metals and speciation	Eight metals in sediment samples at 15 sites from the Shantou Bay were analysed for metal distribution patterns in the bay using BCR sequential extraction technique. Authors reported

		high heavy metal pollutions in upper bay than in middle and down reaches of the bay. More than 50% of the total concentrations of some metals existed in the acid soluble fraction. Large concentration of Ni, Co, Cr and Fe occurred in the residual fraction. Principal component analysis (PCA) indicated that the heavy metals associated in the non-residual fractions resulted from anthropogenic sources.
Raju et al. (2012)	Total metals and speciation of metals	Twenty-five sampling points were selected depending upon geographical proximity of agricultural fields and industrial discharges, river-tributary confluence points, settlements located along the river bank, ritual and recreational activities. Metals were analysed using flame furnace atomic absorption spectrophotometer. The sediment geo-accumulation index (I_{geo}) showed maximum value of Cd and least value of Mn. Metal concentrations in sediments of river Cauvery in Karnataka not exceeded the toxic limit, and there is no peril to the aquatic life.
Bai et al. (2011)	Total metals, risk assessment	Surface sediment (0–15 cm) samples were collected from 31 different grid points throughout the Yilong Lake. Samples were subjected to a total digestion technique and analysed for As, Cd, Cr, Pb, Ni, Cu, and Zn and their ecological risk also were assessed.
Siraswar and Nayak (2011)	Sediment components, organic carbon and metals	Twenty sediment samples collected from mouth, lower and upper middle region of Mandovi estuary during monsoon were analysed for sediment components, organic carbon and selected metals. Sand percentage was found to be high towards the mouth, whereas, finer sediment towards the lower and upper middle regions. Organic carbon was found to be associated with finer sediments. Trace

		metals association with Fe and Mn has been discussed.
Fernandes et al. (2011)	Sediment components, pH, TOC, TN, TP and metals	Two core sediment samples from Manori were analysed for sediment components, total organic carbon, pH, total phosphorus, total nitrogen and metals. Authors reported contamination with metals in both the cores.
Hejabi et al. (2011)	pH, Electrical Conductivity (EC) in sediments, Total metals, metal speciation	Water and bed sediments from Kabini river were analysed for pH, EC, total metals and chemical speciation. Studies indicated that Cr and Cu were highly concentrated in the sediments near the vicinity of the industry and Cr, Zn and Ni were high near the influx of paper mill.
Liu et al. (2011)	pH, TOC, total metals, chemical speciation,	A sediment core collected near the Qiao Island in the Pearl River Estuary was analysed for total metal concentrations, chemical partitioning, and physico-chemical properties. Cu, Pb, Cr, and Zn were associated with residual and Fe/Mn oxides fractions. Cd in all sediments was mainly associated with exchangeable fraction. Sand content might have played an important role in the distributions of residual phases. Sediment pH had also an important influence on the Fe/Mn oxides, organic/sulfide and residual fractions of Cr, Cu, and Zn. Geoaccumulation Index showed different levels of contamination for different metals. The contaminations were attributed to the various anthropogenic activities around the vicinity.
Harikumar and Nasir (2010)	Organic matter and metals	Down core variation of heavy metals was studied in three sediment cores from Cochin estuary. Quality of the sediments was evaluated based on sediment quality guidelines, pollution load index, and sum of toxic units. The degree of contamination for each station was determined. The results of the study revealed higher

		concentration of heavy metals in recent sediments than in past. The concentration of heavy metals exceeded the different levels of toxicity in which adverse biological effects frequently occur. The spatial variation of heavy metals showed high contamination in the downstream at Pathalam industrial site.
Esen et al. (2010)	Grain size and metals	Surface sediments from nine stations in Nemrut Bay, Aegean Sea were analysed for trace metals and grain sizes. The results were compared with the numerical sediment guidelines used in North America. The metal levels were also evaluated according to the EF and CF analyses. The analyses revealed significant anthropogenic pollution of Hg, Pb, Zn, and As in the sediments of Nemrut Bay.
Ho et al. (2010)	pH, organic carbon, grain size, metals	36 surface sediment samples were collected from Cua Ong Habor, Ha Long Bay (Vietnam) and analysed for major elements (Al, Ca, Fe, K, Mg, S), heavy metals, organic matter, loss on ignition (LOI), grain size composition and pH. The results illustrated that the distribution patterns of metals are mainly controlled by organic matter and clay minerals and determined by the distribution of the fine grained fraction in the sediments. Co was largely controlled by Fe-Mn oxides. Carbonates partly control the distribution of Mn. Canadian, Wisconsin-United States and Flemish numerical Sediment Quality Guidelines, and calculation of Geo-accumulation Index (I_{geo}) and Enrichment Factor (EF) results indicated that natural processes such as weathering and erosion of bedrock are the main supply sources of heavy metals in sediments.
Luo et al.	Metals	Estuarine surface sediments from the northern

(2010)		Boai and Yellow Seas were analysed for metals. An ecological risk assessment of metals in the sediments was calculated by various approaches. Sediments from the estuaries of the Wuli and Yalu Rivers contained highest concentrations of metals. Authors reported very high level of pollution of arsenic in sediments with moderately pollution level by chromium, lead, and cadmium. Further, the authors stated that chronic exposures would cause an adverse effect on benthic invertebrates.
Mohiuddin et al. (2010)	Metals	In this study, twenty samples were investigated for trace metal pollution of water and also sediments of downstream of Tsurumi River, Yokohama, Japan. Authors reported high concentrations of some metals in water than in the surface water standard. The concentration of Pb and Mo was also higher than standard values, however, Fe and Mn was much lower than that of surface water standard. The mean concentration of metals was reported to be higher than the average worldwide shale concentrations and average Japanese river sediment values.
Nasrabadi et al. (2010)	Total metals and chemical speciation	Bulk concentrations and chemical speciation of metals Haraz River (Iran) bed sediments were measured. The level of sediment contamination was evaluated using EF, I_{geo}, and I_{poll}. Higher concentrations of Cd, As, Sr, and Pb were noted when compared with those of shale values. Sr, Pb, Co, and Cd were reported to be the most mobile metals. As concentrations were laregly available in residual fraction and hence, it was not considered to be hazardous. Fe, Cr, and Ni were also present in the highest percentages in the residual fraction, indicated that these metals are inert.
Natesan and	Grain size and	Four sediment cores were investigated for heavy

Seshan (2010)	metals	metals from Ennore creek and one core from the sea. Mn showed highest concentration in sediments. Fine sediments and organic matter showed positive correlation with the metals. I_{geo} showed very highly contaminated sediments in the interior of the Ennore creek and moderate degree of pollution according to PLI.
Zhou et al. (2010)	Sediment texture, organic carbon, pH, total metals and chemical speciation	Core sediments from a mudflat in Yifeng estuary (south-eastern China) and adjacent restored mangrove forest were investigated to check the influence of mangrove reforestation on heavy metal accumulation and speciation. Authors reported that mangrove reforestation increased metal concentrations in the oxidizable fraction and decreased the concentrations of all metals in the acid-soluble fraction. They have further reported high Pb, Zn and Cu concentrations in the reducible fraction. From this study the authors concluded that though the mangrove reforestation seems to accumulate heavy metals in the upper sediment layers it has decreased their bioavailability and mobility.

1.3 Objectives

Estuaries in Karnataka are continuously influenced by geological processes like weathering, erosion, deposition, periodic storms and floods and changing sea level. Increasing population, industrial establishments and developments are common near the river banks along this coast. Coastal Karnataka is emerging as an urbanized region with industrial growth. Soil erosion is the biggest problem along river banks and coasts, which poses greater threats to natural habitats and agro-ecosystem with the growing problem of pollution. Life in the rivers, estuaries and the coastal seas is therefore under greater stress. Estuaries act as a sink to many types of pollutants due to effluent discharge by industries of different kind, port activities and dumping of fish and organic wastes. Industrial effluents with toxic chemicals enhance the level of bioavailability of metals which can pose a risk to biota. Estuaries in Karnataka have also been affected

greatly due to construction of dams on rivers. This has led to change in deposition pattern of sediments, organic matter and metals over a period of time. Therefore, it has become a necessity to understand the level of metal pollution in the estuaries along Karnataka coast. An attempt has been made to investigate, with this background and with following objectives

1. To study the spatial and temporal variation of sediment components within the estuaries along the southern Karnataka coast.
2. To understand the depositional environment and diagenetic processes using the distribution pattern of sediment components and metals.
3. To determine chemical speciation of selected metals and to understand the bioavailability of metals.

1.4 Study area

Karnataka coastline extends over a length of 320 km. Along the coastal zone of Karnataka, in the recent years large number of economic developmental activities have come up and the area is also with high density of population. The occupational pressures along this coast are due to aquaculture, port maintenance, fish landing and processing, agricultural activities coir retting, mining for lime shell, bauxite and silica sand. There are several ports out of which major one at Mangalore and Nine minor ports at Karwar, Belikere, Tadri, Honavar, Bhatkal, Kundapur, Hangarkatta, Malpe and Old Mangalore. Many coastal lowlands in the vicinity of mangrove habitats are filled up with mud scooped from lagoons to cultivate coconut plantations. The coir retting carried out mainly in the mangrove cleared areas. The microbial process here causes pollution of water, air and soil, which in turn, affects the marine resources, quality of estuarine banks and nearby beaches. For the present study, eight estuaries along the south Karnataka coast were selected. Among the studied estuaries, Sharavati is a large estuary while Chakra Nadi, Haladi, Sita Nadi, Swarna, Udyavara, Pavanje and Gurpur are smaller estuaries (Fig. 2.2) as, Sharavati is having relatively large catchment area and it is also the longest estuary as compared to the smaller ones.

The Sharavati River is one of the important rivers flowing from Western Ghats into Arabian Sea (Fig 2.3a). On this river a hydroelectric dam Linganamakki was commissioned in 1964. The catchment area of Sharavati estuary is about 2985 km².

The length of the river is 128 km. In Sharavati estuary, the tidal influence is up to 15 km from the mouth. The soil texture in this region is largely clayey, sand and sandy loam in the catchment area. The rock types within the catchment area of River Sharavati includes granite, granodiorite, migmatites, greywacke, grey metabasalt, quartz chlorite schist with orthoquartzite, laterite and alluvium. Annual rainfall in Sharavati river catchment area ranges from 3521 to 4339 mm.

The Kollur and Chakra are the tributaries of Haladi River and join it near Kundapur (Fig. 2.3b). The Haladi River originates above the Ghats in the eastern part of the basin, flows across the Ghats and descends the slope with a fall of 20 m at the top of the Ghats. The rivers Kollur and Chakra originate on the slopes of the Western Ghats. The channel length of Kollur, Chakra and Haladi Rivers is 36, 42, and 60 km, respectively. The Kollur River flows in a highly meandering course before joining the river Chakra and cobble-gravel association dominates in the first half of the course, whereas it is sandy in the second half.

Sita Nadi basin (Figure 2.3c) is located in the Udupi district of Karnataka, India. The total geographical area of the basin is about 643.65 sq km. In Sita Nadi basin, physiographical divisions consist of low land, mid-land and high land. The low land region is 2-8 km wide sandy tract running parallel to the coast. It extends up to a distance of 16 km along the river course. It has small lateritic ridges with cultivable low lands, in between small exposures of gneisses and laterite hillocks with sparse vegetation. The mid-land region consists of laterite ridges, mesas and also structural hills composed of gneisses with incised narrow valleys of younger cycle. High land hills comprise mostly of archaean gneisses and metavolcanics and metasediments of Dharwar super group of proterozoic age. The major lithological units of Sita Nadi catchment area are banded granitic gneisses and laterites and some parts are covered by chlorite schist's. Some intrusive bodies like dolerite dykes and pegmatite veins are also noticed. Thin layer of coastal sediments is also found in the western part of the catchment. The rocks of the area belong to different geological periods like Archaean, Proterozoic, Cretaceous, Tertiary and Quaternary.

The river Swarna originates in the Western Ghats that flows westward and joins Arabian Sea (Fig. 2.3c). The water from this river is also a main source of drinking water. The major tributaries of this river are Durga, Kada, Andar and Happanadka. The basin of Swarna River is about an area of 603 km^2. The basin is located on the south-western part of the Western Dharwar Craton (WDC) (Rogers et al. 1986). Major rock types exposed in the river basin include granitic gneiss, dolerite dyke, and laterite (Balasubramanyan 1978; Tripti et al. 2013).

Udyavara River originates in the foothills of the Western Ghats and flows parallel to the sea for a distance of about 10 km before it joins the Arabian Sea near Malpe (Fig. 2.3d). The length of river is about 60 km and tidal influence is up to 11 km.

Pavanje River originates below the Western Ghats and empties into the Arabian Sea at Mulki after flowing over 12 km (Fig. 2.3e). The river is connected to the Arabian Sea throughout the year and is subjected to tidal influence to a length of 6.6 km in Pavanje River. The estuary has an average depth of 3 m and the tidal range is about 1 m. The bottom of the estuary is mostly a mixture of silt and sand. This is a typical tropical estuary which experiences wide variations in salinity.

Gurpur estuary is known to have a mixed type of semidiurnal tides (Fig. 2.3f). Currents in the river mouth are controlled by fresh water discharge during the southwest monsoon and by tides during the rest of the year. For this reason, ebb flow is dominant during the southwest monsoon and flood flow during winter and summer. Geologically the river basin is composed of rock types belonging to tertiary to quaternary periods in the lower catchments and older (Archaean) gneissic complex in the upper catchments. The basin is located at the western part of the WDC with major lithounit as Peninsular Gneiss/Archean Tonalitic-Trondhjemitic-Granodioritic (TTG) gneiss. The greenstone-amphibolitic facies metamorphic rocks and granulites could be seen in patches. The basin is lithologically composed of about 83% migmatites and granodiorites, 5% of charnockites, about 6% metabasalts and 2% laterites and amphibolites. A 200 m long sand bar is present near the Netravati-Gurpur river mouth at a depth of 2-3 m (Reddy et al. 1979).

Chapter 2

Methodology

2.1 Introduction

A sample is a small portion that is representative of an area or environment. Before sample collection, it is necessary to acquire thorough knowledge on the study area and also procedure involved in sample collection, preservation and analysis. Sample should be collected from an undisturbed area. Care should also be taken while sampling to avoid contamination, as it may lead to incorrect results. Sample preservation is important in order to avoid alteration of chemical components in the sediment which may lead to erroneous results. Further, standard methods should be employed to carry out the analysis. The experiment should be repeated to obtain accurate readings. Considering standard protocols, the methods adopted in collection and analyses in the present investigation are detailed in this chapter and are also outlined in the figure. 2.1.

2.2 Field methods

2.2a. Sampling

Fourteen shallow cores, eight representing mudflat environment and six mangrove environment were collected by using a hand driven PVC coring tube along Karnataka coast (Fig. 2.2 and 2.3a,b,c,d,e,f), south-central west coast of India.

2.2b. Field observations

Station location of all the cores was recorded by using a handheld Global Positioning System (GPS). Further, before sub sampling, each core was described with reference to colour and the length was measured (Table 2.1).

2.2c. Sub sampling/Storage

Sediment cores were sub-sampled at 2 cm interval with a plastic spatula to avoid the metal contamination and transferred to pre-numbered plastic bags. The packed bags were then stored in the icebox and transported to laboratory.

2.3 Laboratory procedures

In the laboratory, every sample was homogenized and half of each sub sample was transferred to pre-cleaned petri-dish and oven-dried at 60^{o} C. Following this, a portion of each of the oven-dried sample was grounded and homogenised by using an agate

mortar and pestle, and used for geochemical analysis. Other portion was used for sedimentological analysis.

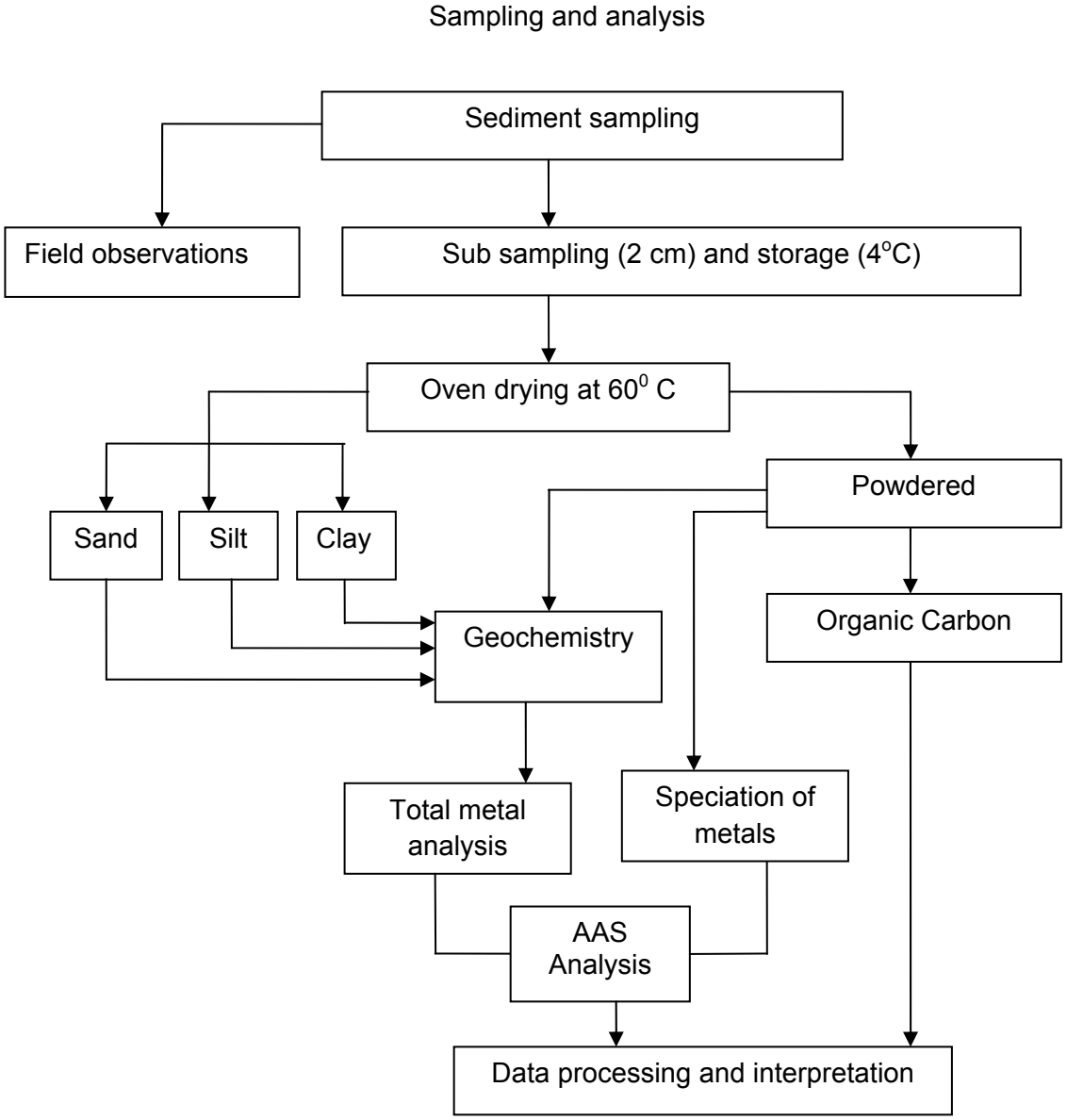

Figure 2.1: Flowchart of the methods followed

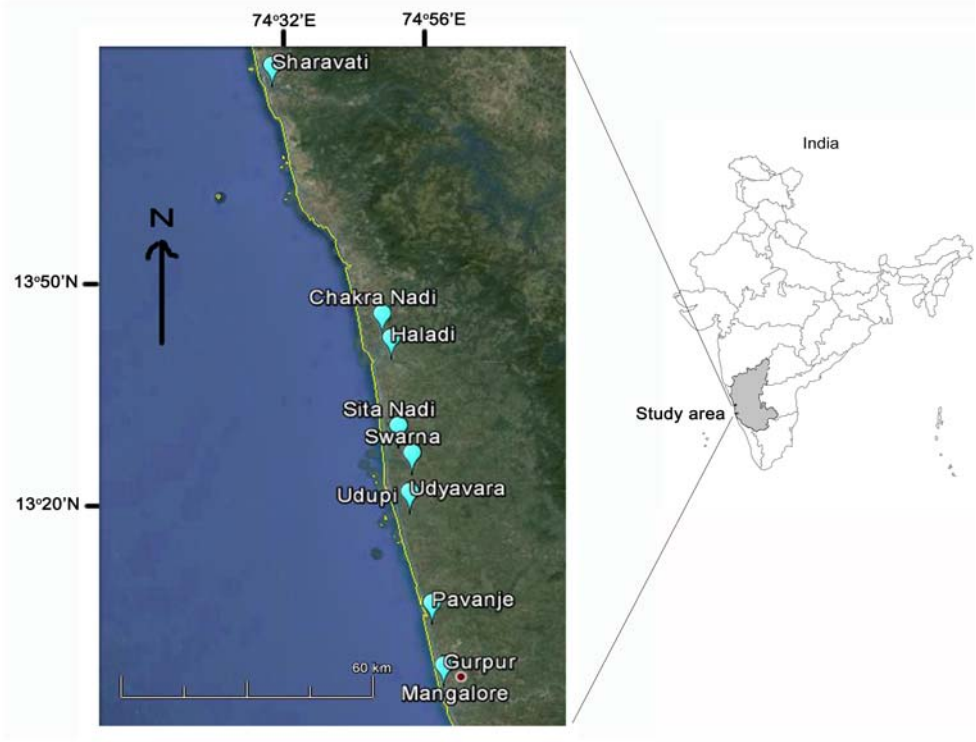

Figure 2.2 Map showing locations of sediment core collection along the south central west coast of India

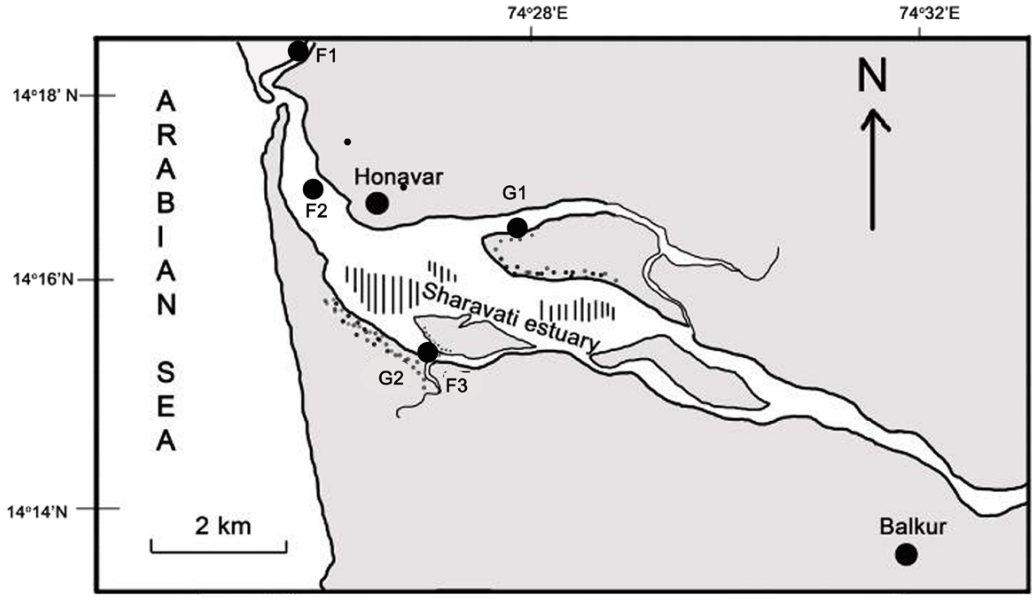

Figure 2.3a Map showing locations of sediment core collection in Sharavati estuary

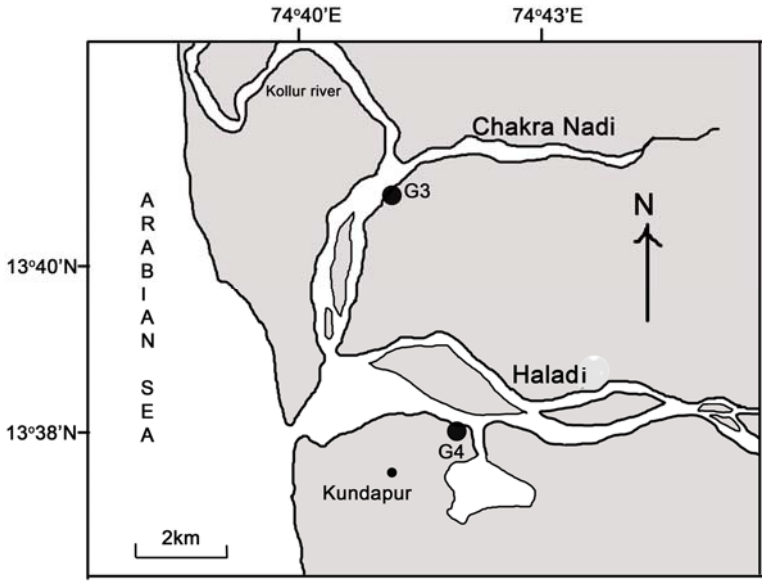

Figure 2.3b Map showing locations of sediment core collection in Chakra Nadi and Haladi estuary

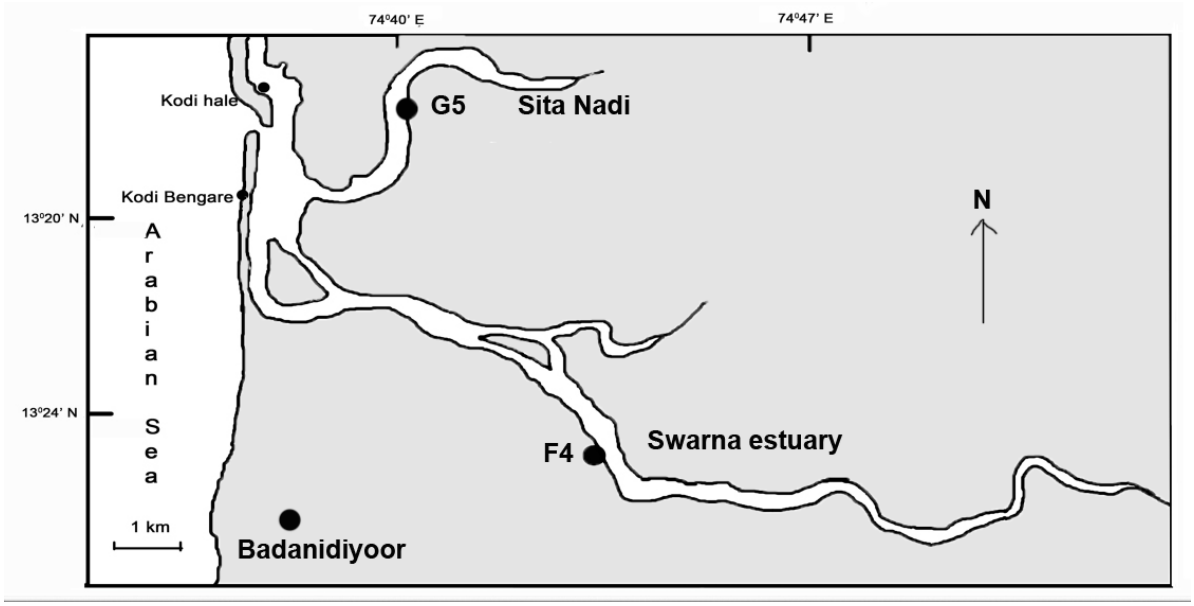

Figure 2.3c Map showing locations of sediment core collection in Sita Nadi and Swarna estuary

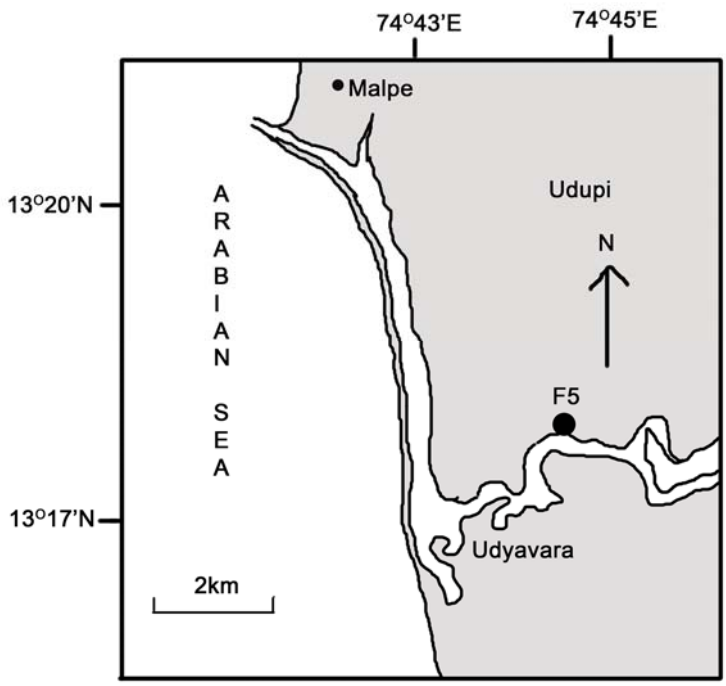

Figure 2.3d Map showing locations of sediment core collection in Udyavara estuary

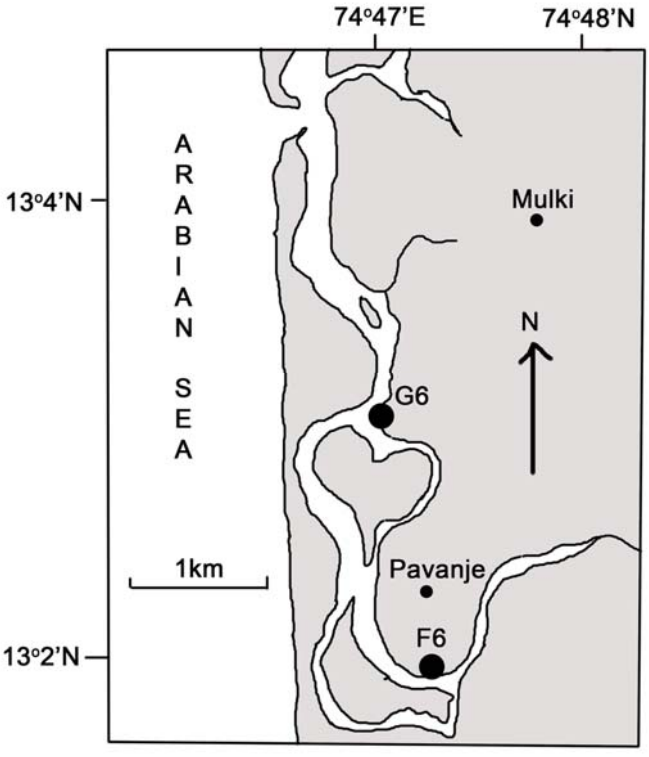

Figure 2.3e Map showing locations of sediment core collection in Pavanje estuary

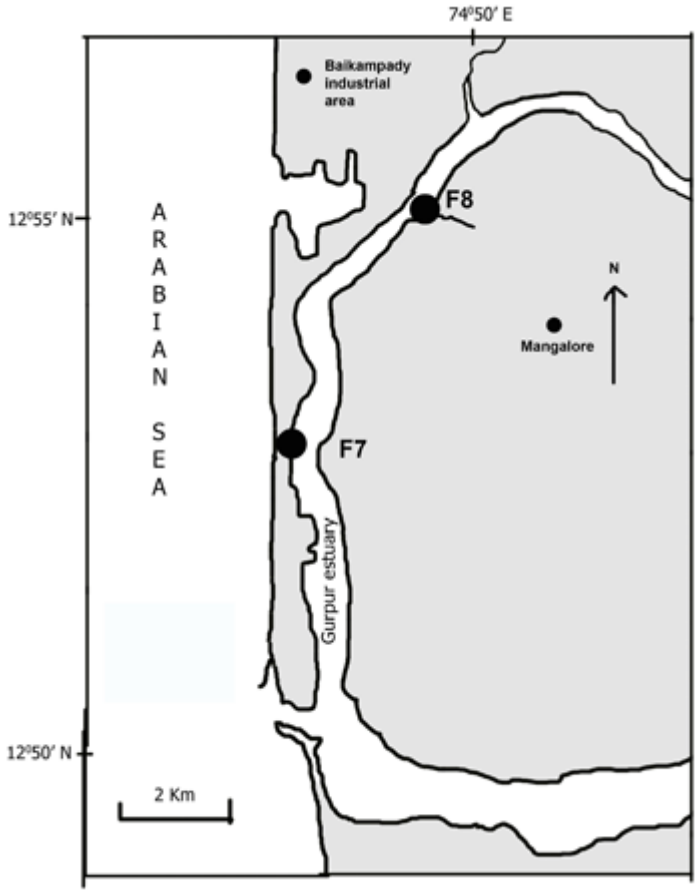

Figure 2.3f Map showing locations of sediment core collection in Gurpur estuary

Table 2.1 a Description of mudflat cores

Core	Estuary	Region	Lat	Long	Length (cm)	Colour
F1	Sharavati	Lower	14° 18’ 32.39” N	74° 25’ 34.81” E	0 - 14 14 - 28	Greyish brown Grey
F2	Sharavati	Lower	14° 16’ 44.25” N	74° 26’ 04.94” E	0 - 34 34 - 61	Brown Grey
F3	Sharavati	Middle	14° 15’ 12.82” N	74° 27’ 13.77” E	0 - 8 8 - 46	Brown Grey
F4	Swarna	Upper Middle	13° 23’ 21.83” N	74° 44’ 41.92” E	0 - 12 12 - 56	Grey-light Grey-dark
F5	Udyavara	Upper Middle	13° 17’ 52.10” N	74° 44’ 41.40” E	0 - 10 10 - 62	Brown Grey
F6	Pavanje	Upper Middle	13° 01’ 59.10” N	74° 47’ 36.49” E	0 - 4 4 - 50	Brown Grey
F7	Gurpur	Lower Middle	12° 53’ 18.62” N	74° 49’ 03.57” E	0 - 4 4 - 46	Brown Grey
F8	Gurpur	Upper Middle	12° 55’ 40.70” N	74° 49’ 50.20” E	0 - 16 16 - 40	Brown Grey

Table 2.1 b Description of mangrove cores

Core	Estuary	Region	Lat	Long	Length (cm)	Colour
G1	Sharavati	Middle	14° 15' 11.15" N	74° 27' 10.55" E	0 - 40	Grey
G2	Sharavati	Middle	14° 16' 37.90" N	74° 27' 41.10" E	0 - 6 6 - 52	Brown-dark Grey
G3	Chakra Nadi	Middle	13° 41' 03.30" N	74° 41' 13.60" E	0 - 8 8 - 20 20 - 40	Brick red Greyish red Red
G4	Haladi	Middle	13° 38' 12.44" N	74° 42' 09.86" E	0 - 46	Grey
G5	Sita Nadi	Middle	13° 27' 00.30" N	74° 43' 12.40" E	0 – 10 10 – 32	Brown Grey
G6	Pavanje	Middle	13° 03' 00.93" N	74° 47' 14.61" E	0 - 4 4 - 42	Brown Grey

2.3a Sediment size analysis (sand: silt: clay)

Sand: silt: clay ratio was determined using pipette analysis (Folk 1968) which is based on Stoke's settling velocity principle. Procedure: 10 g of oven dried (60^0 C) sediment sample was taken and transferred into 1000 ml beaker. Distilled water was added to this beaker and stirred. Sediment was then allowed to settle. Following day, water from the beaker was decanted by using decanting pipe. This step was repeated at least 4 to 5 times to remove the salinity. Salinity was checked using silver nitrate solution till it did not give a milky solution when mixed with decanted water. After decanting, 10 ml of 10 % sodium hexametaphosphate was added for dissociating the clay particles. On the next day 5 ml of 30 % of hydrogen peroxide was added to oxidize the organic matter. Contents of the beaker were then poured over 63-micron (230 mesh) sieve and filtrate was collected in 1000 ml cylinder. The contents from the beaker were washed till solution becomes clear and then volume was made up to 1000 ml. The solution from the cylinder was used for pipette analysis. Before withdrawal, the contents were homogenized by stirring for about 2 minutes using a stirrer. This was then allowed to settle for certain time according to the room temperature. Stirring time was noted down and pipetting time was kept by referring table 2.2.

25 ml of solution was pipetted out at 8 ϕ by inserting pipette up to 10 cm depth from the water level in the cylinder. Pipetted solution was then transferred into preweighed 100 ml beaker and dried at 60^0C overnight. After drying, beaker containing clay was weighed. The sand, which remained on the sieve, was transferred to preweighed

beaker. This was then dried and kept in desiccator to remove any moisture and then weighed. Further, three sediment size fractions viz. sand (4Ø); medium silt (6Ø) and clay (8Ø) were also mechanically separated for selected samples. Medium silt obtained was a mixture of large portion of silt and minor quantity of clay.

Percentage of sand, silt and clay were calculated as follows:

Sand % = (Weight of sand / Total Weight of the sediment) * 100

Clay % = [(Weight of clay / 25) * 1000] – 1 = x

= (x / Weight of the sediment) * 100

Silt %= 100 - (% of sand + % of clay)

Table 2.2 Time schedule used for pipette analysis.

Size Ø	Depth to which pipette is to Inserted (cm)	Time after which water is to be pipetted out Hours: Minutes: Seconds				
		28^0C	29^0C	30^0C	31^0C	32^0C
4	20	0:00:48	0:00:46	0:00:46	0:00:44	0:00:44
5	10	0:01:36	0:01:34	0:01:32	0:01:29	0:01:28
6	10	0:06:25	0:06:15	0:06:06	0:06:57	0:05:52
7	10	0:25:40	0:25:02	0:24:25	0:24:49	0:23:27
8	10	1:42:45	1:40:13	1:37:42	1:37:15	1:33:51
9	10	6:30:00	6:40:40	6:32:50	6:32:10	6:11:30
10	10	27:06:00	26:30:00	-	-	-

2.3b Organic carbon in sediments

Organic carbon was determined for all the sediment samples by using the Walkley-Black method (1947), which was later modified by Jackson (1958). Before performing the experiment all the glassware's were washed with chromic acid, which was prepared by adding potassium dichromate to the concentrated H_2SO_4. An aliquot of the sample (0.5 g) was treated with a known excess of the standard dichromate solution (10 ml) and 20 ml of concentrated H_2SO_4 with silver sulphate (Ag_2SO_4). This was then mixed by gently rotating the flask for about 1 minute. The mixture was then allowed to stand for 30 minutes. After 30 minutes the same solution was then treated with 200 ml milli-Q water, 10 ml of 85 % phosphoric acid (H_3PO_4) and 0.2 g sodium fluoride (NaF). This solution was then back titrated with standard ferrous ammonium sulphate solution using diphenylamine as an indicator to a one-drop end point (brilliant green). Silver sulfate

was used to prevent the oxidation of chloride ions. Standardization blank without sample was run following the same above procedure. Dextrose was taken as a reference standard for the determination of organic carbon.

Percentage of organic carbon was calculated as follows

% Organic carbon = 10 (1-T/S) * F

Where,

S = Standardization blank titration, ml of ferrous solution

T = Sample titration, ml of ferrous solution

F = Factor which is derived as follows:

F = (1.0 N) * 12/4000 * 100/Sample weight

= 0.6 when sample weight is exactly 0.5 g

Where,

12/4000 = m. eq. wt. carbon

2.3c Digestion of sediment for total metal analysis

The sediments were digested using the procedure described by Jarvis and Jarvis (1985) to extract the metals. Procedure: Known quantity (0.2 g) of finely ground sediment sample was transferred into a clean acid washed Teflon beaker. To this, a mixture of 10 ml of HF, HNO_3 and $HClO_4$ (7:3:1) was added slowly to avoid excessive frothing and was completely dried keeping it on the hot plate at around 150^0 C. Further, after drying, 5 ml of the above mixture was added again and dried on the hot plate for one hour and later, 2 ml of concentrated HCl was added to it and dried completely. Final residue was then dissolved in the 10 ml of 1:1 HNO_3. After obtaining a clear solution of the digested mixture, of the sediment sample, the contents from the Teflon beakers were slowly transferred into the pre-acid washed polypropylene volumetric flaks and the solution was made up to 50 ml with milli-Q water. This procedure was adopted for bulk samples and selected samples of three different sediment size fractions viz. sand (4Ø); medium silt (6Ø) and clay (8Ø). Same procedure was also followed for reference standard 2702 obtained from National Institute of Standards and Technology (NIST) to ensure accuracy of the analytical method. The diluted solution was used for metal analysis for eight different metals viz. Al, Fe, Mn, Ni, Zn, Cu, Co and Cr using Atomic Absorption Spectrophotometer.

2.3d Chemical partition / Speciation of elements

A modified sequential extraction procedure (Tessier et al. 1979) was adopted in the present study. Although the sequential extraction procedure is time consuming, the results obtained provide information on the source of metals, its mode of occurrence, bioavailability and remobilization.

Selected sub- samples of some cores were chosen to evaluate chemical partition / speciation of sediments. The procedure involves following five steps, which are referred here as fractions/phases.

i. Exchangeable metal fraction (F1): One gram of the previously dried, finely-ground sediment sample was treated with 8 ml of magnesium chloride solution (1 M $MgCl_2$, pH 7) at room temperature in 50 ml plastic centrifuging tube with frequent agitation for 1 h. After centrifuging at 8000 rpm for 10 minutes the supernatant was collected for metal analysis. The residue was washed with deionised water.

ii. Carbonate metal fraction (F2): The residue from first fraction was further treated with 8 ml of 1 M sodium acetate (NaOAc) at room temperature and adjusted to pH 5 with acetic acid (HOAc) and then periodically agitated for 5 h at room temperature on orbital shaker. Solution was then centrifuged and the supernatant was collected for metal analysis. The residue was washed with deionised water.

iii. Fe - Mn oxide metal fraction (F3): The residue from fraction F2 was extracted with 20 ml of 0.04 M Hydroxylamine hydrochloride in 25 % (volume / volume) acetic acid. Further, the mixture was kept at 96 $\pm$ 3^0C with agitation at regular intervals for 5 hours. Solution was then centrifuged at 8000 rpm and the supernatant was collected for metal analysis. The residue was washed with deionised water.

iv. Organic matter bound metal fraction (F4): 3 ml of 0.02 M nitric acid and 5 ml of 30 % hydrogen peroxide were added to the residue from third fraction which was adjusted to pH 2 with nitric acid. Then this mixture was heated to 85 $\pm$ 2^0 C for 2 hours with agitation at regular intervals. Further, 3 ml of 30 % hydrogen peroxide (pH 2 with nitric acid) was again added and the sample was heated again to 85 $\pm$ 2^0 C for 3 hours with regular agitation. Once cooled, 5 ml of 3.2 M ammonium acetate in 20 % (volume/volume) nitric acid was added to the above mixture and the sample was diluted to 20 ml and agitated continuously for half an hour. After agitation, solution was

centrifuged and the supernatant was collected for metal analysis. The residue was washed with deionised water.

v. Residual metal fraction (F5): The residue from fraction F4 was washed with deionised water and was transferred into the acid washed teflon beaker and then digested completely following the same procedure used for the total metal digestion.

The centrifuging machine used for the sequential extraction procedure was Remi centrifuge (model PR-23) and orbital shaker used for agitation of samples was Orbital shaking incubator (model RC2100).

2.3e Atomic Absorption Spectrophotometer (AAS) analysis

The digested sediment samples for total metal analysis and sediment samples of different size fractions were analyzed for various metals viz. Al, Fe, Mn, Ni, Zn, Cu, Co and Cr; and sequentially extracted samples were analyzed for various metals viz. Fe, Mn, Ni, Zn, Cu, Co and Cr on Atomic Absorption Spectrophotometer (AAS) (Varian 240FS model) with air acetylene fuel mixture. Al was determined using nitrous-oxide flame. The instrument is equipped with deuterium background corrections. During the analysis, blank corrections were applied wherever it was necessary. The average recoveries obtained were around 90-97%. Calibration of the instrument was done using chemical standards obtained from Merck. Recalibration check was also carried out at regular intervals. Blank corrections were applied wherever necessary. Precision was monitored by analyzing triplicate samples for some selected samples.

2.4 Data processing

a) Statistical analysis

The softwares MS Excel and Grapher 7 were used for computations and plotting different parameters. The data was subjected to different statistical analysis for studying large and cumbersome data. STATISTICA 7 (computer software) was used to obtain Pearson's correlation between different parameters.

b) Pollution indices

Enrichment Factor (EF) provides the actual level of contamination and was used to differentiate between the anthropogenic and natural source. The following equation is used to compute EF.

EF= (C_m/C_{Al}) sediment / (C_m/C_{Al}) Shale

Where, (C_m/C_{Al}) sediment is the metal concentration (C_m) (µg/g dry weight) in relation to Al (% dry weight) within sediment samples.

(C_m/C_{Al}) shale is the metal concentration (C_m) within shale in relation to Al (% dry weight). Shale values are taken from Turekian and Wedepohl (1961).

EF values were interpreted following Zhang and Liu (2002) as EF value between 0.5 and 1.5, suggests natural input and if an EF value is greater than 1.5, it suggest anthropogenic input of metals.

Pollution load index (PLI) was computed following Tomlinson et al. (1980), which is as follows:

PLI=n √ (CF1xCF2xCF3x…xCFn)

Wherein,

CF = Contamination Factor, n = number of metals

CF is the quotient obtained by dividing the concentration of each metal with its background value.

The PLI value if > 1 is polluted, whereas <1 indicates no pollution. The background values were taken from Turekian and Wedepohl (1961).

Table 2.3 (a) Screening Quick Reference Table (SQUIRT) for metals in marine sediments (Buchman, 1999)

Elements	Threshold Effect Level (TEL)	Effects Range Low (ERL)	Probable Effects Level (PEL)	Effects Range Median (ERM)	Apparent Effects Threshold (AET)
Fe	-	-	-	-	22 % (Neanthes)
Mn	-	-	-	-	260 (Neanthes)
Ni	15.9	20.9	42.8	51.6	110 (Echinoderm Larvae)
Zn	124	150	271	410	410 (Infaunal community)
Cr	52.3	81	160.4	370	62 (Neanthes)
Cu	18.7	34	108.2	270	390 (Microtox and Oyster larvey)
Co	-	-	-	-	10 (Neanthes)

Further, to understand the potential bioavailability or the risk of toxicity of the studied metals to the biota, the average data of total metal concentrations obtained after total acid digestion as well as average metal concentrations obtained from sequentially

extracted fractions (sum of the bioavailable fractions viz. exchangeable, carbonate, Fe - Mn oxide and organic bound) were compared with the "Sediment Quality Values (SQV) given in the Screening Quick Reference Table (SQUIRT)" (Table 2.3a,b). The implication of the SQV was to achieve information on risk of toxicity of metals to biota. SQUIRT was given by NOAA for screening purposes. The guideline values for SQUIRT were given by Buchman (1999) and are categorized into five classes indicating the different levels of toxicity of metals.

(b) Sediment guidelines and terms used in SQUIRT.

Sediment Guidelines	
Threshold Effect Level (TEL)	Maximum concentration at which no toxic effects are observed
Effects Range Low (ERL)	10^{th} percentile values in effects or toxicity may begin to be observed in sensitive species
Probable Effects Level (PEL)	Lower limit of concentrations at which toxic effects are observed
Effects Range Median (ERM)	50^{th} percentile value in effects
Apparent Effects Threshold (AET)	Concentration above which adverse biological impacts are observed.

Table 2.4 Criteria for risk assessment code (RAC) by Perin et al. (1985).

Risk Assessment Code (RAC)	Criteria (%)
No risk	< 1
Low risk	1 – 10
Medium risk	11 – 30
High risk	31 – 50
Very high risk	> 50

The Risk Assessment Code (RAC) as proposed by Perin et al. (1985) was calculated. If the given metal released from the sediment in the form of exchangeable and carbonate fraction is less than 1% of the total metal, then it will be considered safe for the environment. On the contrary, if the metal released from sediment is more than 50% of the total metal, in the same fractions is considered to be highly dangerous as it can easily enter the food chain. The values are interpreted in accordance with the RAC percentage classifications, given by Perin et al. (1985) (Table 2.4).

Chapter 3

Results and Discussion

3.1 Section I

Sharavati estuary

Five sediment cores were collected from large estuary Sharavati estuary namely F1, F2 and F3, from mudflat sedimentary environment and G1 and G2 from mangrove sedimentary environment. Core F1 and F2 were representing the lower estuary and F3, G1 and G2 were collected from the middle estuary.

3.1A Sediment component and organic matter

3.1A.1a. Mudflats

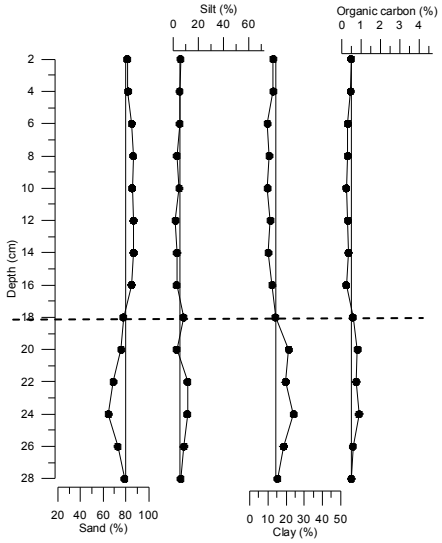

Fig. 3.1.1 Vertical profiles of sediment components and organic carbon in core F1 (Sharavati estuary – lower region)

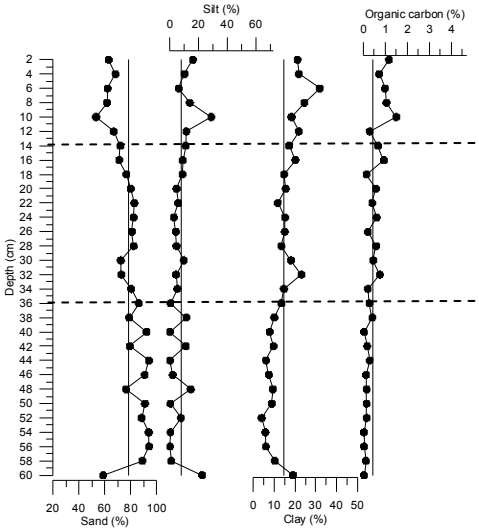

Fig. 3.1.2 Vertical profiles of sediment components and organic carbon in core F2 (Sharavati estuary – lower region)

In core F1, sand content varies from 65 to 87 % whereas silt and clay content vary from 2 to 11 % and 10 to 24 % respectively with mean values for sand, 80 %; silt, 6 % and clay, 15 % (Table 3.1.1). Organic carbon content varies from 0.24 to 0.9 % with its mean value 0.49 %. In core F2 sand varies from 53 to 94 % whereas silt, clay and organic carbon vary from 0.07 to 29 %, 4 to 32 % and 0.03 to 1.5 % respectively with mean values of sand, 78 %; silt, 8 %; clay, 14 % and organic carbon, 0.44 %. In core F3 sand varies from 42 to 96 % whereas silt, clay and organic carbon vary from 0.28 to 32 %, 3 to 33 % and 0.03 to 2 % respectively with mean values of sand, 76 %; silt, 8 %; clay, 16 % and organic carbon, 0.79 %. When the average values of sediment components and organic carbon of cores F1, F2 and F3 were compared, it is noted that

all the three cores were highly dominated by sand content and organic carbon was found to be relatively higher in core F3 which was collected at the middle estuary as compared to cores F1 and F2 which were collected at the lower estuary. On the basis of the distribution of sediment components, core F1 can be divided into two sections. Section 1 from 28 to 18 cm and section 2 from 18 cm to the surface. Core F2 can be divided into three sections. Section 1 from 60 to 36 cm; section 2 from 36 to 14 cm and section 3 from 14 cm to the surface. Core F3 can be divided into three sections; section 1 (46 – 22cm), section 2 (22 – 8 cm) and section 3 (8 – 0 cm). Range and average values for each section is provided in table 3.1.2.

Table 3.1.1 Range and average values of sand, silt, clay and organic carbon (OC) in mudflats and mangroves

Core	Sand			Silt			Clay			OC		
	Min	Max	Avg	Min	Max	Avg	Min	Max	Avg	Min	Max	Avg
F1	65	87	80	2	11	6	10	24	15	0.24	0.9	0.49
F2	53	94	78	0.07	29	8	4	32	14	0.03	1.5	0.44
F3	42	96	76	0.28	32	8	3	33	16	0.03	2	0.79
G1	59	94	82	0.01	13	4	6	34	14	0.06	2	0.41
G2	23	78	58	1	58	25	11	34	18	0.4	5	2

In core F1, section 1, sand content varies from 65 to 79 % whereas silt and clay content vary from 2.7 to 11 % and 15 to 24 % respectively with mean values for sand, 72 %; silt, 8 % and clay, 20 %. Organic carbon content varies from 0.50 to 0.9 % with its mean value 0.72 %. In section 2, sand content varies from 78 to 87 % whereas silt and clay content vary from 1.8 to 8 % and 10 to 14 % respectively with mean values for sand, 84 %; silt, 4 % and clay, 12 %. Organic carbon content varies from 0.24 to 0.58 % with its mean value 0.37 %. In core F2, section 1, sand content varies from 59 to 94

Table 3.1.2 Range and average values of sections of sand, silt, clay and organic carbon (OC) in mudflats and mangroves

Core	section	Sand			Silt			Clay			OC		
		min	max	avg	min	max	Avg	min	max	avg	min	max	avg
F1	2	78	87	84	1.8	8	4	10	14	12	0.24	0.58	0.37
	1	65	79	72	2.7	11	8	15	24	20	0.50	0.90	0.72
F2	3	53	68	62	6.1	29	14	18	32	23	0.29	1.49	0.95
	2	71	83	77	2.8	11	6	12	23	16	0.15	0.94	0.51
	1	59	94	85	0.1	22	6	4	19	9	0.03	0.41	0.15

F3	3	42	84	57	6	32	20	10	29	23	0.5	2.1	1.5
	2	46	77	64	6	26	13	16	33	23	0.8	1.8	1.2
	1	82	96	89	0.3	4	1	3	15	10	0.03	0.9	0.3
G1	3	59	83	72	3.9	8	6	13	34	22	0.06	1.61	0.98
	2	70	86	79	0.7	13	6	11	19	15	0.06	0.72	0.40
	1	81	94	89	0.01	3	1	6	19	10	0.09	0.34	0.23
G2	2	23	53	34	24.5	58	46	15	31	20	1.61	4.62	3.23
	1	57	78	68	1	21	15	11	34	17	0.44	1.32	1.00

% whereas silt and clay content vary from 0.1 to 22 % and 4 to 19 % respectively with mean values for sand, 85 %; silt, 6 % and clay, 9 %. Organic carbon content varies from 0.03 to 0.41 % with its mean value 0.15 %. In section 2, sand content varies from 71 to 83 % whereas silt and clay content vary from 2.8 to 11 % and 12 to 23 % respectively with mean values for sand, 77 %; silt, 6 % and clay, 16 %. Organic carbon content varies from 0.15 to 0.94 % with its mean value 0.51 %. In section 3, sand, silt and clay vary from 53 to 68 %, 6.1 to 29 % and 18 to 32 %, respectively with mean values for sand 62 %; silt, 14 %; and clay, 23 %. Organic carbon varies from 0.29 to 1.49 % with its mean value 0.95 %. In core F3, section 1, sand content varies from 82 to 96 % whereas silt and clay content vary from 0.3 to 4 % and 3 to 15 % respectively with mean values for sand, 89 %; silt, 1 % and clay, 10 %. Organic carbon content varies from 0.03 to 0.9 % with its mean value 0.3 %. In section 2, sand content varies from 46 to 77 % whereas silt and clay content vary from 6 to 26 % and 16 to 33 % respectively with mean values for sand, 64 %; silt, 13 % and clay, 23 %. Organic carbon content varies from 0.8 to 1.8 % with its mean value 1.2 %. In section 3, sand, silt and clay vary from 42 to 84 %, 6 to 32 % and 10 to 29 %, respectively with mean values for sand 57 %; silt, 20 %; and clay, 23 %. Organic carbon varies from 0.5 to 2.1 % with its mean value 1.5 %. Among all the three cores, core F3 showed large range in variation of sand, silt, clay and organic carbon (Table 3.1.1) and in section 3 it showed maximum variation (Table 3.1.2). The mean

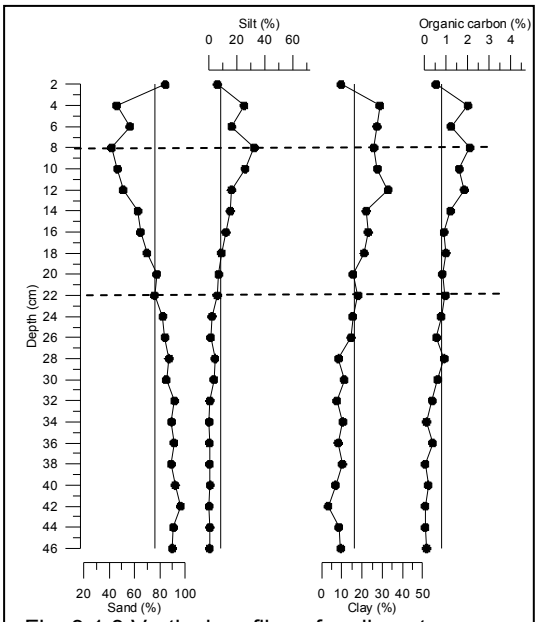

Fig. 3.1.3 Vertical profiles of sediment components and organic carbon in core F3 (Sharavati estuary – middle region)

value of sand (89 %) was high in section 1, whereas, silt (20 %), clay (23 %) and organic carbon (1.5 %), were high in section 3, of core F3 (Table 3.1.2).

In core F1, sand profile shows a decreasing trend from the bottom of the core up to 24 cm, followed by increase up to 12 cm and then decrease again up to surface (Fig. 3.1.1). Silt profile shows an increasing trend from the bottom of the core up to 24 cm and further, maintains a constant trend along the average line up to the surface. Clay profile compensates to that of sand profile throughout the core. Organic carbon profile largely agrees with the clay profile. In core F2, sand profile shows sharp increase from the bottom of the core up to 58 cm which further shows a decreasing trend up to the surface with fluctuations (Fig. 3.1.2). It is observed that the silt and to some extent clay profile show exactly opposite trend to that of sand thereby, compensating it. Organic carbon shows a gradual increasing trend from the bottom of the core up to the surface which largely agrees to that of finer sediment profiles. In core F3, it is observed that sand profile shows a decreasing trend in section 1 and 2 and increasing trend in section 3 (Fig. 3.1.3). The distribution pattern of sand is compensated by that of silt and clay. Further, the distribution pattern of organic carbon is largely similar to the distribution pattern of silt and clay.

3.1A.1b. Mangroves

In core G1 sand content varies from 59 – 94 % (avg. 82 %), whereas silt and clay content vary from 0.01 – 13 % (avg. 4 %) and 6 – 34 % (avg. 14%) respectively and organic carbon varies from 0.06 – 2 % (avg. 0.41 %). In core G2 sand content varies from 23 – 78 % (avg. 58 %), whereas silt and clay content vary from 1 – 58 % (avg. 25 %) and 11 – 34 % (avg. 18%) respectively (Table 3.1.1). Organic carbon varies from 0.4 – 5 % (avg. 2%). When the average values of sediment components and organic carbon of cores G1 and G2 were compared, it is noted that the average sand content was higher in core G1 which was collected at lower middle region and mud content (silt + clay) was found to be higher in core G2 which was collected from the upper middle region. The average organic carbon was also found to be higher in core G2.

On the basis of the distribution of sediment components, core G1 can be divided into three sections; section 1 (40 – 22 cm), section 2 (22 – 6 cm) and section 3 (6 – 0 cm).

Core G2 can be divided into two sections; section 1(52 – 16 cm) and section 2 (16 – 0 cm). The range and average values for each section is given in table 3.1.2. In core G1, section 1, sand content varies from 81 to 94 % whereas silt and clay content vary from 0.01 to 3 % and 6 to 19 % respectively with mean values for sand, 89 %; silt, 1 % and clay, 10 %. Organic carbon content varies from 0.09 to 0.34 % with its mean value 0.23 %. In section 2, sand content varies from 70 to 86 % whereas silt and clay content vary from 0.7 to 13 % and 11 to 19 % respectively with mean values for sand, 79 %; silt, 6 % and clay, 15 %. Organic carbon content varies from 0.06 to 0.72 % with its mean value

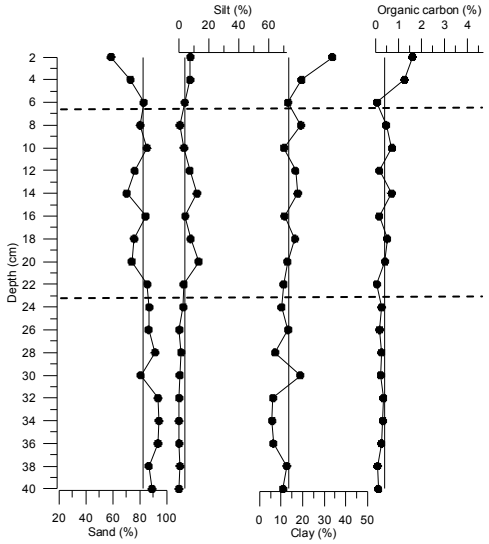

Fig. 3.1.4 Vertical profiles of sediment components and organic carbon in core G1 (Sharavati estuary – lower middle region)

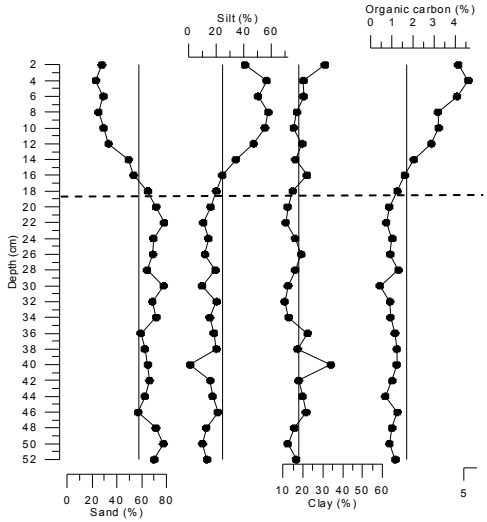

Fig. 3.1.5 Vertical profiles of sediment components and organic carbon in core G2 (Sharavati estuary – upper middle region)

0.4 %. In section 3, sand, silt and clay vary from 59 to 83 %, 3.9 to 8 % and 13 to 34 %, respectively with mean values for sand 72 %; silt, 6 %; and clay, 22 %. Organic carbon varies from 0.06 to 1.61 % with its mean value 0.98 %. In core G2, section 1, sand content varies from 57 to 78 % whereas silt and clay content vary from 1 to 21 % and 11 to 34 % respectively with mean values for sand, 68 %; silt, 15 % and clay, 17 %. Organic carbon content varies from 0.44 to 1.32 % with its mean value 1 %. In section 2, sand, silt and clay vary from 23 to 53 %, 24.5 to 58 % and 15 to 31 %, respectively with mean values for sand 34 %; silt, 46 %; and clay, 20 %. Organic carbon varies from 1.61 to 4.62 % with its mean value 3.23 %. Among all the two cores, core G2 showed large range in variation of sand, silt and organic carbon (Table 3.1.1) and section 2 showed maximum variation, however, clay showed variation in section 1 of core G2

(Table 3.1.2). The mean value of sand (89 %) and clay (22 %) was high in section 1 and 3, respectively, of core G1, whereas, silt (46 %) and organic carbon (3.23 %), were high in section 2, of core G2 (Table 3.1.2).

In core G1, the sand profile shows a decreasing trend in section 1, with some fluctuations (Fig. 3.1.4). Further, it maintains lower values than average line in section 2 showing negative peak values at 20 and 14 cm depth. Sharp decrease in sand content is noticed in section 3. The silt profile shows a constant trend in section 1. Distribution of silt compensates that of sand in section 2 with two positive peak values at 20 cm and 14 cm depth which later show a slight increase at the surface. Clay shows an increasing trend in section 1 and 2, which later shows a sharp increase in section 3. Organic carbon profile shows a similar trend to that of silt and clay. In core G2, the sand profile shows a constant trend from the bottom of core up to 22 cm with fluctuating values more than average line (Fig. 3.1.5). Further, it decreases gradually up to the surface in section 2. Silt also shows a constant trend from the bottom of the core up to 22 cm but with lower than average value and later increases up to the surface, thereby compensating the sand values. Clay profile shows fluctuating trends throughout the core with a peak at 40 cm higher values of clay are also seen at the surface. Organic carbon profile shows a similar trend to that of silt which remains constant from the bottom of the core up to 22 cm with lower than average value and further increases gradually up to the surface.

3.1B Metal distribution

3.1B.1a. Distribution of Al, Fe and Mn in the bulk sediments of mudflats

The geochemical data shows 3-5 % (avg. 4 %) Al, 2 - 3% (avg. 2 %) Fe, 223 - 331 ppm (avg. 280 ppm) Mn in core F1, 2 – 8 % (avg. 4 %) Al, 1-5 % (avg. 2 %) Fe, 83 - 181 ppm (avg. 121 ppm) Mn in core F2 (Table 3.1.3) and core F3 showed, 3 – 11 % (avg. 5 %%) Al, 1 - 6% (avg. 3 %) Fe and 73 - 232 ppm (avg. 149 ppm) Mn.

Table 3.1.3 Range and average values of metals in mudflats and mangroves

Core	Al (%)			Fe (%)			Mn (ppm)		
	min	max	avg	min	max	avg	min	max	avg
F1	3	5	4	2	3	2	223	331	280
F2	2	8	4	1	5	2	83	181	121
F3	3	11	5	1	6	3	73	232	149
G1	2	6	3.4	1	3	1.6	94	252	130
G2	3	8	5	3	9	5	226	552	364

	Ni (ppm)			Zn (ppm)			Cu (ppm)			Co (ppm)			Cr (ppm)		
	min	max	avg	min	max	avg	min	max	avg	min	max	avg	min	max	avg
F1	12	60	27	15	30	22	40	67	53	2	12	5	37	75	54
F2	3	32	11	3	37	15	43	79	55	6	17	9	26	129	49
F3	13	46	24	6	41	17	3	33	11	1	11	5	12	205	62
G1	6	19	11	7	31	17	5	17	9	1	7	4	36	88	52
G2	6	86	36	26	70	42	32	105	55	13	33	20	73	153	107

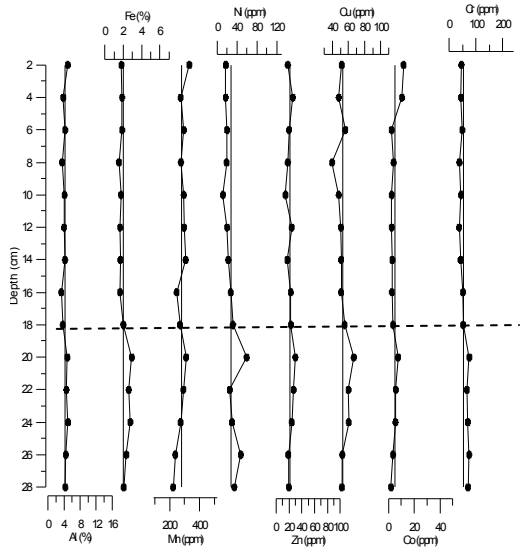

Fig. 3.1.6 Vertical profiles of metals in core F1 (Sharavati estuary – lower region)

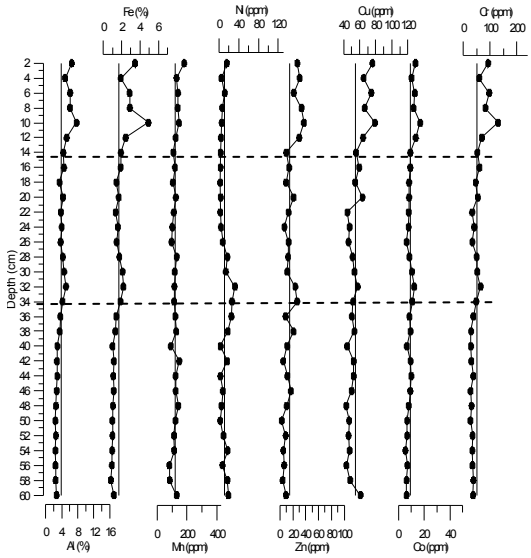

Fig. 3.1.7 Vertical profiles of metals in core F2 (Sharavati estuary – lower region)

The range and average values for each section is given in table 3.1.4. In core F1, section 1, geochemical data showed 4.3 - 5 % (avg. 4.6 %) Al, 2.1 – 2.9% (avg. 2.5 %) Fe, 223 - 310 ppm (avg. 267 ppm) Mn and; section 2 showed, 3.3 – 4.9 % (avg. 4 %) Al, 1.5 - 2 % (avg. 1.8 %) Fe, 247 - 331 ppm (avg. 287 ppm) Mn. In core F2, section 1, showed, 2.4 - 3.7 % (avg. 2.8 %) Al, 0.8 – 1.4% (avg. 1.1 %) Fe, 83 - 148 ppm (avg. 117 ppm) Mn; section 2 showed, 3.4 – 5.1% (avg. 4.2 %) Al, 1.3-2.2 % (avg. 1.8 %) Fe,

98 - 131 ppm (avg. 114 ppm) Mn; section 3 showed, 4.9 - 7.7 % (avg. 6.1 %) Al, 1.9 – 4.9 % (avg. 3.1 %) Fe, 124 - 181 ppm (avg. 143 ppm) Mn. In core F3, section 1, showed 2 - 4 % (avg. 3 %) Al, 1 – 2% (avg. 2 %) Fe, 73 - 224 ppm (avg. 125 ppm) Mn; section 2 showed, 6 – 11 % (avg. 7 %) Al, 3 - 6 % (avg. 4 %) Fe, 152 - 232 ppm (avg. 182 ppm) Mn and section 3 showed, 3 - 8 % (avg. 6 %) Al, 2 – 6% (avg. 4 %) Fe, 153 - 179 ppm (avg. 166 ppm) Mn. Among the mudflat cores, Al, Fe and Mn showed maximum range in variation in core F3 (Table 3.1.3) and; Al, Fe and Mn had largest variation in section 2, 3 and 1, respectively, in core F3 (Table 3.1.4)

In core F1, Al profile maintained a constant trend along the average line (Fig. 3.1.6). However, it showed higher values in section 1 as compared to section 2. Similar distribution pattern is also observed in case of Fe and to some extent Mn profiles. Al, Fe and Mn showed peak values at 20 cm depth. In core F2, Al showed lower values than the average in section 1. Further, it remained constant along the average line (Fig. 3.1.7) in section 2. In section 3, it showed higher values. Similar profile was also observed in case of Fe. However, Mn profile maintained a constant trend throughout the core. In core F3, the distribution of Al shows an increasing trend in section 1 and 2 followed by a decreasing trend in section 3 showing positive peak value at depth 12 (prominent) and 4 cm (Fig. 3.1.8). Similar distribution pattern is also observed for Fe throughout the core and in section 1 and 2 in case of Mn. All the three elements maintain lower than average values in section 1 in core F2 and F3 and higher than average in section 2 in core F3. In section 3, Al and Fe, showed a peak at 4 cm depth in core F3 and at 10 cm depth in core F2 and then decrease. Mn, however, maintained a constant value in section 3. Higher values of Fe and Al, between 20 cm and 4 cm with peaks at 12 cm of Al, Fe and Mn and at 4 cm of Fe and Al in core F3 and peak at 10 cm depth of Al and Fe in core F2 indicate either additional input of sediments with these metals or remobilization of Fe during early diagenesis. Low

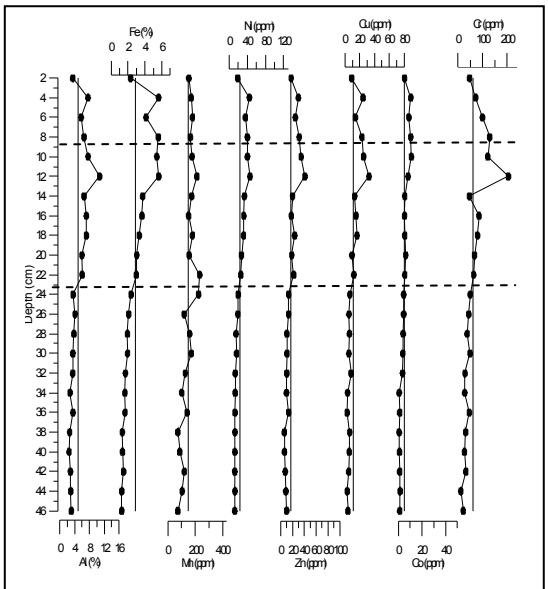

Fig. 3.1.8 Vertical profiles of metals in core F3 (Sharavati estuary – middle region)

values of metals at the surface are probably due to the removal of these ions from the sediments to the water column above, through diffusion processes (Badr et al. 2009). Like fine sediments and organic carbon, Al, Fe and Mn maintained higher values in section 1 for core F1.

Table 3.1.4 Range and average values of sections of metals in mudflats and mangroves

Core	section	Al (%)			Fe (%)			Mn (ppm)		
		min	max	avg	min	max	Avg	min	max	avg
F1	2	3.3	4.9	4.0	1.5	2.0	1.8	247	331	287
	1	4.3	5.0	4.6	2.1	2.9	2.5	223	310	267
F2	3	4.9	7.7	6.1	1.9	4.9	3.1	124	181	143
	2	3.4	5.1	4.2	1.3	2.2	1.8	98	131	114
	1	2.4	3.7	2.8	0.8	1.4	1.1	83	148	117
F3	3	3	8	6	2	6	4	153	179	166
	2	6	11	7	3	6	4	152	232	182
	1	2	4	3	1	2	2	73	224	125
G1	3	3.7	5.3	4.6	1.7	3.5	2.7	122	144	131
	2	2.9	6.2	4.2	1.3	3.4	2.1	111	252	149
	1	1.8	2.4	2.2	0.5	1.1	0.8	94	141	113
G2	2	5.3	7.7	6.7	5.1	8.6	7.1	360	552	454
	1	3.2	5.3	4.3	2.6	4.7	3.8	226	385	324

		Ni (ppm)			Zn (ppm)			Cu (ppm)			Co (ppm)			Cr (ppm)		
	Sections	min	max	avg	min	max	avg	Min	max	avg	min	max	avg	min	max	avg
F1	2	12	32	21	15	26	21	40	56	50	3	12	4.8	37	52	44
	1	25	60	39	19	30	24	52	67	58	2	8	4.9	65	75	70
F2	3	4	16	8	22	37	30	64	79	71	10	17	13	59	129	88
	2	3	32	11	7	27	15	45	64	53	6	12	9	33	64	48
	1	3	25	12	3	21	9	43	61	49	6	10	8	26	37	32
F3	3	19	45	35	18	31	26	9	25	18	5	11	9	47	129	87
	2	26	46	34	18	41	25	10	33	18	5	11	7	47	205	95
	1	13	20	15	6	14	10	3	8	5	1	5	2	12	49	34
G1	3	11	19	15	12	24	18	9	17	14	5	7	6	44	69	54
	2	6	18	12	11	31	20	5	17	9	5	6	5	47	88	64
	1	6	11	8	7	20	13	5	12	8	1	5	3	36	57	41
G2	2	11	61	32	41	70	52	55	105	81	21	33	27	110	153	130
	1	6	86	38	26	45	37	32	54	43	13	20	17	73	122	97

3.1B.1b. Distribution of Ni, Zn, Cu, Co and Cr in the bulk sediments of mudflats

In core F1, trace metal concentration shows 12 – 60 ppm (avg. 27 ppm) Ni, 15 – 30 ppm (avg. 22 ppm) Zn, 40 – 67 ppm (avg. 53 ppm) Cu, 2- 12 ppm (avg. 5 ppm) Co and

37 – 75 ppm (avg. 54 ppm) Cr (Table 3.1.3). Trace metal concentration shows 3 – 32 ppm (avg. 11 ppm) Ni, 3 – 37 ppm (avg. 15 ppm) Zn, 43 – 79 ppm (avg. 55 ppm) Cu, 6-17 ppm (avg. 9 ppm) Co and 26 – 129 ppm (avg. 49 ppm) Cr in core F2. In core F3, trace metal concentration shows 13 – 46 ppm (avg. 24 ppm) Ni, 6 – 41 ppm (avg. 17 ppm) Zn, 3 – 33 ppm (avg. 11 ppm) Cu, 1- 11 ppm (avg. 5 ppm) Co and 12 – 205 ppm (avg. 62 ppm) Cr.

The range and average values for each section is given in table 3.1.4. In core F1, section 1, trace metal concentration showed 25 – 60 ppm (avg. 39 ppm) Ni, 19– 30 ppm (avg. 24 ppm) Zn, 52 – 67 ppm (avg. 58 ppm) Cu, 2- 8 ppm (avg. 4.9 ppm) Co and 65 – 75 ppm (avg. 70 ppm) Cr; section 2 showed, 12 – 32 ppm (avg. 21 ppm) Ni, 15–26 ppm (avg. 21 ppm) Zn, 40 – 56 ppm (avg. 50 ppm) Cu, 3–12 ppm (avg. 5 ppm) Co and 37 – 52 ppm (avg. 44 ppm) Cr. In core F2, section 1, shows 3 – 25 ppm (avg. 12 ppm) Ni, 3 – 21 ppm (avg. 9 ppm) Zn, 43 – 61 ppm (avg. 49 ppm) Cu, 6- 10 ppm (avg. 8 ppm) Co and 26 – 37 ppm (avg. 32 ppm) Cr; section 2 showed, 3 – 32 ppm (avg. 11 ppm) Ni, 7 – 27 ppm (avg. 15 ppm) Zn, 45 – 64 ppm (avg. 53 ppm) Cu, 6- 12 ppm (avg. 9 ppm) Co and 33 – 64 ppm (avg. 48 ppm) Cr and section 3, 4 – 16 ppm (avg. 8 ppm) Ni, 22 – 37 ppm (avg. 30 ppm) Zn, 64 – 79 ppm (avg. 71 ppm) Cu, 10- 17 ppm (avg. 13 ppm) Co and 59 – 129 ppm (avg. 88 ppm) Cr. In core F3, section 1, shows 13 – 20 ppm (avg. 15 ppm) Ni, 6 – 14 ppm (avg. 10 ppm) Zn, 3 – 8 ppm (avg. 5 ppm) Cu, 1- 5 ppm (avg. 2 ppm) Co and 12 – 49 ppm (avg. 34 ppm) Cr; section 2 showed, 26 – 46 ppm (avg. 34 ppm) Ni, 18 – 41 ppm (avg. 25 ppm) Zn, 10 – 33 ppm (avg. 18 ppm) Cu, 5- 11 ppm (avg. 7 ppm) Co and 47 – 205 ppm (avg. 95 ppm) Cr and section 3 showed, 19 – 45 ppm (avg. 35 ppm) Ni, 18 – 31 ppm (avg. 26 ppm) Zn, 9 – 25 ppm (avg. 18 ppm) Cu, 5- 11 ppm (avg. 9 ppm) Co and 47 – 129 ppm (avg. 87 ppm) Cr. Among the trace metals, Cr showed maximum range in variation in core F3 (Table 3.1.3) and in section 2 it was maximum with high mean value (95 ppm) (Table 3.1.4).

In core F1, Ni shows higher values than average in section 1 with a peak at 20 cm depth. Further, it shows a decreasing trend in section 2 (Fig. 3.1.6). Zn, Cu, Co and Cr show similar distribution trend to that of Fe indicating a similar source or remobilization. Cu and Co, however show higher values near surface like Mn. In core F2, Ni shows almost constant value in section 1 with slightly higher values between 38 and 32 cm

depth whereas in section 2 it shows lower values than average line (Fig. 3.1.7). Zn shows an increasing trend in section 1 remains constant in section 2 and shows increasing values in section 3 having a peak value at 10 cm depth similar to Al and Fe. Similar distribution is also noticed by Cu, Co and Cr. It is further noted that Zn, Cu, Co and Cr show similar distribution to that of Al indicating their association with Al and natural source. Further, concentration of metals is also similar to that of Fe especially near surface which indicates precipitation of Fe oxyhydroxides and co-precipitation of metals in the top sections of the core (Selvaraj et al. 2010). In core F3, all trace metals show an increasing trend from section 1 to section 2 and decreasing trend in section 3 (Fig. 3.1.8). They show similar trend to that of Al, Fe and Mn, with peak value at 12 cm depth. Except Cr, all metals also show small peak at 4 cm.

3.1B.1c. Distribution of Al, Fe and Mn in the bulk sediments of mangroves

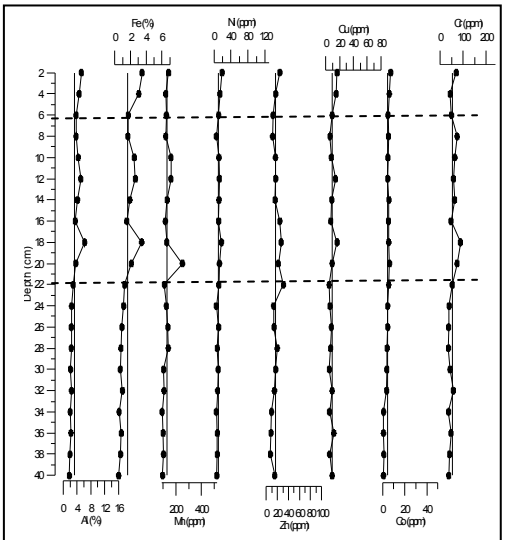

Fig. 3.1.9 Vertical profiles of metals in core G1 (Sharavati estuary – lower middle region)

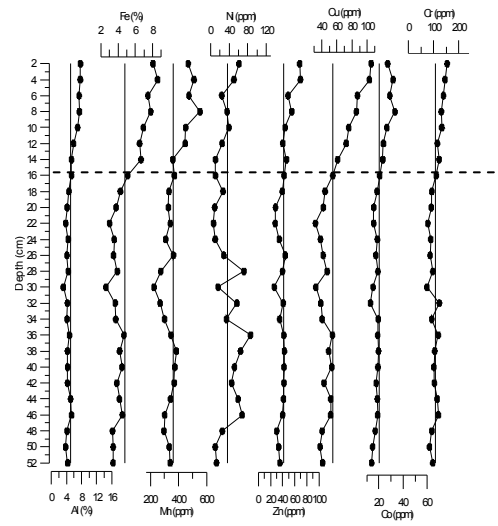

Fig. 3.1.10 Vertical profiles of metals in core G2 (Sharavati estuary – upper middle region)

The geochemical data shows 2 – 6 % (avg. 3.4 %) Al, 1 - 3% (avg. 1.6 %) Fe, 94 - 252 ppm (avg. 130 ppm) Mn in core G1 and 3 – 8 % (avg. 5 %) Al, 3 – 9 % (avg. 5 %) Fe, 226 - 552 ppm (avg. 364 ppm) Mn in core G2 (Table 3.1.3). When the range and average values of Al, Fe and Mn were considered of cores G1 and G2, it was observed that core G2 shows higher range and average value than core G1. The range and average values for each section is given in table 3.1.4. In core G1, section 1,

geochemical data showed1.8 - 2.4 % (avg. 2.2 %) Al, 0.5 – 1.1% (avg. 0.8 %) Fe, 94 - 141 ppm (avg. 113 ppm) Mn; section 2 showed, 2.9 – 6.2 % (avg. 4.2 %) Al, 1.3-3.4 % (avg. 2.1 %) Fe, 111 - 252 ppm (avg. 149 ppm) Mn and; section 3 showed, 3.7 - 5.3 % (avg. 4.6 %) Al, 1.7 – 3.5% (avg. 2.7 %) Fe, 122 - 144 ppm (avg. 131 ppm) Mn. In core G2, section 1, showed, 3.2 - 5.3 % (avg. 4.3 %) Al, 2.6 – 4.7% (avg. 3.8 %) Fe, 226 - 385 ppm (avg. 324 ppm) Mn and; section 2 showed, 5.3 – 7.7% (avg. 6.7 %) Al, 5.1-8.6 % (avg. 7.1 %) Fe, 360 - 552 ppm (avg. 454 ppm) Mn. Al, Fe and Mn showed large variation core G2 (Table 3.1.3) and in section 2 (Table 3.1.4).

In core G1, Al showed an increasing trend from section 1 to 3 with positive peak at 18 cm (prominent) and elevated values at the surface. Similar distribution pattern was also observed for Fe (Fig. 3.1.9). However, Mn showed similar distribution pattern to Al and Fe only in section 1 and 2 but having a prominent peak at 20 cm depth. In section 3 it exhibited constant trend. Peak values of Al and Fe coincides with peaks of clay and organic carbon and peak of Mn coincide with that of silt peak at 20 cm depth. In core G2, Al showed constant trend in section 1 (Fig. 3.1.10). Further, in section 2 it showed increasing trend up to the surface. Fe and Mn showed similar fluctuating distribution profiles with lower values than average line in section 1, whereas in section 2 they showed large increase. They showed higher value at 40 cm which coincides with peak of clay in section 1 and peaks at 8 and 4 cm which largely coincides with silt and organic carbon in section 2.

3.1B.1d. Distribution of Ni, Zn, Cu, Co and Cr in the bulk sediments of mangroves

Trace metal concentration shows 6 – 19 ppm (avg. 11 ppm) Ni, 7 – 31 ppm (avg. 17 ppm) Zn, 5 – 17 ppm (avg. 9 ppm) Cu, 1- 7 ppm (avg. 4 ppm) Co and 36 – 88 ppm (avg. 52 ppm) Cr in core G1 and; 6 – 86 ppm (avg. 36 ppm) Ni, 26 – 70 ppm (avg. 42 ppm) Zn, 32 – 105 ppm (avg. 55 ppm) Cu, 13 - 33 ppm (avg. 20 ppm) Co and 73 – 153 ppm (avg. 107 ppm) Cr in core G2. The range and average of trace metals were higher in core G2 than core G1 (Table 3.1.3). Range and average values for each section is given in table 3.1.4. In core G1, section 1, trace metal concentration showed 6 – 11 ppm (avg. 8 ppm) Ni, 7– 20 ppm (avg. 13 ppm) Zn, 5 – 12 ppm (avg. 8 ppm) Cu, 1- 5 ppm (avg. 3 ppm) Co and 36 – 57 ppm (avg. 41 ppm) Cr; section 2 showed, 6 – 18 ppm (avg. 12 ppm) Ni, 11– 31 ppm (avg. 20 ppm) Zn, 5 – 17 ppm (avg. 9 ppm) Cu, 5- 6

ppm (avg. 5 ppm) Co and 47 – 88 ppm (avg. 64 ppm) Cr and; section 3 showed, 11 – 19 ppm (avg. 15 ppm) Ni, 12 – 24 ppm (avg. 18 ppm) Zn, 9 – 17 ppm (avg. 14 ppm) Cu, 5- 7 ppm (avg. 6 ppm) Co and 44 – 69 ppm (avg. 54 ppm) Cr. In core G2, section 1, shows 6 – 86 ppm (avg. 38 ppm) Ni, 26 – 45 ppm (avg. 37 ppm) Zn, 32 – 54 ppm (avg. 43 ppm) Cu, 13- 20 ppm (avg. 17 ppm) Co and 73 – 122 ppm (avg. 97 ppm) Cr; section 2 showed, 11 – 61 ppm (avg. 32 ppm) Ni, 41 – 70 ppm (avg. 52 ppm) Zn, 55 – 105 ppm (avg. 81 ppm) Cu, 21- 33 ppm (avg. 27 ppm) Co and 110 – 153 ppm (avg. 130 ppm) Cr. Ni and Cr showed large range in variation in core G2 (Table 3.1.3) and among the sections, all trace metals showed variation in section 2 of core G2 (Cr maximum variation) except Ni which highly varied in section 1 (Table 3.1.4).

In core G1, all trace metals show similar distribution trend in section 1 which is almost constant along the average line, probably originating from the same source (Fig. 3.1.9). In section 2, Ni, Zn Cu and Cr show small peak at 18 cm which coincide with peaks of Al and Fe. Cu shows a peak at 12 cm which coincide with peaks of Al, Fe and Mn as well. In section 3, however they show slight increase similar trend to that of Al and Fe. In core G2, Ni and Cu show largely similar distribution trend to that of Fe and Mn indicating a diagenetic remobilization and enrichment towards surface (Fig. 3.1.10). However, Zn, Co and Cr show similar trend to that of Al indicating their association and lithogenous source.

Sand is the major sediment components in all the five cores studied. Sand content in an area generally reflects high hydrodynamic energy condition due to its size and settling velocity. In core F1 (lower estuary), collected at the northern part of mouth of Sharavati estuary, sand showed higher than average values in section 1 as compared to core F2 (lower estuary) which was collected from the southern part of the mouth. Sand showed decreasing trend in core F2 (lower estuary) and F3 (middle estuary) from section 1 to 2, however, higher sand content was noted in section 3 at the surface of core F3. Among the mangrove cores, in core G1 (lower middle estuary), sand showed constant value with more than average line in section 1, fluctuating along the average line in section 2, and lower values in section 3. In core G2 (upper middle estuary), sand showed constant trend in section 1 and decreasing trend in section 2. When the average sand content in mudflat and mangrove cores were compared, higher sand

content was noted in mangrove core G1 with 83 % followed by F1 (80 %) > F2 (78 %) > F3 (76 %) > G2 (58 %). In general, mangroves environment is known to retain finer sediments as compared to the mudflats, however, higher sand content in core G1 could be due to the coarser material brought by the adjoining tributary. Sand content in mudflat cores F1, F2 and F3 reflects decrease in hydrodynamic energy conditions from lower estuary to middle estuary. Higher mud (silt and clay) content in cores G2 and F3 reflects processes like coagulation and flocculation of sediments which facilitate the deposition of finer sediments in the middle estuarine region due to the mixing of fresh water and saline water. Organic carbon profiles of all the cores showed similar distribution trend to that of the finer sediments indicating its association. Among the mudflat cores, higher average value was found in core F3, collected at the middle estuarine region, favoring its deposition. Organic carbon was found to be increasing from bottom to surface in cores F2 and F3 whereas in core F1, it showed decreasing trend. Among the mangrove cores, higher average organic carbon was noted in core G2 collected at upper middle estuarine region as compared to core G1. In core G1, it showed constant trend in section 1 and 2 and higher values at the surface, whereas, in core G2, it showed constant trend in section 1 and increasing trend in section 2.

Higher sand percentage in section 1 of cores F2, F3, G1 and G2 suggest that sediments in the past were probably deposited in the high hydrodynamic energy conditions. Decrease in the sand percentage from 14 cm could be due reduced supply of coarser material due to the activities within the catchment area like building dams, change in rainfall pattern and runoff, and sea level changes (Singh et al. 2013a) bringing a change in sedimentation pattern. The Linganmakki and Gersoppa dams built in the upstream of Sharavati estuary must have contributed significantly in the reduction of sand content. Dredging activities within the lower reaches must have also contributed for the distribution of sediment components (Huaiyang et al. 2004) as it amounts the resuspension and settling of finer sediments. Increase of clay percentage in the top section of these cores probably reflects a calmer hydrodynamic energy condition during their deposition (Dolch and Hass 2008). The depth wise distribution pattern suggests the prevalence of relatively high hydrodynamic energy conditions facilitating greater deposition of coarser sediments in the past. Finer sediments towards the surface must have been deposited in calmer hydrodynamic energy condition in the

recent year. However, in case of core F1, it is noted that sand percentage is higher in section 2 and mud fraction is higher in section 1. Besides the hydrodynamic condition, sediment source also play an important role in the distribution of grain size (Yang et al. 2008). The high sand percentage, almost 80 % throughout this core could be due tidal energy flushing the finer sediment component leaving behind the coarser ones. The source of sediment for this core could be also from Badagani River which flows from north to south and a part of it must be entering the Sharavati estuary. It is also observed that the average sand content decreases in core collected from lower estuary (core F1) to lower middle estuary (core F3) which is probably due to decreasing wave action towards the upstream of the estuary facilitating deposition of finer sediment. Compared to all the cores collected, mangrove core G2 showed higher mud content (42 %). This core was collected in the interior region, which generally provides quiet hydrodynamic energy condition thereby, allowing the deposition of finer sediment components. It is well understood that mangroves are known to retain relatively higher finer sediments (Zhou et al. 2010).

Organic carbon profile in all the cores (mudflat and mangrove) shows a similar trend to that of silt and clay though; in core G2 it shows association only with silt. It is well established that organic carbon is generally associated with the finer sediments as compared to the coarser sediments (Dessai et al. 2009) which is mainly due to surface area/ volume ratio of the sediment grain (Muzuka and Shaghude 2000). The decline in the organic carbon with depth in cores F2, F3, G1 and G2 can be attributed to its degradation. In sandy marine sediments, oxygenated water can easily percolate through the coarser sediments leading to high rate of degradation as compared to the finer sediments (Singh and Nayak 2009). Higher values of organic carbon in the upper sections of these cores indicate enhanced supply of organic material from the overlying water column or these organic matter are yet to undergo degradation. In mangrove core G2, highest percentage of organic carbon is noted (2%) as compared to other cores. This is probably due to additional organic matter supplied from the surrounding mangrove litter (Clough et al 2000; Alongi, 1998).

The distribution of Al is largely governed by the distribution of finer sediments throughout the cores as Al is largely associated with Aluminosilicates. When the

distribution of metals were compared among the cores collected in different regions and different sub-environments, it was noted that, in core F1, Al along with Fe and Mn oxides played important role in distribution of studied trace metals viz. Zn, Cu, Cr, Co and Ni along with finer sediments and organic carbon. Mn, Co and to some extent Cu showed higher value at the surface indicating that Mn must have influenced the distribution of Co and Cu at the surface. However, Al, Fe and organic carbon showed lower values at the surface along with trace metals Ni, Zn and Cr indicating the role played by Al, Fe and organic carbon in their distribution at the surface. Similar distribution of Fe and Mn with Al indicate their common terrigenous source. In core F2, Al and Fe oxides seem to be controlling the distribution of Zn, Cu and Cr in section 1, Mn shows some similarity to the distribution of Co and Ni in section 1. In section 2 and 3, Al along with Fe oxides plays a major role in the distribution of all the trace metals except Ni in section 3. Metals also show similar distribution trend to that of finer sediments and organic carbon, thereby indicating their association and role played by finer sediments and organic carbon. In core F3, Al, Fe and Mn along with finer sediments and organic carbon largely controls the distribution of all trace metals in section 1 and 2. However in section 3, only Al and Fe along with finer sediments and organic carbon seem to be the controlling factor for Ni, Zn, Cu and Co whereas Mn seems to be controlling factor for Cr. Among the mangrove cores, in core G1, Al, Fe-Mn oxides, silt, organic carbon and to some extent clay govern the distribution of trace metals in section 1 and section 2. In section 3, Al, Fe oxides along with finer sediments and organic carbon control the distribution of Zn, Cu and Cr. Ni and Co show similar trend to that of Mn. In core G2, Al seems to control the distribution of Zn, Co and Cr whereas Fe-Mn oxides seem to control the distribution of Ni and Cu throughout the cores.

Fe and Mn show largely similar distribution pattern in core G2 and section 1 and 2 of core F3, indicating similar source and/or show similar early digenetic mobilization. The redox sensitive elements, Fe and Mn have been widely used to understand the diagenetic processes (Caetano et al. 2009). Normally, Fe^{2+} and Mn^{2+} species get precipitated in the top layers of sediment after being removed through the pore water of subsurface sediments (Klinkhammer et al. 1982) as observed at 10 cm depth in section 3 of core F2; at 12 and 4 cm of core F3; at 10 and 12 cm in in core G1 and in section 2

of core G2. Enrichment of Fe and Mn in top layers indicates the precipitation of these redox sensitive elements as oxides and hydroxides, and the low Fe and Mn content in the bottom layers reflect their dissolution (Pande and Nayak 2013) and possible migration.

In case of core F1, however, higher concentration of Al and Fe at deeper layer and their association to finer sediments was explained through the supply by Badagani River, as stated earlier. It is noted that the distribution pattern of all studied trace metals except Co in core F1, Ni in core F2 and Cr in core F3 largely follows the distribution pattern of Al and Fe indicating similar source and post diagenetic processes. The exceptions viz. Co in core F1, Ni in core F2 and Cr in core F3, especially near surface follow the trend of Mn. When the Fe (II) and Mn (II) cations which are produced due to bacterial reduction of Fe and Mn in the bottom sediments diffuse and migrate upwards and precipitate under oxic conditions, scavenge other trace metals from pore water (Volvoikar and Nayak 2013). Brown colour noted in the upper portion (Table 2.1) of core F1, F2, F3 and G2, is mainly due to the formation of red/brown Mn (IV) and Fe (III) oxyhydroxides in an upper oxidised zone and of reduced black/grey Fe (II) sulphides in a deeper reducing zone (Thomson et al. 2002). While the presence of distinct Fe and Mn peaks in core G2 at 28 and 26 cm respectively must be the result of their variation in oxidation levels. Higher stability of Fe oxyhydroxides under mildly reducing conditions and faster oxidation kinetics of Fe^{2+} compared to Mn^{2+} leads to diagenetic enrichment of Fe at greater depth as compared to Mn (Zwolsman et al. 1993). Enrichment of metals towards the surface in cores F2, F3, G1 and G2 indicated either additional input received during recent years or diagenetic remobilization. The protected area of core G2 must have facilitated the accretion of sediments under relatively less violent hydrodynamic energy conditions thereby recording the changes in metal input from past to present. Decrease in fresh water inflow over a period of time is known to be one of the factors which may contribute to the gradual accumulation of metals along with finer sediments within the estuary (Ruiz and Saiz-Salinas 2000). The metal input could also be from other sources like agriculture, domestic waste, industrial effluents etc.

3.1C. Ia. Pearson's correlation for parameters of bulk sediments in mudflats

In order to understand the elemental association, correlation tests were carried out for the data set of F1, F2 and F3 (Table 3.1.5 a, b, c). Analysis of correlation coefficient among the different chemical components for core F1 shows a significant positive correlation of Al with clay, organic carbon, Fe along with trace metals Cu and Cr. In core F2 and F3, Al showed a significant correlation with finer sediments, organic carbon, Fe and Mn along with all trace metals (except Ni in core F2). In core F1, Fe showed significant positive correlation with finer sediments, organic carbon and trace metals (except Co). In core F2 and F3, Fe and Mn showed a significant positive correlation with finer sediments, organic carbon and trace metals (except Ni in core F2). A significant negative correlation of sand with all other parameters was observed in all three cores.

Al indicates terrigenous input and is the major component in the clay lattice. Al exhibited significant positive correlation with clay indicating its natural source. The association of Al with fine grained sediments in cores F1, F2 and F3 suggests that the sediments include detrital minerals dominated by phyllosilicates (Jonathan et al. 2004). Also, most metals show positive correlation with fine grained sediments in core F1 (except Mn and Co), F2 (except Ni)and F3 as they have greater affinity for adsorption of metals due to their large surface area as compared to the coarser grained sediment fraction (Mikulic et al. 2008). The strong correlation between these elements and organic carbon reveals an association in the form of organo-metallic complexes (Zourarah et al. 2009). A significant correlation of trace metals with Fe and Mn in core F3 suggests that the distribution of trace metals was largely controlled Fe and Mn cycle which is also reflected by brown colour in the top portion as mentioned earlier. In core F1, Mn and Co show weak correlation with finer sediments, organic carbon and also with Al, Fe indicating their input from different source. Core F1 collected from lower estuary receives input from river Badagani River flowing from north direction and joining Sharavati River at its mouth region, can be source for these metals which may be anthropogenic source like agriculture, municipal wastewater discharges, sewage sludge.

3.1C. Ib. Pearson’s correlation for parameters of bulk sediments in mangroves

In core G1 (Table 3.1.6a) and G2 (Table 3.1.6b), Al showed significant positive correlation with finer sediments, organic carbon and Fe along with all the trace metals (except Ni in core G2). Further, in core G1, Fe cycling seems to play a major role in the trace metal distribution whereas Mn is associated with Co and Cr only. Therefore, the major controlling factors for the distribution of metals in mangrove core G1 are Al, Fe along with finer sediment components and organic carbon. In core G2, along with fine sediments, organic carbon, Al and Fe, Mn also played a role in distribution of trace elements. Ni in core G2 must be from different source.

Table 3.1.5 Pearson's correlation between sand, silt, clay, organic carbon (OC) and metals of: (a) core F1, (b) core F2 and (c) core F3

F1	Sand	Silt	Clay	OC	Al	Fe	Mn	Ni	Zn	Cu	Co	Cr
Sand	1.00											
Silt	-0.86	1.00										
Clay	-0.94	**0.64**	1.00									
OC	-0.92	**0.68**	**0.95**	1.00								
Al	-0.62	0.47	**0.63**	**0.69**	1.00							
Fe	-0.89	**0.60**	**0.95**	**0.94**	**0.69**	1.00						
Mn	0.20	-0.22	-0.16	0.02	0.39	-0.02	1.00					
Ni	-0.51	0.13	**0.69**	**0.63**	0.33	**0.72**	-0.27	1.00				
Zn	-0.48	0.17	**0.61**	**0.63**	0.17	**0.62**	0.05	0.47	1.00			
Cu	-0.66	0.40	**0.73**	**0.76**	**0.65**	**0.85**	0.19	**0.63**	**0.65**	1.00		
Co	-0.23	0.14	0.25	0.38	0.40	0.23	0.46	-0.01	0.34	0.15	1.00	
Cr	-0.81	**0.56**	**0.86**	**0.77**	**0.55**	**0.87**	-0.40	**0.82**	0.40	**0.70**	0.01	1.00

(a)

F2	Sand	Silt	Clay	OC	Al	Fe	Mn	Ni	Zn	Cu	Co	Cr
Sand	1.00											
Silt	-0.85	1.00										
Clay	-0.84	**0.43**	1.00									
OC	-0.72	**0.51**	**0.70**	1.00								
Al	-0.79	**0.54**	**0.80**	**0.92**	1.00							
Fe	-0.79	**0.64**	**0.69**	**0.89**	**0.96**	1.00						
Mn	-0.60	**0.61**	**0.40**	**0.55**	**0.52**	**0.57**	1.00					
Ni	-0.04	-0.04	0.11	-0.07	0.01	0.00	0.12	1.00				
Zn	-0.67	**0.51**	**0.63**	**0.69**	**0.82**	**0.79**	**0.49**	0.04	1.00			
Cu	-0.84	**0.64**	**0.78**	**0.81**	**0.86**	**0.86**	**0.67**	0.02	**0.76**	1.00		
Co	-0.70	**0.55**	**0.63**	**0.77**	**0.87**	**0.89**	**0.60**	0.08	**0.82**	**0.80**	1.00	
Cr	-0.78	**0.59**	**0.74**	**0.89**	**0.94**	**0.97**	**0.52**	-0.01	**0.76**	**0.90**	**0.86**	1.00

(b)

F3	Sand	Silt	Clay	OC	Al	Fe	Mn	Ni	Zn	Cu	Co	Cr
Sand	1.00											

Silt	-0.97	1.00										
Clay	-0.96	**0.86**	1.00									
OC	-0.95	**0.93**	**0.90**	1.00								
Al	-0.87	**0.77**	**0.92**	**0.86**	1.00							
Fe	-0.99	**0.95**	**0.95**	**0.97**	**0.91**	1.00						
Mn	-0.56	**0.47**	**0.62**	**0.69**	**0.65**	**0.62**	1.00					
Ni	-0.98	**0.91**	**0.97**	**0.94**	**0.94**	**0.99**	**0.63**	1.00				
Zn	-0.92	**0.86**	**0.92**	**0.92**	**0.93**	**0.96**	**0.67**	**0.95**	1.00			
Cu	-0.92	**0.87**	**0.91**	**0.90**	**0.93**	**0.95**	**0.56**	**0.94**	**0.95**	1.00		
Co	-0.93	**0.92**	**0.88**	**0.94**	**0.81**	**0.94**	**0.66**	**0.92**	**0.90**	**0.86**	1.00	
Cr	-0.82	**0.73**	**0.85**	**0.81**	**0.88**	**0.86**	**0.60**	**0.85**	**0.92**	**0.90**	**0.77**	1.00

(c)

Table 3.1.6 Pearson's correlation between sand, silt, clay, organic carbon (OC) and metals of: a) G1 and b) G2

G1	Sand	Silt	Clay	OC	Al	Fe	Mn	Ni	Zn	Cu	Co	Cr
Sand	1.00											
Silt	**-0.78**	1.00										
Clay	**-0.92**	**0.47**	1.00									
OC	**-0.72**	**0.47**	**0.72**	1.00								
Al	**-0.77**	**0.72**	**0.63**	**0.59**	1.00							
Fe	**-0.81**	**0.73**	**0.68**	**0.72**	**0.97**	1.00						
Mn	-0.44	**0.69**	0.18	0.19	0.41	**0.45**	1.00					
Ni	**-0.79**	**0.69**	**0.67**	**0.61**	**0.82**	**0.86**	0.41	1.00				
Zn	-0.43	**0.47**	0.31	0.23	**0.49**	**0.48**	0.30	**0.65**	1.00			
Cu	**-0.59**	**0.50**	**0.51**	**0.61**	**0.75**	**0.79**	0.22	**0.76**	0.27	1.00		
Co	**-0.75**	**0.69**	**0.62**	**0.53**	**0.72**	**0.73**	**0.55**	**0.69**	**0.66**	0.35	1.00	
Cr	**-0.59**	**0.60**	**0.46**	0.40	**0.78**	**0.73**	**0.48**	**0.61**	0.43	**0.48**	**0.58**	1.00

(a)

G2	Sand	Silt	Clay	OC	Al	Fe	Mn	Ni	Zn	Cu	Co	Cr
Sand	1.00											
Silt	**-0.95**	1.00										
Clay	**-0.42**	0.13	1.00									
OC	**-0.95**	**0.91**	**0.39**	1.00								
Al	**-0.97**	**0.92**	**0.42**	**0.95**	1.00							
Fe	**-0.98**	**0.92**	**0.43**	**0.96**	**0.96**	1.00						
Mn	**-0.88**	**0.83**	**0.41**	**0.86**	**0.87**	**0.88**	1.00					
Ni	-0.21	0.09	**0.43**	0.12	0.21	0.17	0.07	1.00				
Zn	**-0.82**	**0.70**	**0.57**	**0.83**	**0.84**	**0.86**	**0.77**	**0.42**	1.00			
Cu	**-0.96**	**0.88**	**0.52**	**0.97**	**0.97**	**0.97**	**0.87**	0.27	**0.89**	1.00		
Co	**-0.94**	**0.90**	0.38	**0.91**	**0.93**	**0.94**	**0.88**	0.16	**0.80**	**0.92**	1.00	
Cr	**-0.89**	**0.81**	**0.48**	**0.84**	**0.91**	**0.89**	**0.72**	**0.45**	**0.86**	**0.90**	**0.78**	1.00

(b)

3.1D. Isocon

3.1D.1a. Isocon plot for mudflat cores

Further, an isocon plot was used to compare the distribution and concentration of sediment components, organic carbon and studied metals within two regions. Isocon plots allow an easy visual comparison of the average composition of each parameter (Grant 1986; Rosales-Hoz et al. 2003). The plot between core F1 and core F2 (Fig. 3.1.11a) indicated, Mn and Ni are higher in core F1 whereas Co is higher in core F2. The results between core F2 and F3 (Fig. 3.1.11b) indicated Al, Fe, Mn, organic carbon along with trace metals Ni and Cr were higher in core F3 suggesting the role of Fe and Mn oxides along with organic carbon coating, in the distribution of Ni and Cr. The plot between core F1 and F3 (Fig. 3.1.11c) indicated the values of Mn, Ni, Cu and Zn are higher towards core F1 whereas Al, Fe, finer sediments along with organic carbon are higher in core F3. This indicates higher concentration of Mn and Ni in core F1 of different source and other trace metals along with Al and Fe are received from detrital source at core F2 and core F3.

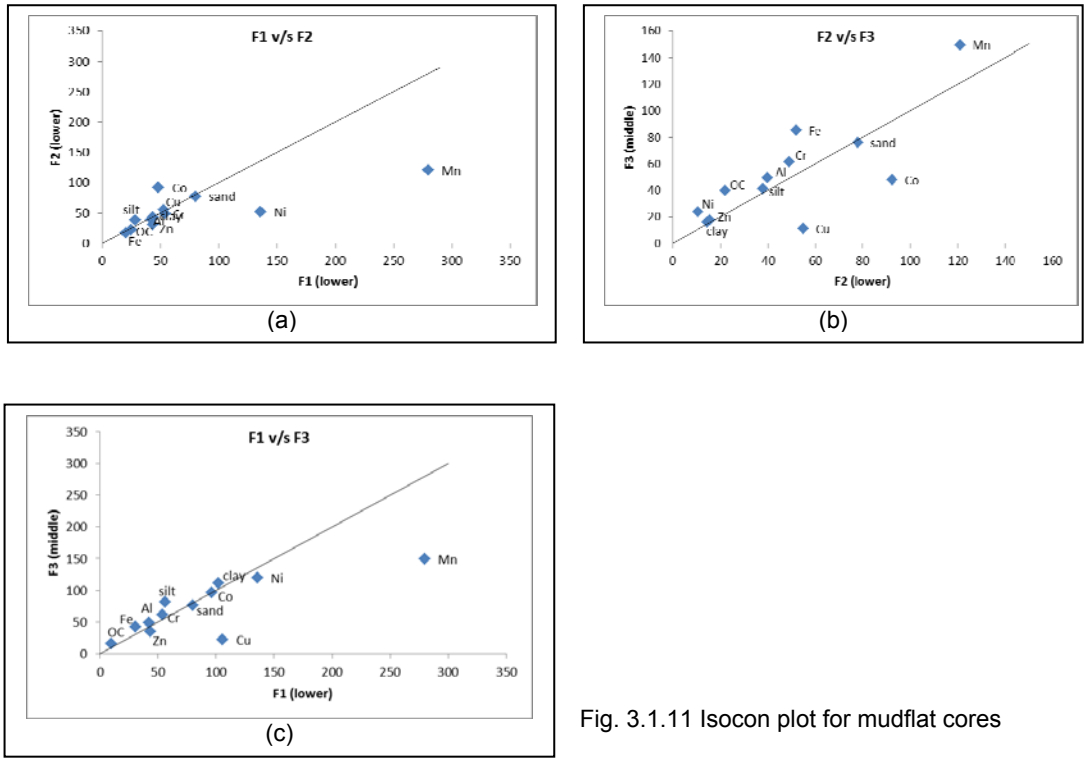

Fig. 3.1.11 Isocon plot for mudflat cores

3.1D 1b Isocon plot for mangrove cores

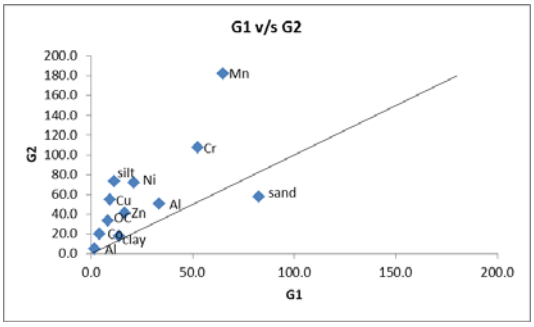

Fig. 3.1.12 Isocon plot for mangrove cores

The plot between core G1 and G2 (Fig. 3.1.12) indicated the values of Al, Fe, Mn, finer sediments, organic carbon along with trace metals Ni, Zn, Cu, Co and Cr are higher in core G2 whereas sand is higher in core G1 indicating a dynamic environment towards core G1 and a calmer environment towards core G2, facilitating the deposition of finer sediments along with metals. Besides wave induced high energy hydrodynamics, there is also a small channel that joins at core G1 which could be a possible source for sand to this location.

3.1E Enrichment Factor (EF) and Pollution Load Index (PLI)

Table 3.1.7 Enrichment Factor (EF) and Pollution Load Index (PLI)

core	Fe (EF)	Mn (EF)	Ni (EF)	Zn (EF)	Cu (EF)	Co (EF)	Cr (EF)	PLI
F1	0.9	0.7	1.1	0.5	2.5	0.5	1.2	0.4
F2	0.8	0.3	0.5	0.3	2.9	1.1	1.2	0.3
F3	1.0	0.3	0.8	0.3	0.4	0.4	1.1	0.3
G1	0.8	0.4	0.6	0.5	0.6	0.6	1.6	0.2
G2	1.7	0.8	1.3	0.8	2.1	1.9	2.1	0.8

Further, Enrichment Factor and Pollution Load Index were compared to understand metal loading in Sharavati estuary. Among the mudflat cores, (Table 3.1.7) it is noticed that there is minor enrichment of Ni, Cu and Cr in core F1; Cu, Co and Cr in core F2 and; Fe and Cr in core F3. In case of mangrove cores, there is minor enrichment of Cr in core G1, whereas in core G2, all metals are enriched except Mn. However, from the PLI results, it is observed that there is no high metal loading at any of the core locations collected in Sharavati estuary. But the value for core G2 is relatively higher.

3.2 Section II

This section includes five small estuaries from north to south in the study area, which are named as Chakra Nadi and Haladi River which flows into Arabian Sea through a common mouth, similarly, Sita Nadi and Swarna Nadi have a common mouth, River Udyavara, River Pavanje and River Gurpur.

3.2 A. Sediment components and organic carbon

3.2 A. 1a Mudflats

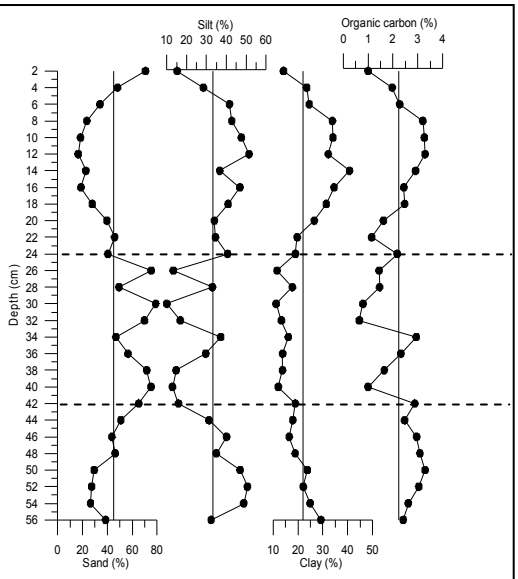

Fig. 3.2.1 Vertical profiles of sediment components and organic carbon in core F4 (Swarna estuary – upper middle)

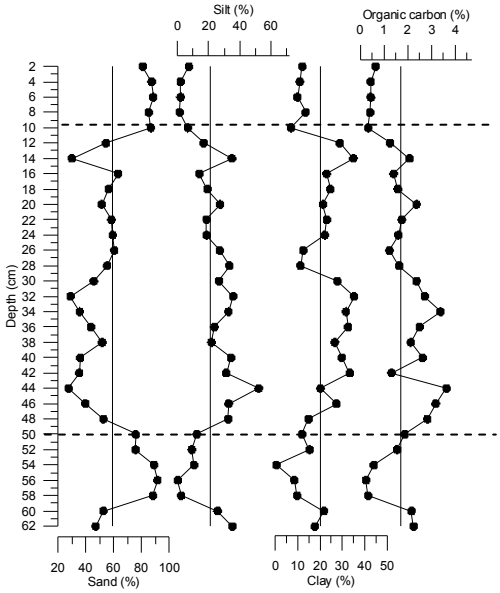

Fig. 3.2.2 Vertical profiles of sediment components and organic carbon in core F5 (Udyavara estuary – upper middle)

In core F4 (Table 3.2.1) sand content varies from 16 – 79 % (avg. 45 %), whereas silt and clay content vary from 10 – 51 % (avg. 33 %) and 11 – 41 % (avg. 22%) respectively. Organic carbon varies from 0.65 – 3.3 % (avg. 2.2%). In core F5 sand content varies from 28 to 92 % whereas silt and clay content vary from 0.02 to 52 % and 0.44 to 35 % respectively with mean values for sand, 59 %; silt, 21 % and clay, 20 %. Organic carbon content varies from 0.23 to 3.6 % with its mean value 1.7 %. In core F6 sand varies from 7 to 80 % whereas silt, clay and organic carbon vary from 6 to 71 %, 11 to 52 % and 0.79 to 4.2 % respectively with mean values of sand, 38 %; silt, 34 %; clay, 29 % and organic carbon, 2.36 %. In core F7 sand varies from 49 – 90 % (avg. 77 %), whereas silt and clay content vary from 3 – 26 % (avg. 8 %) and 7 – 35 % (avg. 15 %) respectively. Organic carbon ranges from 0.37 – 1.2 % (avg. 0.6 %). In core F8

sand varies from 74 – 93 % (avg. 87 %), whereas silt and clay content vary from 0.003 – 12 % (avg. 3 %) and 2 – 16 % (avg. 10 %) respectively. Organic carbon ranges from 0.09 – 0.73 % (avg. 0.31 %). Among the five cores collected from mudflat environment F7 is from lower middle and other four are from upper middle region. Between lower middle and upper middle mudflats within Gurpur estuary, sand content is slightly less in lower middle estuary.

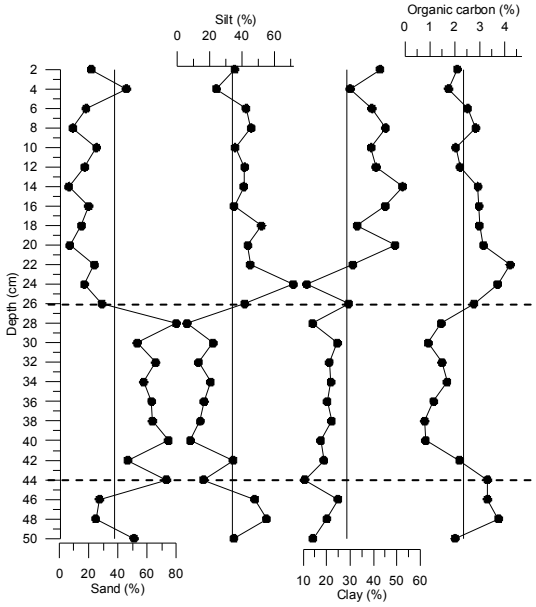

Fig. 3.2.3 Vertical profiles of sediment components and organic carbon in core F6 (Pavanje estuary – upper middle

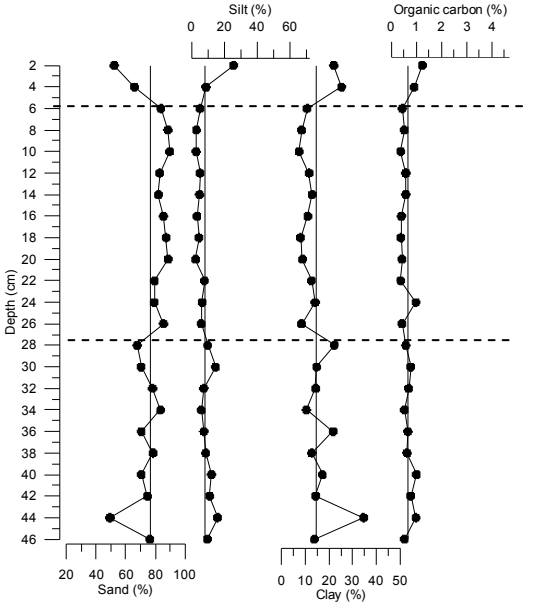

Fig. 3.2.4 Vertical profiles of sediment components and organic carbon in core F7 (Gurpur estuary – lower middle)

On the basis of the distribution of sediment components each core is divided into three sections. In core F4, section 1 is from 56 to 42 cm, section 2 (42 – 24 cm) and section 3 (24 – 0 cm). Core F5 is divided as; section 1 (62-50 cm), section 2 (50-10 cm), section 3 (10-0cm). Core F6 is divided as; section 1(50-44 cm), section 2 (44-26 cm), section 3 (26-0 cm). Core F7 is divided as; section 1 (46-2 cm), section 2 (26-6 cm), section 3 (6-0 cm) and core F8 is divided as; section 1 (34-22 cm), section 2 (22-18 cm), section 3 (18-0 cm). The range and average for each section is provided in table 3.2.2. In core F4 (Table 3.2.2), section 1, sand content varies from 26 to 51 % whereas silt and clay content vary from 31 to 51 % and 16 to 29 % respectively with mean values for sand, 37 %; silt, 41 % and clay, 22 %. Organic carbon content varies from 2.4 to 3.3 % with its mean value 2.8 %. In section 2, sand content varies from 47 to 79 % whereas silt

and clay content vary from 10 to 37 % and 11 to 19 % respectively with mean values for sand, 65 %; silt, 20 % and clay, 14 %. Organic carbon content varies from

Table 3.2.1 Range and average values of sand, silt, clay and organic carbon (OC) in mudflats and mangroves

Core	Sand			Silt			Clay			OC		
	Min	Max	Avg	Min	Max	Avg	Min	Max	Avg	Min	Max	Avg
F4	16	79	45	10	51	33	11	41	22	0.65	3.3	2.2
F5	28	92	59	0.02	52	21	0.44	35	20	0.23	3.6	1.7
F6	7	80	38	6	71	34	11	52	29	0.79	4.2	2.36
F7	49	90	77	3	26	8	7	35	15	0.37	1.2	0.6
F8	74	93	87	0.003	12	3	2	16	10	0.09	0.73	0.31
G3	51	87	79	11	40	19	0.04	9	1.88	0.2	1.55	0.54
G4	8	64	34	14	43	31	22	49	35	0.32	3.32	1.6
G5	5	71	41	9	40	24	20	57	36	0.85	3	2
G6	52	89	67	2	18	10	9	33	23	0.46	3.54	1.26

0.6 to 2.9 % with its mean value 1.7 %. In section 3, sand, silt and clay vary from 16 to 71 %, 15 to 51 % and 14 to 41 %, respectively with mean values for sand 34 %; silt, 38 %; and clay, 28 %. Organic carbon varies from 1 to 3.3 % with its mean value 2.3 %. In core F5, section 1, sand content varies from 47 to 92 % whereas silt and clay content vary from 0.02 to 35 % and 0.44 to 22 % respectively with mean values for sand, 74 %; silt, 14 % and clay, 12 %. Organic carbon content varies from 0.2 to 2.2 % with its mean value 1.3 %. In section 2, sand content varies from 28 to 63 % whereas silt and clay content vary from 14 to 52 % and 11 to 35 % respectively with mean values for sand, 47 %; silt, 28 % and clay, 25 %. Organic carbon content varies from 1.2 to 3.6 % with its mean value 2.2 %. In section 3, sand, silt and clay vary from 81 to 88 %, 1.37 to 7.20 % and 6.99 to 13.48 %, respectively with mean values for sand 86 %; silt, 3.74 %; and clay, 10.65 %. Organic carbon varies from 0.3 to 0.6 % with its mean value 0.4 %. In core F6, section 1, sand content varies from 25 to 51 % whereas silt and clay content vary from 35 to 55 % and 14 to 25 % respectively with mean values for sand, 35 %; silt, 46 % and clay, 20 %. Organic carbon content varies from 2 to 3.8 % with its mean value 3 %. In section 2, sand content varies from 47 to 80 % whereas silt and clay content vary from 6 to 34 % and 11 to 25 % respectively with mean values for sand, 64 %; silt, 17 % and clay, 19 %. Organic carbon content varies from 0.8 to 3.3 % with its mean value 1.5 %. In section 3, sand, silt and clay vary from 7 to 46 %, 24.1 to 71.4 % and 11.5 to 52.4 %, respectively with mean values for sand 20 %; silt, 42.6 %; and clay,

37.6 %. Organic carbon varies from 1.7 to 4.2 % with its mean value 2.8 %. In core F7, section 1, sand content varies from 49 to 84 % whereas silt and clay content vary from 6 to 16 % and 10 to 35 % respectively with mean values for sand, 72 %; silt, 10 % and clay, 18 %. Organic carbon content varies from 0.5 to 1 % with its mean value 0.7 %. In section 2, sand content varies from 79 to 90 % whereas silt and clay content vary from 3 to 8 % and 7 to 14 % respectively with mean values for sand, 85 %; silt, 5 % and clay, 10 %. Organic carbon content varies from 0.4 to 1 % with its mean value 0.5 %. In section 3, sand, silt and clay vary from 52 to 66 %, 9 to 26 % and 22 to 25 %, respectively with mean values for sand 59 %; silt, 17 %; and clay, 24 %. Organic carbon varies from 0.9 to 1.2 % with its mean value 1.1 %. In core F8, in section 1, sand content varies from 84 to 90 % whereas silt and clay content vary from 0.003 to

Table 3.2.2 Range and average values of sections of sand, silt, clay and organic carbon (OC) in mudflats and mangroves

Core	section	Sand			Silt			Clay			OC		
		min	max	avg	min	max	Avg	min	max	avg	min	max	avg
F4	3	16	71	34	15	51	38	14	41	28	1.0	3.3	2.3
	2	47	79	65	10	37	20	11	19	14	0.6	2.9	1.7
	1	26	51	37	31	51	41	16	29	22	2.4	3.3	2.8
F5	3	81	88	86	1.37	7.20	3.74	6.99	13.48	10.65	0.3	0.6	0.4
	2	28	63	47	14	52	28	11	35	25	1.2	3.6	2.2
	1	47	92	74	0.02	35	14	0.44	22	12	0.2	2.2	1.3
F6	3	7	46	20	24.1	71.4	42.6	11.5	52.4	37.6	1.7	4.2	2.8
	2	47	80	64	6	34	17	11	25	19	0.8	3.3	1.5
	1	25	51	35	35	55	46	14	25	20	2.0	3.8	3.0
F7	3	52	66	59	9	26	17	22	25	24	0.9	1.2	1.1
	2	79	90	85	3	8	5	7	14	10	0.4	1.0	0.5
	1	49	84	72	6	16	10	10	35	18	0.5	1.0	0.7
F8	3	85	93	90	0.02	2.2	0.8	6.9	13.2	9.3	0.1	0.7	0.2
	2	74	76	75	9.7	10.4	10.1	14.4	16.0	15.2	0.64	0.73	0.68
	1	84	90	87	0.003	12.1	3.3	1.9	12.8	9.9	0.21	0.32	0.27
G3	2	51	75	64	23.5	40.1	31.5	1.3	8.6	4.3	0.8	1.6	1.2
	1	71	87	82	11.0	28.4	16.3	0.04	3.6	1.3	0.2	0.7	0.4
G4	3	8	31	20	29.9	42.8	36.1	38.2	49.4	44.0	2.5	3.0	2.7
	2	21	51	35	22.2	41.8	30.9	26.0	43.3	34.3	0.3	3.3	1.5
	1	33	64	44	13.5	30.3	25.2	22.4	37.1	30.6	0.6	1.3	1.0
G5	2	5	34	22	27.5	39.6	31.8	38.2	56.6	45.8	2.2	3.1	2.7
	1	42	71	59	9.2	24.5	16.1	19.8	33.6	25.2	0.9	2.1	1.4
G6	2	52	66	58	10.4	17.6	13.9	23.8	32.6	27.8	1.0	3.5	1.9
	1	60	89	75	2.3	13.5	6.8	8.6	26.9	18.2	0.5	1.2	0.7

12.1 % and 1.9 to 12.8 % respectively with mean values for sand, 87 %; silt, 3.3 % and clay, 9.9 %. Organic carbon content varies from 0.21 to 0.32 % with its mean value 0.27 %. In section 2, sand content varies from 74 to 76 % whereas silt and clay content vary from 9.7 to 10.4 % and 14.4 to 16 % respectively with mean values for sand, 75 %; silt, 10.1 % and clay, 15.2 %. Organic carbon content varies from 0.64 to 0.73 % with its mean value 0.68 %. In section 3, sand, silt and clay vary from 85 to 93 %, 0.02 to 2.2 % and 6.9 to 13.2 %, respectively with mean values for sand 90 %; silt, 0.8 %; and clay, 9.3 %. Organic carbon varies from 0.1 to 0.7 % with its mean value 0.2 %.

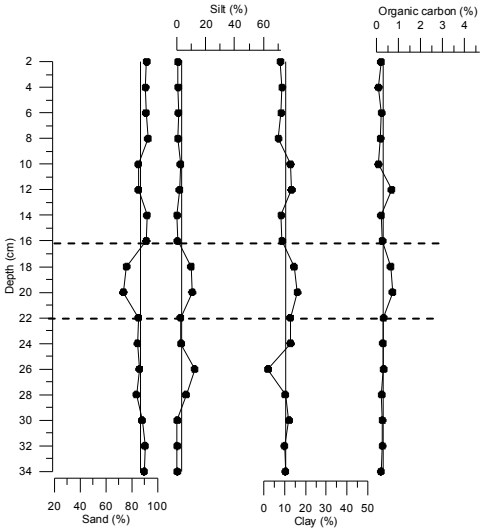

Fig. 3.2.5 Vertical profiles of sediment components and organic carbon in core F8 (Gurpur estuary – upper middle)

In core F4 (Fig. 3.2.1) sand profile shows an increasing trend from the bottom of core up to 40 cm and further, large fluctuation is observed in section 2. In section 3, sand concentration values maintain below the average line but increases towards surface after a decrease up to 12 cm. It is also noted that sand profile is largely compensated by silt and clay profiles throughout the core. Organic carbon profile shows a similar trend to that of silt and clay profiles. In core F5 (Fig. 3.2.2), sand content shows a sudden increase from 60 to 58 cm which further maintains a constant value up to 54 cm and later shows a decreasing trend up to 44 cm. Further, it shows an increasing trend up to the surface with a prominent negative peak at 14 cm depth. It is noted that the sand profile is largely compensated by the silt and clay profile throughout the core. Organic carbon shows similar profile to that of finer sediment components. In core F6 (Fig. 3.2.3), sand content shows lower values than average in section 1. However, in section 2, it maintains a constant trend, above the average line. In section 3, it again shows lower values than average line maintaining a constant value up to the surface. Like core F5, sand profile is largely compensated by silt and clay profiles and also, organic carbon shows a similar trend to that of finer sediment components. In core F7 (Fig. 3.2.4), in section 1, the sand profile shows a negative peak at 44 cm and

fluctuating pattern whereas in section 2 it maintains a constant trend above the average line which further decreases up to the surface in section 3. Silt profile shows constant values with the average line in section 1. However, silt in section 2 shows lower values than average line which later shows elevated values at the surface. Clay also shows opposite distribution pattern to that of sand with minor fluctuations in section 1. Organic carbon shows similar distribution trend to that of silt in this core. In core F8 (Fig. 3.2.5), there is no much variation in the distribution of sediment components and organic carbon. Sand profile maintains constant trend throughout the core having lower values at 20 and 18 cm (section 2). Silt and clay profile compensate sand percentage and organic carbon shows similar trend to finer sediment components.

When the range and average values of sediment components and organic carbon of cores F4, F5, F6 and F8 which were collected from upper middle region were compared, it is noted that core F8 (Gurpur) was highly dominated by sand content whereas, higher mud content (silt + clay) was found in core F6 with 63 %. The range of variation in sediment components and organic carbon is much larger in core F4 (Swarna estuary), F5 (Udyavara estuary) and F6 (Pavanje estuary) as compared to core F8 collected from Gurpur estuary. This indicates larger fluctuation in hydrodynamics in core Swarna, Udyavara and Pavanje estuaries. Higher average (avg) sand component in core F8 (Gurpur estuary) indicates uniform high hydrodynamic energy conditions prevailed in this estuary. Large fluctuations in hydrodynamics with intermittent quiet conditions must have facilitated deposition of sediment during calmer periods which must have helped in the formation of small islands in Swarna estuary (Avinash et al. 2012). Distribution of sediment component in core F4 and F6 are found to be similar pattern. It is noted that, these estuaries have experienced alternate repeated occurrence of high and low input of sand. However, sand percentage increased in core F4 and decreased in core F6 at surface. The sediment deposition in section 2 of both of these cores was probably under fluctuating high energy hydrodynamic conditions which lead to deposition of higher coarser sediments. Alternate high coarser and finer sediments are also seen (Table 3.2.2). Fluctuating sand profiles with low percentage in section 1 of core F4 and F6; and section 2 of F5 could be due to various factors like change in rainfall pattern and runoff, dredging activities and sea level changes bringing a change in sedimentation pattern. Higher

deposition of mud content (silt + clay) reflects periods of calmer hydrodynamic energy conditions which facilitated mud deposition and are well depicted in the profiles. Gurpur estuary maintained high sand values uniformly with time indicating availability of high hydrodynamic energy conditions throughout the core. Core collected from upper middle estuarine region of Gurpur show high sand content as compared to lower middle estuarine region. Core collected from lower middle estuary shows gradual increase in sand content from section 1 to 2; however, it decreases in section 3 unlike the distribution of sediments in core from upper middle region. This could be due to the input of sand from mouth region from shifting of material of Mangalore spit and shifting of the mouth of Gurpur estuary towards north (Nasnodkar and Nayak 2015).

It is observed that organic carbon in all the mudflat cores shows similar profile to that of finer sediment components indicating its association (Mayer and Xing 2001; Falco et al. 2004). The higher concentration of organic carbon in section 1 of cores F4 and F6 corresponding with lower sand content suggested deposition of organic matter together with finer sediments under calm hydrodynamic energy conditions which were probably prevalent in the past (Kumar and Edward 2009) and low organic carbon at the surface of core F4, F5, F6 is probably because of its dilution by input of sand.

3.2 A. 1b Mangroves

In core G3 (Table 3.2.1), sand content varies from 51 – 87 % (avg. 79 %), whereas silt and clay content vary from 11 – 40 % (avg. 19 %) and 0.04 – 9 % (avg. 1.88 %) respectively. Organic carbon varies from 0.2 – 1.55 % (avg. 0.54 %). In core G4, sand content varies from 8 to 64 % whereas silt and clay content vary from 14 to 43 % and 22 to 49 % respectively with mean values for sand, 34 %; silt, 31 % and clay, 35 %. Organic carbon content varies from 0.32 to 3.32 % with its mean value 1.6 %. In core G5, sand value varies from 5 to 71 % whereas silt, clay and organic carbon vary from 9 to 40 %, 20 to 57 % and 0.85 to 3 % respectively with mean values of sand, 41 %; silt, 24 %; clay, 36 % and organic carbon, 2 %. In core G6, sand varies from 52 – 89 % (avg. 67 %), whereas silt and clay content vary from 2 – 18 % (avg. 10 %) and 9 – 33 % (avg. 23 %) respectively. Organic carbon ranges from 0.46 – 3.54 % (avg. 1.26 %).

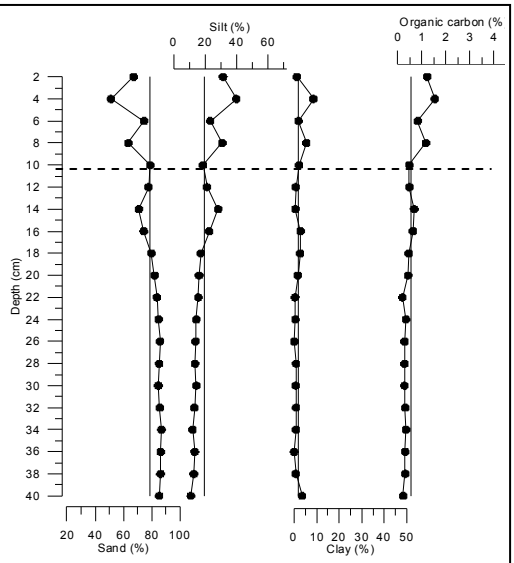

Fig. 3.2.6 Vertical profiles of sediment components and organic carbon in core G3 (Chakra Nadi-middle estuary)

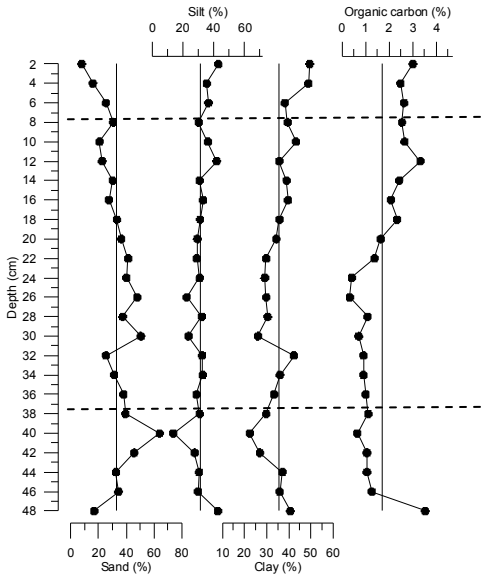

Fig. 3.2.7 Vertical profiles of sediment components and organic carbon in core G4 (Haladi-middle estuary)

On the basis of the distribution of sediment components, core G3 is divided into two sections, section 1 (40 – 10 cm) and section 2 (10 – 0 cm). Core G4 is divided as; section 1 (48 - 38 cm), section 2 (38 - 8 cm) and section 3 (8 - 0 cm). Core G5 is divided as; section 1(32-18 cm) and section 2 (18-0 cm). Core G6 is divided as; section 1 (42-20 cm) and section 2 (20-0 cm). Range and average values for each section is provided in table 3.2.2. In core G3, section 1, sand content varies from 71 to 87 % whereas silt and clay content vary from 11 to 28.4 % and 0.04 to 3.6 % respectively with mean values for sand, 82 %; silt, 16.3 % and clay, 1.3 %. Organic carbon content varies from 0.2 to 0.7 % with its mean value 0.4 %. In section 2, sand content varies from 51 to 75 % whereas silt and clay content vary from 23.5 to 40.1 % and 1.3 to 8.6 % respectively with mean values for sand, 64 %; silt, 31.5 % and clay, 4.3 %. Organic carbon content varies from 0.8 to 1.6 % with its mean value 1.2 %. In core G4, section 1, sand content varies from 33 to 64 % whereas silt and clay content vary from 13.5 to 30.3 % and 22.4 to 37.1 % respectively with mean values for sand, 44 %; silt, 25.2 % and clay, 30.6 %. Organic carbon content varies from 0.6 to 1.3 % with its mean value 1 %. In section 2, sand content varies from 21 to 51 % whereas silt and clay content vary from 22.2 to 41.8 % and 26 to 43.3 % respectively with mean values for sand, 35 %; silt, 30.9 % and clay, 34.3 %. Organic carbon content varies from 0.3 to 3.3 % with its mean value 1.5 %. In section 3, sand content varies from 8 to 31 % whereas silt and

clay content vary from 29.9 to 42.8 % and 38.2 to 49.4 % respectively with mean values for sand, 20 %; silt, 36.1 % and clay, 44 %. Organic carbon content varies from 2.5 to 3.0 % with its mean value 2.7 %. In core G5, section 1, sand content varies from 42 to 71 % whereas silt and clay content vary from 9.2 to 24.5 % and 19.8 to 33.6 % respectively with mean values for sand, 59 %; silt, 16.1 % and clay, 25.2 %. Organic carbon content varies from 0.9 to 2.1 % with its mean value 1.4 %. In section 2, sand content varies from 5 to 34 % whereas silt and clay content vary from 27.5 to 39.6 % and 38.2 to 56.6 % respectively with mean values for sand, 22 %; silt, 31.8 % and clay, 45.8 %. Organic carbon content varies from 2.2 to 3.1 % with its mean value 2.7 %. In core G6, section 1, sand content varies from 60 to 89 % whereas silt and clay content vary from 2.3 to 13.5 % and 8.6 to 26.9 % respectively with mean values for sand, 75 %; silt, 6.8 % and clay, 18.2 %. Organic carbon content varies from 0.5 to 1.2 % with its mean value 0.7 %. In section 2, sand content varies from 52 to 66 % whereas silt and clay content vary from 10.4 to 17.6 % and 23.8 to 32.6 % respectively with mean values for sand, 58 %; silt, 13.9 % and clay, 27.8 %. Organic carbon content varies from 1 to 3.5 % with its mean value 1.9 %

Among the four cores collected from mangrove environment, G3 and G4 are from upper middle region whereas G5 and G6 are from lower middle region of estuaries. When the cores from upper middle region were compared, it is noted the sand is highly dominated in core G3 (79 %) as compared to core G4 (34 %). In the lower middle region, sand is high in core G6 (67 %) as compared to G5 (41 %). The range of variation in sediment components and organic carbon is much larger in core G4 (Haladi) and G5 (Sita Nadi) indicating fluctuation in hydrodynamics and higher average sand component in Chakra Nadi (G3) indicates uniform high hydrodynamic energy conditions, possibly due to the influence of fresh water influx.

In core G3 (Fig. 3.2.6), sand profile shows a decreasing trend in section 1, further it continues to decrease but with fluctuations in section 2. Silt and clay percentage compensates to that of sand percentage. Organic carbon show similar profile to that of finer sediment components. In core G4 (Fig. 3.2.7), sand profile shows an increasing

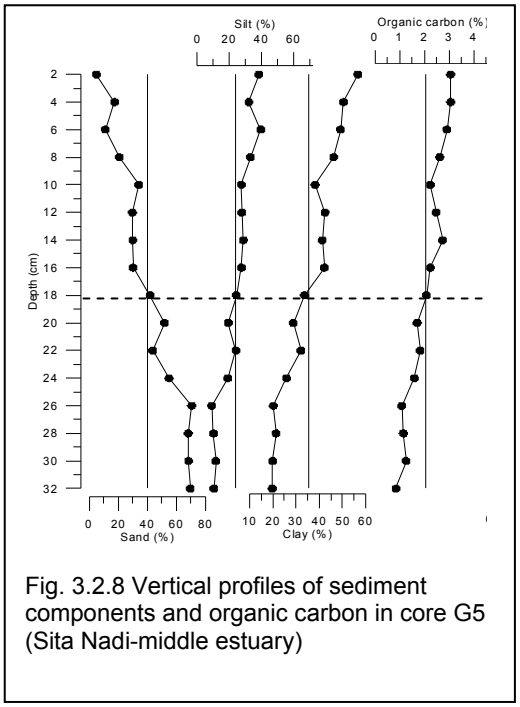

Fig. 3.2.8 Vertical profiles of sediment components and organic carbon in core G5 (Sita Nadi-middle estuary)

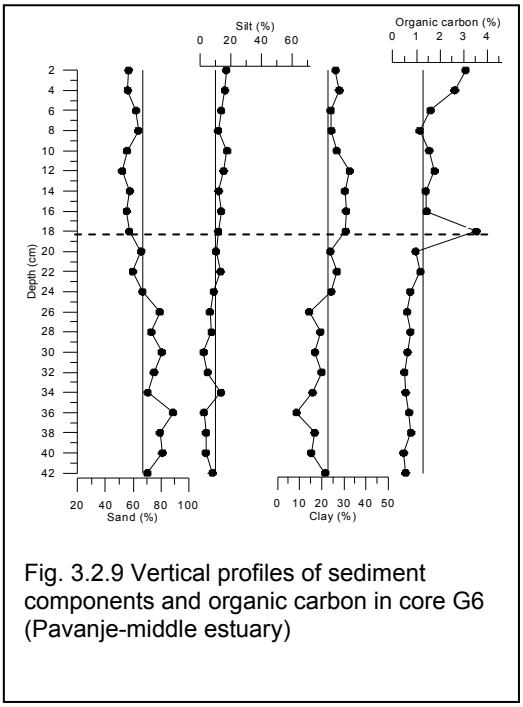

Fig. 3.2.9 Vertical profiles of sediment components and organic carbon in core G6 (Pavanje-middle estuary)

trend in section 1, however in section 2, it shows a decreasing trend. In section 3, it shows a sharp decreasing trend below the average values up to the surface. Silt and the clay profile compensates to that of sand profile in all the three sections. Similar to core G3, organic carbon profile largely agrees with the profiles of finer sediments in core G4. In core G5 (Fig. 3.2.8), sand profile shows a decreasing trend from section 1 to section 2 and from higher than average to lower than average. Silt and clay profiles maintain an opposite trend to sand profile thereby compensating the sand profile. Organic carbon again shows similar trend to finer sediment components. Similar to core G5, sand profile in core G6 (Fig. 3.2.9), showed decreasing trend from section 1 to section 2. Silt and clay profile shows an increasing trend. Clay largely compensates sand. Organic carbon shows an increasing trend from section 1 to section 2 with elevated valued at the surface and a prominent peak at 18 cm.

When the range and average values of sediment components and organic carbon of all mangrove cores were compared, it is noted that core G3 (Chakra Nadi) was highly dominated by sand content whereas, higher mud content (silt + clay) was noted in core G4 with 66 %. The range of variation in sediment components and organic carbon is much larger in core G5 as compared to cores G3, G4 and G6. Higher average sand component along with minimum and maximum values in core G6 indicates uniform high

hydrodynamic energy conditions in Panvanje estuary. A decrease in sand percentage from bottom to top is noted in all the mangrove cores. In general, mangroves are known to retain higher finer sediments (Zhou et al. 2010) thereby preventing erosion. Highest mud content was noted in core G4 (67 %).

Among the upper middle region, organic carbon was high in core G4 and among lower middle region it was high in core G5. Overall when the average organic carbon was compared, it was found to be higher in core G5 (2 %). Organic carbon profiles of all the mangroves cores were similar to that of finer sediments profiles indicating their association. High amount of organic matter was noted in the upper 8 cm which could be due to the litters of surrounding mangroves. Prevailing calmer hydrodynamic energy conditions must have favoured the deposition of mud content (silt + clay) in mangroves, in the recent years.

When sand, silt and clay trends between mudflats and mangroves were compared, more systematic distribution is noted in mangroves. All the mangrove cores show decrease in sand and increase in silt, clay and organic carbon towards surface. This trend is not seen in mudflats. Variation in hydrodynamics therefore affected sediment deposition in mudflats and not mangroves. Sediment deposition showed large fluctuation in mudflat environment and systematic deposition in mangrove environment as mangrove ecosystems holds and stabilizes the sediments. Mangroves are known to reduce wave energy as waves travel through them and therefore prevent erosion (Cat et al. 2006).

3.2 B Metal distribution

3.2 B. 2a Distribution of Al, Fe and Mn in the bulk sediments of mudflats

The geochemical data shows, 7-14 % (avg. 11 %) Al, 2 - 6% (avg. 4 %) Fe, 110 - 314 ppm (avg. 193 ppm) Mn in core F4 (Table 3.2.3) and; 3 – 12 % (avg. 8 %) Al, 2-6 % (avg. 4 %) Fe, 74 - 406 ppm (avg. 186 ppm) Mn in core F5. Core F6 showed 4 -18 % (avg. 10 %) Al, 3 - 7% (avg. 5 %) Fe, 125 - 553 ppm (avg. 213 ppm) Mn. In core F7, the data shows, 3 – 10% (avg. 5 %) Al, 1 – 3 % (avg. 2 %) Fe, 119 – 229 ppm (avg. 177 ppm) Mn and; core F8 showed, 4 – 7% (avg. 5 %) Al, 1 – 3 % (avg. 2 %) Fe, 166 – 275 ppm (avg. 203 ppm) Mn.

Table 3.2.3 Range and average values of metals in mudflats and mangroves

Core	Al (%)			Fe (%)			Mn (ppm)		
	min	max	avg	min	max	Avg	min	max	avg
F4	7	14	11	2	6	4	110	314	193
F5	3	12	8	2	6	4	74	406	186
F6	4	18	10	3	7	5	125	553	213
F7	3	10	5	1	3	2	119	229	177
F8	4	7	5	1	3	2	166	275	203
G3	4	7	4	3	5	3	181	365	233
G4	6	10	8	3	5	4	119	192	168
G5	4	11	7	2	5	4	160	304	219
G6	4	8	6	2	6	4	55	115	85

core	Ni (ppm)			Zn (ppm)			Cu (ppm)			Co (ppm)			Cr (ppm)		
	min	max	avg	Min	max	avg	min	Max	avg	min	max	avg	min	max	avg
F4	34	117	77	24	78	52	38	68	54	5	35	19	74	180	134
F5	45	155	100	16	97	60	32	78	57	18	54	36	79	314	202
F6	64	179	124	39	100	72	43	85	66	11	27	19	161	375	266
F7	8	56	30	18	60	37	47	90	65	4	18	12	59	159	89
F8	6	79	39	23	42	31	55	77	65	3	27	12	41	100	68
G3	29	85	48	33	48	39	30	56	41	2	20	9	93	168	114
G4	5	83	47	52	121	75	48	70	57	3	22	12	123	206	166
G5	39	112	69	18	62	38	31	59	44	3	16	9	69	197	126
G6	27	126	55	17	55	33	38	61	47	2	23	9	157	282	198

Table 3.2.4 Range and average values of sections of metals in mudflats and mangroves

Core	section	Al (%)			Fe (%)			Mn (ppm)		
		min	Max	avg	min	max	avg	min	max	avg
F4	3	7.8	13.8	11.5	3.4	5.8	4.6	138	314	220
	2	6.8	12.9	9.6	2.5	5.0	4.0	110	177	155
	1	11.2	12.9	12.0	4.0	4.8	4.4	170	215	195
F5	3	4.1	5.4	4.5	1.6	2.4	1.9	74	120	92
	2	5.6	11.7	8.7	3.3	6.3	4.7	135	406	222
	1	3.3	11.9	6.7	1.8	5.4	3.2	107	213	153
F6	3	9.0	18.2	12.9	4.5	7.3	6.0	156	553	243
	2	3.7	5.9	5.0	2.7	4.1	3.3	125	193	152
	1	6.3	11.4	9.6	3.6	6.3	5.5	191	274	239
F7	3	8.2	9.7	9.0	2.38	2.45	2.42	208	215	211
	2	3.0	5.5	3.7	1.1	2.3	1.4	124	213	179
	1	3.7	8.1	5.0	1.4	3.3	2.0	119	229	168
F8	3	3.5	6.6	4.5	1.3	2.1	1.6	166	275	208
	2	6.86	6.87	6.86	3.0	3.1	3.1	191	210	201

	1	4.2	5.0	4.6	1.6	2.0	1.8	174	244	200
G3	2	4.9	7.2	6.0	3.4	4.6	4.0	219	294	267
	1	3.6	5.1	4.0	2.6	3.5	2.8	181	365	225
G4	3	6.4	9.2	8.30	3.0	4.8	4.2	157	176	167
	2	7.09	10.0	8.20	3.4	4.8	3.9	119	189	166
	1	7.10	9.2	8.31	3.5	3.9	3.6	160	192	180
G5	2	7.7	10.7	8.9	3.7	5.3	4.5	226	304	254
	1	4.1	7.3	5.3	2.1	3.2	2.6	160	206	185
G6	2	5.4	7.6	6.4	2.2	6.1	4.2	80	115	94
	1	3.8	5.7	4.7	1.9	5.8	3.0	55	93	77

Core	section	Ni (ppm)			Zn (ppm)			Cu (ppm)			Co (ppm)			Cr (ppm)		
		min	max	avg	min	max	avg	min	max	avg	min	max	avg	min	max	avg
F4	3	34	112	83	32	78	57	38	59	51	11.75	28.25	20.54	103	180	145
	2	36	117	67	24	66	42	39	59	52	4.50	34.50	18.28	74	142	119
	1	51	95	82	50	71	56	55	68	63	12.25	23.25	16.07	117	155	134
F5	3	45	73	58	16	29	25	41	51	46	17.50	25.00	21.10	79	130	96
	2	69	155	116	53	97	73	32	78	62	21.00	54.00	40.42	187	314	249
	1	55	122	87	28	75	50	32	71	49	20.75	50.75	32.68	98	221	153
F6	3	101	179	145	63	100	85	61	85	74	11.25	26.25	19.04	234	375	301
	2	64	96	82	39	59	50	43	57	50	11.25	19.50	15.75	161	239	201
	1	86	163	140	48	87	73	53	76	69	15.25	27.00	23.63	209	313	280
F7	3	32	44	38	46	53	50	88	90	89	14.50	17.00	15.75	112	119	116
	2	8	50	21	18	50	31	47	70	58	5.75	15.00	10.23	59	110	75
	1	22	56	38	27	60	41	56	89	68	4.00	17.75	13.18	74	159	100
F8	3	6	40	20	23	38	29	55	68	60	3.00	18.25	9.88	41	86	60
	2	71	79	75	41.8	42.3	42.0	74	77	75	14.25	15.75	15.00	98	100	99
	1	33	66	51	26	35	30	60	76	68	8.00	26.75	13.64	59	88	70
G3	2	52	85	64	33	45	40	41	56	46	8.25	12.50	9.88	100	168	132
	1	29	65	44	33	48	39	30	45	39	1.50	19.75	8.25	93	126	109
G4	3	49	83	61	52	121	92	58	70	65	10.75	21.00	16.06	175	206	193
	2	24	67	47	53	112	74	48	70	57	3.25	19.75	11.05	123	203	166
	1	5	60	35	57	67	62	49	52	50	4.75	21.50	12.69	136	145	140
G5	2	62	112	83	41	62	49	46	59	51	8.25	15.75	12.38	125	197	152
	1	39	67	55	18	35	27	31	42	37	2.50	7.00	4.94	69	165	99
G6	2	48	86	64	23	55	39	44	61	51	3.00	23.25	9.78	171	282	204
	1	27	126	47	17	38	27	38	50	44	2.25	21.25	8.77	157	250	192

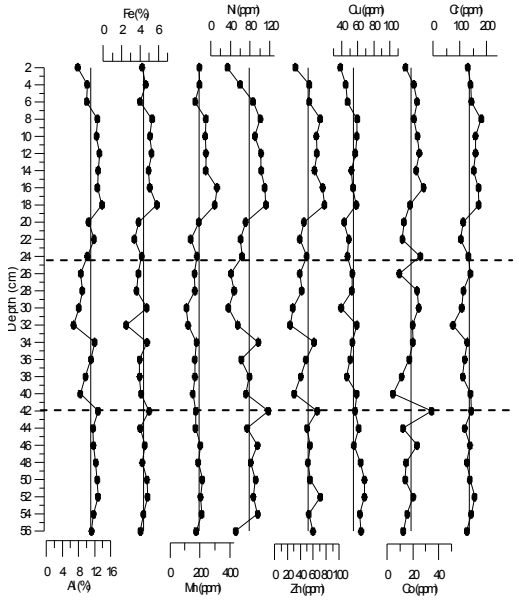

Fig. 3.2.10 Vertical profiles of metals in core F4 (Swarna – upper middle estuary)

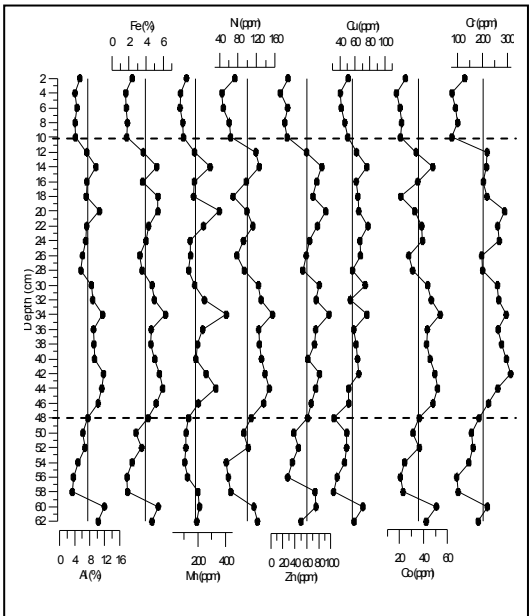

Fig. 3.2.11 Vertical profiles of metals in core F5 (Udyavara – upper middle estuary)

Range and average values for each section is given in table 3.2.4. In core F4, section 1, showed, 11.2-12.9 % (avg. 12 %) Al, 4 – 4.8% (avg. 4.4 %) Fe, 170 - 215 ppm (avg. 195 ppm) Mn; section 2 showed, 6.8 – 12.9 % (avg. 9.6 %) Al, 2.5-5 % (avg. 4 %) Fe, 110 - 177 ppm (avg. 155 ppm) Mn; section 3 showed, 7.8-13.8 % (avg. 11.5 %) Al, 3.4 – 5.8 % (avg. 4.6 %) Fe, 138 – 314 ppm (avg. 220 ppm) Mn. In core F5, section 1, showed, 3.3 -11.9 % (avg. 6.7 %) Al, 1.8 – 5.4 % (avg. 3.2 %) Fe, 107 - 213 ppm (avg. 153 ppm) Mn; section 2 showed, 5.6 – 11.7 % (avg. 8.7 %) Al, 3.3-6.3 % (avg. 4.7 %) Fe, 135 - 406 ppm (avg. 222 ppm) Mn and section 3, 4.1-5.4 % (avg. 4.5 %) Al, 1.6 – 2.4 % (avg. 1.9 %) Fe, 74 –120 ppm (avg. 92 ppm) Mn. In core F6, section 1, showed, 6.3-11.4 % (avg. 9.6 %) Al, 3.6 – 6.3% (avg. 5.5 %) Fe, 191 - 274 ppm (avg. 239 ppm) Mn; section 2 showed, 3.7–5.9 % (avg. 5 %) Al, 2.7-4.1 % (avg. 3.3 %) Fe, 125 - 193 ppm (avg. 152 ppm) Mn; section 3 showed, 9-18.2 % (avg. 12.9 %) Al, 4.5 – 7.3 % (avg. 6 %) Fe, 156 –553 ppm (avg. 243 ppm) Mn. In core F7, section 1, showed, 3.7-8.1 % (avg. 5 %) Al, 1.4 – 3.3 % (avg. 2 %) Fe, 119 - 229 ppm (avg. 168 ppm) Mn; section 2 showed, 3–5.5 % (avg. 3.7 %) Al, 1.1-2.3 % (avg. 1.4 %) Fe, 124 - 213 ppm (avg. 179 ppm) Mn; section 3 showed, 8.2-9.7 % (avg. 9 %) Al, 2.38 – 2.45 % (avg. 2.42 %) Fe, 208 –215 ppm (avg. 211 ppm) Mn. In core F8, section 1, showed, 4.2-5 %

(avg. 4.6 %) Al, 1.6 – 2 % (avg. 1.8 %) Fe, 174 - 244 ppm (avg. 200 ppm) Mn; section 2 showed, 6.86 –6.87 % (avg. 6.86 %) Al, 3-3.1 % (avg. 3.1 %) Fe, 191 - 210 ppm (avg. 201 ppm) Mn; in section 3 showed, 3.5-6.6 % (avg. 4.5 %) Al, 1.3 – 2.1 % (avg. 1.6 %) Fe, 166 –275 ppm (avg. 208 ppm) Mn.

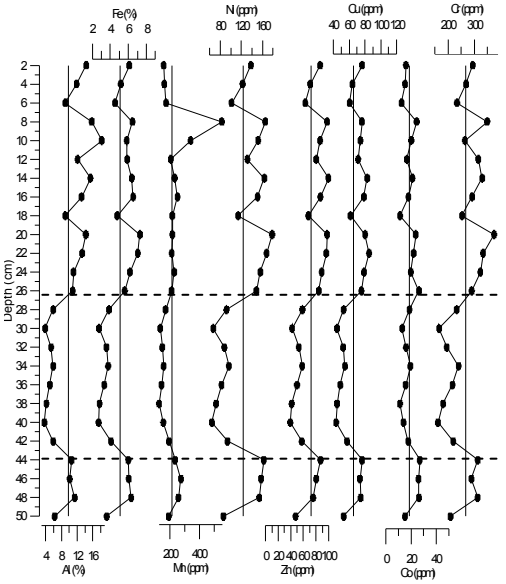

Fig. 3.2.12 Vertical profiles of metals in core F6 (Pavanje – upper middle estuary)

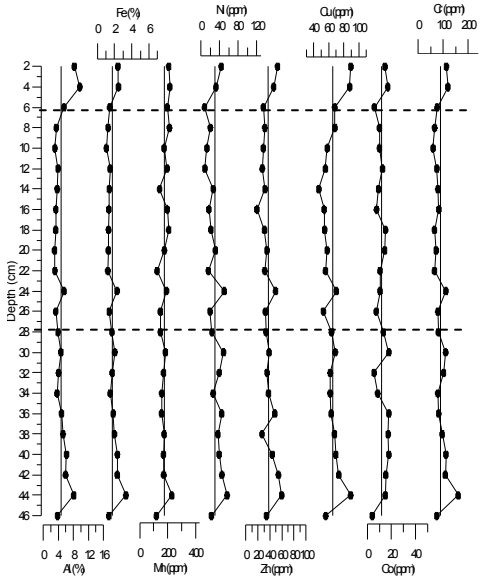

Fig. 3.2.13 Vertical profiles of metals in core F7 (Gurpur – lower middle estuary)

In core F4 (Fig. 3.2.10), Al maintained a constant trend above average line in section 1, lower than average line with two prominent negative peaks at 40 and 32 cm depth in section 2. In section 3, it maintains constant trend above average line up to 8 cm which further decreases up to the surface. Similar distribution trend is also shown by Fe and Mn. In core F5 (Fig. 3.2.11), Al concentration decreases sharply from 60 cm to 58 cm depth, further it shows increasing trend in section 1. In section 2, it shows a decreasing trend with fluctuations. Al maintains constant values below average line in section 3. Fe and Mn also follows similar distribution trend to that of Al with larger fluctuations in section 2. In core F6 (Fig. 3.2.12), Al shows decreasing trend from section 1 to 2 with lower than average values in section 2. Further in section 3, it shows higher than average values up to the surface with fluctuations. Similar distribution trend is also observed in case of Fe. Mn shows similar profile to Al and Fe in section 1 and section 2, a decreasing trend with a prominent peak at 8 cm depth in section 3. In core F7 (Fig. 3.2.13), Al shows a decreasing trend in section 1, maintains constant trend below

average line in section 2, elevated values in section 3. Fe and Mn show similar distribution to that of Al. In core F8 (Fig. 3.2.14), Al and Fe shows constant values along the average line in section 1, positive peak values at 20 and 18 cm depth in section 2. In section 3, they maintain values below average line. Mn maintains constant values along the average line throughout the core with a small peak value at 32 cm and higher value at the surface.

3.2 B. 3a Distribution of Ni, Zn, Cu, Co and Cr in the bulk sediments of mudflats

In core F4, trace metal concentration shows 34 – 117 ppm (avg. 77 ppm) Ni, 24 – 78 ppm (avg. 52 ppm) Zn, 38 – 68 ppm (avg. 54 ppm) Cu, 5- 35 ppm (avg. 19 ppm) Co and 74 – 180 ppm (avg. 134 ppm) Cr (Table 3.2.3). Core F5, shows 45 – 155 ppm (avg. 100 ppm) Ni, 16 – 97 ppm (avg. 60 ppm) Zn, 32 – 78 ppm (avg. 57 ppm) Cu, 18-54 ppm (avg. 36 ppm) Co and 79 – 314 ppm (avg. 202 ppm) Cr. Trace metal concentration shows 64 – 179 ppm (avg. 124 ppm) Ni, 39 – 100 ppm (avg. 72 ppm) Zn, 43– 85 ppm (avg. 66 ppm) Cu, 11- 27 ppm (avg. 19 ppm) Co and 161 – 375 ppm (avg. 266 ppm) Cr in core F6 and; 8 – 56 ppm (avg. 30 ppm) Ni, 18 – 60 ppm (avg. 37 ppm) Zn, 47 – 90 ppm (avg. 65 ppm) Cu, 4- 18 ppm (avg. 12 ppm) Co and 59 – 159 ppm (avg. 89 ppm) Cr in core F7. In core F8, showed, 6 – 79 ppm (avg. 39 ppm) Ni, 23 – 42 ppm (avg. 31 ppm) Zn, 55 – 77 ppm (avg. 65 ppm) Cu, 3- 27 ppm (avg. 12 ppm) Co and 41 – 100 ppm (avg. 68 ppm) Cr.

The range and average values for each section is given in table 3.2.4. In core F4, section 1, trace metal concentration showed 51 – 95 ppm (avg. 82 ppm) Ni, 50– 71 ppm (avg. 56 ppm) Zn, 55 – 68 ppm (avg. 63 ppm) Cu, 12.25- 23.25 ppm (avg. 16.07 ppm) Co and 117 – 155 ppm (avg. 134 ppm) Cr; section 2 showed, 36 – 117 ppm (avg. 67 ppm) Ni, 24– 66 ppm (avg. 42 ppm) Zn, 39 – 59 ppm (avg. 52 ppm) Cu, 4.5-34.5 ppm (avg. 18.28 ppm) Co and 74 – 142 ppm (avg. 119 ppm) Cr and; section 3 showed, 34 – 112 ppm (avg. 83 ppm) Ni, 32– 78 ppm (avg. 57 ppm) Zn, 38 – 59 ppm (avg. 51 ppm) Cu, 11.75-28.25 ppm (avg. 20.54 ppm) Co and 103 – 180 ppm (avg. 145 ppm) Cr. In core F5, section 1, trace metal concentration ed55 – 122 ppm (avg. 87 ppm) Ni, 28– 75 ppm (avg. 50 ppm) Zn, 32 – 71 ppm (avg. 49 ppm) Cu, 20.75- 50.75 ppm (avg. 32.68 ppm) Co and 98 – 221 ppm (avg. 153 ppm) Cr; section 2 showed, 69 – 155 ppm (avg. 116 ppm) Ni, 53– 97 ppm (avg. 73 ppm) Zn, 32 – 78 ppm (avg. 62 ppm) Cu, 21-

54 ppm (avg. 40.42 ppm) Co and 187 – 314 ppm (avg. 249 ppm) Cr and; section 3 showed, 45 – 73 ppm (avg. 58 ppm) Ni, 16– 29 ppm (avg. 25 ppm) Zn, 41 – 51 ppm (avg. 46 ppm) Cu, 17.5-25 ppm (avg. 21.1 ppm) Co and 79 – 130 ppm (avg. 96 ppm) Cr. In core F6, section 1, trace metal concentration shows 86 – 163 ppm (avg. 140 ppm) Ni, 48– 87 ppm (avg. 73 ppm) Zn, 53 – 76 ppm (avg. 69 ppm) Cu, 15.25- 27 ppm (avg. 23.63 ppm) Co and 209 – 313 ppm (avg. 280 ppm) Cr; section 2 showed, 64 – 96 ppm (avg. 82 ppm) Ni, 39– 59 ppm (avg. 50 ppm) Zn, 43 – 57 ppm (avg. 50 ppm) Cu, 11.25-19.5 ppm (avg. 15.75 ppm) Co and 161 – 239 ppm (avg. 201 ppm) Cr and; section 3 showed, 101 – 179 ppm (avg. 145 ppm) Ni, 63– 100 ppm (avg. 85 ppm) Zn, 61 – 85 ppm (avg. 74 ppm) Cu, 11.25-26.25 ppm (avg. 19.04 ppm) Co and 234 – 375 ppm (avg. 301 ppm) Cr. In core F7, section 1, trace metal concentration shows 22 – 56 ppm (avg. 38 ppm) Ni, 27– 60 ppm (avg. 41 ppm) Zn, 56 – 89 ppm (avg. 68 ppm) Cu, 4 – 17.75 ppm (avg. 13.18 ppm) Co and 74 – 159 ppm (avg. 100 ppm) Cr; section 2 showed, 8 – 50 ppm (avg. 21 ppm) Ni, 18– 50 ppm (avg. 31 ppm) Zn, 47 – 70 ppm (avg. 58 ppm) Cu, 5.75-15 ppm (avg. 10.23 ppm) Co and 59 –110 ppm (avg. 75 ppm) Cr and; section 3 showed, 32 – 44 ppm (avg. 38 ppm) Ni, 46– 53 ppm (avg. 50 ppm) Zn, 88 – 90 ppm (avg. 89 ppm) Cu, 14.5-17 ppm (avg. 15.75 ppm) Co and 112 – 119 ppm (avg. 116 ppm) Cr. In core F8, section 1, trace metal concentration showed 33 – 66 ppm (avg. 51 ppm) Ni, 26– 35 ppm (avg. 30 ppm) Zn, 60 – 76 ppm (avg. 68 ppm) Cu, 8 – 26.75 ppm (avg. 13.64 ppm) Co and 59 – 88 ppm (avg. 70 ppm) Cr; section 2 showed, 71 – 79 ppm (avg. 75 ppm) Ni, 41.8– 42.3 ppm (avg. 42 ppm) Zn, 74 – 77 ppm (avg. 75 ppm) Cu, 14.25-15.75 ppm (avg. 15 ppm) Co and 98 –100 ppm (avg. 99 ppm) Cr and; section 3 showed, 6 – 40 ppm (avg. 20 ppm) Ni, 23– 38 ppm (avg. 29 ppm) Zn, 55 – 68 ppm (avg. 60 ppm) Cu, 3-18.25 ppm (avg. 9.88 ppm) Co and 41 – 86 ppm (avg. 60 ppm) Cr.

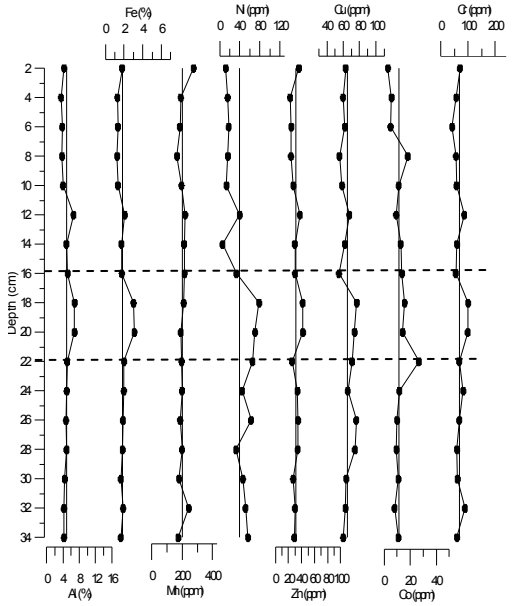

Fig. 3.2.14 Vertical profiles of metals in core F8 (Gurpur – upper middle estuary)

In core F4, among the trace metals, it is seen that Ni, Zn, Cu and Cr show either higher or along the average line in section 1 and lower than average value with decreasing trend in section 2. Further, in section 3, all trace metals show values above the average line up to 6 cm, later decrease up to the surface. These metals show similar distribution trend to that of Al and Fe in section 1 and 2, whereas, to that of Al, Fe and Mn in section 3. Their peaks largely coincide with clay and organic carbon in section 1, however, with silt and organic carbon in section 2 and 3. Co values fluctuate along average line in section 1 and 2. However, in section 3, it follows similar distribution with other trace metals. In core F5, Ni, Zn, Cu, Co and Cr show increasing trend from 58 cm to 34 cm depth, further show decreasing trend up to the surface. Similar distribution trend is also observed in case of Al, Fe and Mn. In core F6, all trace metals maintain slightly increasing trend above average line in section 1. In section 2, they show fluctuating values below the average line. In section 3, they show fluctuating trend with the average line or slightly more than average lines. Trace metals show similar distribution trend in case of Al, Fe and Mn in section 1 and 2 whereas only with Al and Fe in section 3 (except Co). Co distribution is largely similar to Mn. In core F7, all trace metals show decreasing trend from section 1 to 2, however, in section 3 they show elevated values. Similar distribution trend is also shown by Al, Fe and Mn. Peak values at 4, 24 and 44 cm depth coincides with finer sediments and organic carbon. In core F8, most of the trace metals maintain constant values with the average line except Ni which shows decreasing trend in section 1 and 3. In section 2, all the trace metals except Co show higher values. Their distribution trend is largely similar to Al and Fe. Also, their peaks at 12, 18 and 20 cm depth largely coincide with the peaks of finer sediment components.

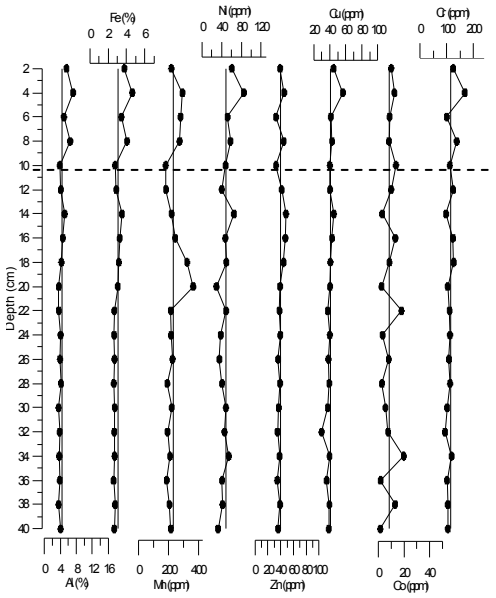

Fig. 3.2.15 Vertical profiles of metals in core G3 (Chakra Nadi – middle estuary)

3.2 B. 2b. Distribution of Al, Fe and Mn in the bulk sediments of mangroves

The geochemical data shows, 4 - 7 % (avg. 4 %) Al, 3 - 5% (avg. 3 %) Fe, 181 - 365 ppm (avg. 233 ppm) Mn in core G3 and; 6 – 10 % (avg. 8 %) Al, 3 - 5 % (avg. 4 %) Fe, 119 - 192 ppm (avg. 168 ppm) Mn in core G4 (Table 3.2.3). Core G5, showed, 4 – 11 % (avg. 7 %) Al, 2 - 5% (avg. 4 %) Fe, 160 – 304 ppm (avg. 219 ppm) Mn. In core G6, the data shows, 4 – 8% (avg. 6 %) Al, 2 – 6 % (avg. 4 %) Fe, 55 – 115 ppm (avg. 85 ppm) Mn.

Range and average values for each section is provided in table 3.2.4. In core G3, section 1, showed, 3.6 - 5.1 % (avg. 4 %) Al, 2.6 – 3.5 % (avg. 2.8 %) Fe, 181 - 365 ppm (avg. 225 ppm) Mn; section 2 showed, 4.9 –7.2 % (avg. 6 %) Al, 3.4 - 4.6 % (avg. 4 %) Fe, 219 - 294 ppm (avg. 267 ppm) Mn. In core G4, section 1 showed, 7.1 -9.2 % (avg. 8.31 %) Al, 3.5 – 3.9% (avg. 3.6 %) Fe, 160 - 192 ppm (avg. 180 ppm) Mn; section 2 showed, 7.09 – 10 % (avg. 8.2 %) Al, 3.4-4.8 % (avg. 3.9 %) Fe, 119 - 189 ppm (avg. 166 ppm) Mn; section 3 showed, 6.4 - 9.2 % (avg. 8.3 %) Al, 3 – 4.8 % (avg. 4.2 %) Fe, 157 –176 ppm (avg. 167 ppm) Mn. In core G5, section 1, showed, 4.1-7.3 % (avg. 5.3 %) Al, 2.1 – 3.2% (avg. 2.6 %) Fe, 160 – 206 ppm (avg. 185 ppm) Mn; section 2 showed, 7.7 –10.7 % (avg. 8.9 %) Al, 3.7-5.3 % (avg. 4.5 %) Fe, 226 – 304 ppm (avg. 254 ppm) Mn. In core G6, section 1 showed, 3.8 - 5.7 % (avg. 4.7 %) Al, 1.9 – 5.8 % (avg. 3 %) Fe, 55 – 93 ppm (avg. 77 ppm) Mn; section 2 showed, 5.4 –7.6 % (avg. 6.4 %) Al, 2.2-6.1 % (avg. 4.2 %) Fe, 80 – 115 ppm (avg. 94 ppm) Mn.

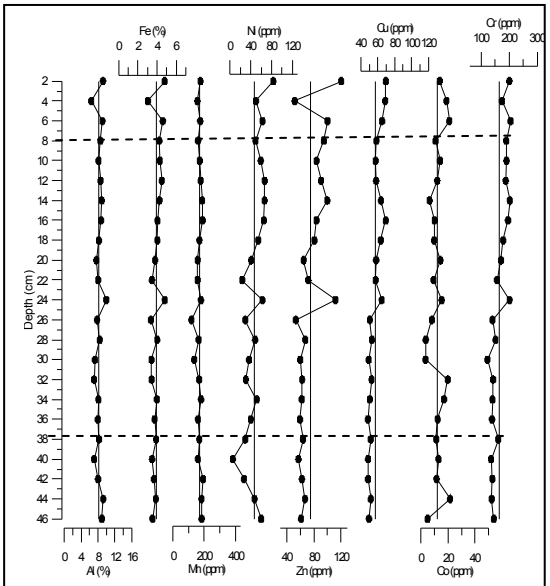

Fig. 3.2.16 Vertical profiles of metals in core G4 (Haladi – middle estuary)

In core G3 (Fig 3.2.15), Al and Fe shows a constant trend along with the average line in section 1. In section 2, they show values above average line with two peaks at 8 and 4 cm and lower values at the surface. However, Mn shows constant trend from bottom of the core up to 22 cm, increases at 20 cm (prominent peak) and decreases up to 10 cm

depth. In section 2, it shows values above average line with lower values at the surface. In core G4 (Fig. 3.2.16), Al and Fe maintains a constant trend in all the sections with positive peak at 24 cm and negative peak at 4 cm depth. However, Mn profile shows a constant trend throughout the core and with a negative peak at 26 cm depth. In core G5 (Fig. 3.2.17), Al, Fe and Mn show an increasing trend from section 1 (having values less than average line) to section 2 (having values greater than average line). In core G6 (Fig. 3.2.18), Al shows an increasing trend from section 1 (values below average line) to 2 (values above average line). Fe also shows an increasing trend with three positive peaks namely at 38, 14 and 10 cm. Mn profile shows similar distribution to that of Al, however, having high values at the surface.

3.2 B. 3b Distribution of Ni, Zn, Cu, Co and Cr in the bulk sediments of mangroves

In core G3, trace metal concentration shows 29 – 85 ppm (avg. 48 ppm) Ni, 33 – 48 ppm (avg. 39 ppm) Zn, 30 – 56 ppm (avg. 41 ppm) Cu, 2- 20 ppm (avg. 9 ppm) Co and 93 – 168 ppm (avg. 114 ppm) Cr (Table 3.2.3). Core G4 shows 5 – 83 ppm (avg.

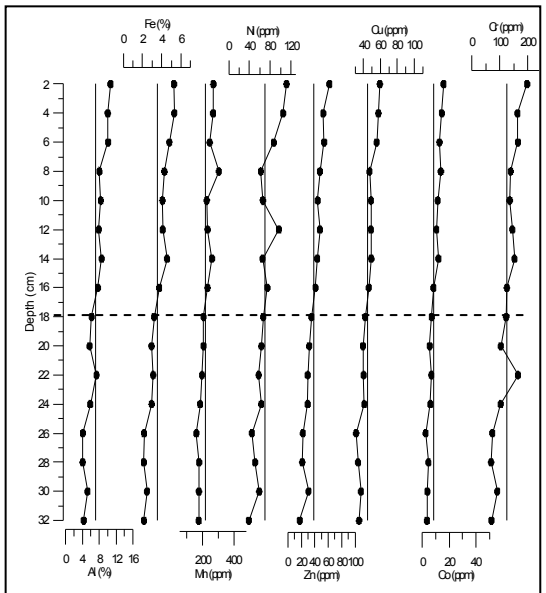

Fig. 3.2.17 Vertical profiles of metals in core G5 (Sita Nadi – middle estuary)

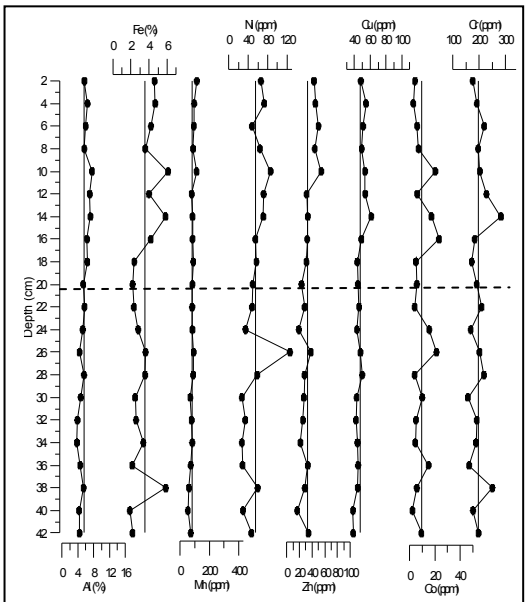

Fig. 3.2.18 Vertical profiles of metals in core G6 (Pavanje – middle estuary)

47 ppm) Ni, 52 – 121 ppm (avg. 75 ppm) Zn, 48 – 70 ppm (avg. 57 ppm) Cu, 3- 22 ppm (avg. 12 ppm) Co and 123 – 206 ppm (avg. 166 ppm) Cr. Trace metal concentration shows 39 – 112 ppm (avg. 69 ppm) Ni, 18 – 62 ppm (avg. 38 ppm) Zn, 31– 59 ppm (avg. 44 ppm) Cu, 3 - 16 ppm (avg. 9 ppm) Co and 69 – 197 ppm (avg. 126 ppm) Cr in

core G5 and; 27 – 126 ppm (avg. 55 ppm) Ni, 17 – 55 ppm (avg. 33 ppm) Zn, 38 – 61 ppm (avg. 47 ppm) Cu, 2 - 23 ppm (avg. 9 ppm) Co and 157 – 282 ppm (avg. 198 ppm) Cr.

Range and average values for each section is given in table 3.2.4. In core G3, section 1, trace metal concentration showed 29 – 65 ppm (avg. 44 ppm) Ni, 33– 48 ppm (avg. 39 ppm) Zn, 30 – 45 ppm (avg. 39 ppm) Cu, 1.5 – 19.75 ppm (avg. 8.25 ppm) Co, 93 – 126 ppm (avg. 109 ppm) Cr; section 2 showed, 52 – 85 ppm (avg. 64 ppm) Ni, 33– 45 ppm (avg. 40 ppm) Zn, 41 – 56 ppm (avg. 46 ppm) Cu, 8.25-12.5 ppm (avg. 9.88 ppm) Co and 100 –168 ppm (avg. 132 ppm) Cr. In core G4, section 1, trace metal concentration showed 5 – 60 ppm (avg. 35 ppm) Ni, 57– 67 ppm (avg. 62 ppm) Zn, 49 – 52 ppm (avg. 50 ppm) Cu, 4.75 – 21.5 ppm (avg. 12.69 ppm) Co, 136 – 145 ppm (avg. 140 ppm) Cr; section 2 showed, 24 – 67 ppm (avg. 47 ppm) Ni, 53– 112 ppm (avg. 74 ppm) Zn, 48– 70 ppm (avg. 57 ppm) Cu, 3.25-19.75 ppm (avg. 11.05 ppm) Co and 123 –203 ppm (avg. 166 ppm) Cr and; section 3 showed, 49 – 83 ppm (avg. 61 ppm) Ni, 52– 121 ppm (avg. 92 ppm) Zn, 58 – 70 ppm (avg. 65 ppm) Cu, 10.75-21 ppm (avg. 16.06 ppm) Co and 175 – 206 ppm (avg. 193 ppm) Cr. In core G5, section 1, trace metal concentration showed 39 – 67 ppm (avg. 55 ppm) Ni, 18– 35 ppm (avg. 27 ppm) Zn, 31 – 42 ppm (avg. 37 ppm) Cu, 2.5 – 7 ppm (avg. 4.94 ppm) Co, 69 – 165 ppm (avg. 99 ppm) Cr; section 2 showed, 62 – 112 ppm (avg. 83 ppm) Ni, 41– 62 ppm (avg. 49 ppm) Zn, 46– 59 ppm (avg. 51 ppm) Cu, 8.25-15.75 ppm (avg. 12.38 ppm) Co and 125 –197 ppm (avg. 152 ppm) Cr. In core G6, section 1, trace metal concentration showed 27 – 126 ppm (avg. 47 ppm) Ni, 17– 38 ppm (avg. 27 ppm) Zn, 38 – 50 ppm (avg. 44 ppm) Cu, 2.25 – 21.25 ppm (avg. 8.77 ppm) Co, 157 – 250 ppm (avg. 192 ppm) Cr; section 2 showed, 48 – 86 ppm (avg. 64 ppm) Ni, 23– 55 ppm (avg. 39 ppm) Zn, 44– 61 ppm (avg. 51 ppm) Cu, 3-23.25 ppm (avg. 9.78 ppm) Co and 171 –282 ppm (avg. 204 ppm) Cr.

In core G3 (Fig. 3.2.15), Ni shows slight fluctuating trend from bottom to surface with peak at 4 cm. Zn, Cu and Cr show constant trend in section 1, however they show peak value at 4 and 8 cm (except Cu) in section 2. Fluctuating trend is observed in case of Co from bottom to surface. Trace metals (except Co), show similar distribution pattern to that of Al and Fe in section 1. In section 2, most of the trace metals show similar

distribution pattern to that of Al and Fe, however peak of Zn and Co coincide with peaks of Al, Fe and Mn at 10 cm depth. In core G4 (Fig. 3.2.16), section 1, Ni showed decreasing trend, however it shows an increasing fluctuating trend from section 2 to 3 with a peak value at 24 cm. Zn shows constant values from bottom up to 26 cm depth, followed by a peak at 24 cm depth, further, it shows an increasing trend. Cu and Cr follow similar tend to that of Zn in section 1 and 2. In section 3 they show an increasing trend. Co shows fluctuating trend throughout the core like in core G3. Trace metals (except Co) show similar distribution trend to that of Al, Fe and Mn in section 1 and 2, however, only with Al and Fe in section 3. In core G5 (Fig. 3.2.17), all trace metals show an increasing trend from bottom to surface which is similar to Al, Fe and Mn. In core G6 (Fig. 3.2.18), Ni, Zn and Cu show slight increasing trend from bottom to surface, similar to Al and Fe. Peak values of Ni, Zn and Co concentration at 26 cm largely coincide with Fe. Peak values of trace metals (except Cr) at 10 cm coincide with Al, Fe and Mn. However, Co and Cr show fluctuating trend. However, the peak value of Cr at 38, 28 and 14 cm coincide with the peak of Fe.

Among the mudflat cores collected from upper middle estuarine region, trace metals in core F4 show similar distribution trend and coinciding to almost all the peaks of Al, Fe and Mn. Cr at surface show similar trend to Mn. Higher values of trace metals between 18 cm and 8 cm indicate a diagenetic remobilization, moving upwards from section 2 to 3, thereby suggesting the role of Fe-Mn oxyhydroxides in controlling their distribution. Mn oxide seems to be controlling the distribution of Cr at the surface whereas Fe oxide seems to control the distribution of Ni, Zn, Cu and Co. Trace metals largely follow similar distribution to that of silt, clay and organic carbon. Therefore, organic coating on silt and clay must have facilitated their deposition. Lower values at the surface must be due flushing activities during tidal processes resulting in the diffusion of these metals to the over lying water column. Low values of metals in section 2 could be due to dilution by the higher sand content. In core F5, section 1, Al and Fe seem to be controlling the distribution of all the trace metals, whereas in section 2 and 3, Mn also seem to be controlling the trace metal distribution along with Al and Fe. Trace metals in this core largely follow the distribution of silt, clay and organic carbon, indicating their association. A diagenetic mobilization is noted in section 2 with higher values of trace metals along with Fe and Mn. Section 1 and 3 probably reflects their dilution by sand

and diffusion to overlying water column, respectively. In core F6, an increasing trend of Al and Fe from section 2 to 3 is observed which is also true in case of all trace metals coinciding at all peaks. Trace metals also show similar trend to Mn but only in section 1 and 2, however, in section 3, Mn shows a constant trend with a prominent peak at 6 cm depth. This suggests that Fe-Mn oxides must have controlled the distribution in section 1 and 2 and only Fe oxide in section 3. Trace metals largely follow finer sediments and organic carbon distribution. Higher sand content in section 2 must have diluted the trace metal concentration. In core F7, collected from lower middle region, Al and Fe show decreasing trend in section 1, constant trend in section 2, further increase in section 3. Trace metals follow similar trend to Al, Fe and Mn. Metals follow similar trend to clay indicating the role of clay in their distribution. In core F8, collected from upper middle region, trace metals (except Co) largely follow the distribution of Al, Fe and Mn in section 1 and 3 and only with Al and Fe in section 2. However, at surface, Al, Fe and Mn seem to control Zn, Cu and Cr distribution whereas Ni and Co seem to be from a different source. In section 1, Trace metals largely follow the silt, clay and organic carbon profile, whereas, in section 3, the peaks at 12 cm depth coincide with clay and organic carbon. Therefore, silt, clay and organic carbon along with Al, Fe and Mn played an important role in the distribution of trace metals in section 1 and organic coating on clay along with Al, Fe and Mn played a role in their distribution in section 3.

In the mangroves cores, collected from the upper estuarine region, in core G3, Ni, Zn, Cr and to some extent Cu show similar distribution trend to that of Al and Fe in section 1 and also with Mn in section 2 including Co. Thereby indicating the role of Al and Fe in section 1 and along with Mn in section 2 (including Co) in the distribution of Ni, Zn, Cr and Cu. Co shows fluctuating distribution in section 1 indicating a different source from that of Ni, Zn, Cr and Cu. Distribution of Al, Fe, Mn along with trace metals follow similar trend to finer sediments and organic carbon indicating a lithogenic source (except Mn and Co in section 1). In core G4, Al, Fe and Mn seem to be controlling the distribution of Zn, Cu, and Cr in section 1. In section 2, Ni, Zn, Cu, Cr and to some extent Co follow similar trend to that of Al, Fe and Mn. In section 3, Al and Fe seem to control Ni, Zn and Cr distribution whereas Cu and Co seem to be from different source. Peaks at 32 cm of Co largely coincide with the peak shown by clay profile. In this section, most of the metals (except Cu and Co) follow similar trend to organic carbon

profile indicating their association. Among the core collected from lower middle estuary, in core G5, Al, Fe and Mn seem to control the distribution of all trace metals. However, Mn at 26 and 8 cm seem to control Co distribution. Increasing trend of metals from bottom to top indicate additional input with time. All metals show similar trend to that of finer sediments and organic carbon indicating their association. In core G6, Al and Fe control the distribution of Ni, Zn, Cu and Cr in section 1. From 34 to 10 cm trace metals (except Co) distribution seemed to be controlled by Al, Fe and Mn. At surface, Al and Fe seem to control Ni, Zn and Cu distribution whereas Mn controlled Co distribution. Co shows fluctuating distribution throughout the core. Al, Fe, Ni, Zn, Cu and Cr show similar trend to clay profile whereas, Mn to silt and organic carbon profile.

3.2 C. 1a Pearson's correlation for parameters of bulk sediments in mudflats

Analysis of correlation coefficient among the different chemical components for core F4 (Table 3.2.5a) shows a significant positive correlation of Al with finer sediments, organic carbon, Fe, Mn along with trace metals except Co. Al, Fe and Mn showed positive correlation with each other. Fe showed positive correlation with trace metals except Cu whereas Mn showed positive correlation with trace metals except Cu and Co. In core F5 (Table 3.2.5b), all parameters (except sand) are significant positively correlated with each other. In core F6 (Table 3.2.5c), Al, Fe and Mn are significantly positively correlated with silt, clay (except Mn) and organic carbon. Al, Fe and Mn are positively correlated with each other and all the trace metals. In core F7 (Table 3.2.5d), Al and Fe are significantly positively correlated with finer sediments and organic carbon along with trace metals whereas, Mn is positively correlated only with Cu and Cr. In core F8 (Table 3.2.5e), Al and Fe are positively correlated with finer sediments and organic carbon along with trace metals (except Co).

3.2 C. 1b Pearson's correlation for parameters of bulk sediments in mangroves

In core G3 (Table 3.2.6a), Al and Fe are positively correlated with finer sediments and organic carbon along with trace metals except Co. In core G4 (Table 3.2.6b), Al shows positive correlation with Fe, Mn, Ni, Zn and Cr. However, Fe shows positive correlation with silt and organic carbon along with trace metals except Co. In core G5 (Table 3.2.6c), all parameters (except sand), are positively correlated with each other. In core

G6 (Table 3.2.6d), Al and Mn are positively correlated with finer sediments and organic carbon and Fe correlated to clay. Among the trace metals, Al and Fe are positively correlated with all trace metals except Co and; Mn is positively correlated only with Ni, Zn and Cu.

Al shows significant positive correlation with finer sediments in all the mudflat and mangroves (except core G4). The association of Al with finer grained sediments suggests that the sediments include detrital minerals. Among the mudflat cores, Al, Fe and Mn shows significant positive correlation with each other in cores F4, F5 and F6 and among mangroves, core G4, G5 and G6, probably indicating its lithogenic origin. In core F4, Fe and Mn oxides could have favoured the distribution of Ni, Zn and Cr and only Fe oxide responsible for the distribution of Co. Metals in core F5 and G5 shows a lithogenic origin as all parameters being significantly positively correlated with each other (except sand). Fe cycling are noted to be responsible for the distribution of trace metals in core F7 (lower middle region) and in cores F8, G3 G4 which belong to upper middle region (except Co). Among the cores of lower middle region, Mn cycling responsible for distribution of Cu and Cr in core F7 and for the distribution of Ni, Zn and Cu in core G6. Most of the metals show positive correlation with fine grained sediments, probably due to their adsorption on larger surface area. Mn probably seems to be from a different source in core F6 and Co in most of the cores (except in core F5 and G5). The possible anthropogenic sources of environmental manganese include mining and mineral processing, emissions from alloy, steel, and iron production; combustion of fossil fuels, municipal wastewater discharges and sewage sludge (Howe et al. 2005).

Table 3.2.5 Pearson's correlation between sand, silt, clay, organic carbon (OC) and metals of: (a) core F4, (b) core F5, (c) core F6 (d) core F7 and (e) F8

F4	Sand	Silt	Clay	OC	Al	Fe	Mn	Ni	Zn	Cu	Co	Cr
Sand	1.00											
Silt	-0.95	1.00										
Clay	-0.88	**0.69**	1.00									
OC	-0.74	**0.75**	**0.59**	1.00								
Al	-0.78	**0.74**	**0.68**	**0.87**	1.00							
Fe	-0.55	**0.45**	**0.59**	**0.67**	**0.71**	1.00						

Mn	-0.76	**0.65**	**0.78**	**0.60**	**0.69**	**0.74**	1.00					
Ni	-0.64	**0.59**	**0.60**	**0.76**	**0.82**	**0.66**	**0.68**	1.00				
Zn	-0.80	**0.73**	**0.75**	**0.85**	**0.89**	**0.78**	**0.80**	**0.80**	1.00			
Cu	-0.42	**0.46**	0.26	**0.58**	**0.51**	0.18	0.27	**0.45**	**0.45**	1.00		
Co	-0.32	0.28	0.32	0.36	0.29	**0.42**	0.27	**0.41**	**0.46**	-0.10	1.00	
Cr	-0.65	**0.55**	**0.67**	**0.66**	**0.65**	**0.85**	**0.82**	**0.65**	**0.81**	0.30	0.30	1.00

(a)

F5	Sand	Silt	Clay	OC	Al	Fe	Mn	Ni	Zn	Cu	Co	Cr
Sand	1.00											
Silt	-0.93	1.00										
Clay	-0.85	**0.60**	1.00									
OC	-0.87	**0.87**	**0.65**	1.00								
Al	-0.88	**0.82**	**0.75**	**0.83**	1.00							
Fe	-0.93	**0.86**	**0.80**	**0.87**	**0.94**	1.00						
Mn	-0.75	**0.68**	**0.67**	**0.70**	**0.78**	**0.81**	1.00					
Ni	-0.91	**0.83**	**0.81**	**0.87**	**0.89**	**0.87**	**0.75**	1.00				
Zn	-0.79	**0.68**	**0.76**	**0.69**	**0.76**	**0.84**	**0.85**	**0.75**	1.00			
Cu	-0.62	**0.48**	**0.66**	**0.43**	**0.62**	**0.67**	**0.56**	**0.56**	**0.65**	1.00		
Co	-0.88	**0.81**	**0.77**	**0.85**	**0.91**	**0.86**	**0.72**	**0.96**	**0.74**	**0.58**	1.00	
Cr	-0.87	**0.76**	**0.81**	**0.76**	**0.83**	**0.90**	**0.74**	**0.84**	**0.84**	**0.72**	**0.81**	1.00

(b)

F6	Sand	Silt	Clay	OC	Al	Fe	Mn	Ni	Zn	Cu	Co	Cr
Sand	1.00											
Silt	-0.86	1.00										
Clay	-0.76	0.33	1.00									
OC	-0.67	**0.79**	0.23	1.00								
Al	-0.77	**0.58**	**0.70**	**0.64**	1.00							
Fe	-0.77	**0.68**	**0.56**	**0.86**	**0.90**	1.00						
Mn	-0.51	**0.45**	0.37	**0.47**	**0.64**	**0.56**	1.00					
Ni	-0.71	**0.65**	**0.49**	**0.86**	**0.89**	**0.98**	**0.61**	1.00				
Zn	-0.75	**0.63**	**0.59**	**0.80**	**0.92**	**0.97**	**0.60**	**0.97**	1.00			
Cu	-0.75	**0.68**	**0.52**	**0.86**	**0.90**	**0.98**	**0.54**	**0.98**	**0.98**	1.00		
Co	-0.26	0.34	0.05	**0.66**	**0.52**	**0.68**	**0.55**	**0.77**	**0.68**	**0.69**	1.00	
Cr	-0.72	**0.65**	**0.51**	**0.82**	**0.84**	**0.96**	**0.57**	**0.96**	**0.95**	**0.94**	**0.71**	1.00

(c)

F7	Sand	Silt	Clay	OC	Al	Fe	Mn	Ni	Zn	Cu	Co	Cr
Sand	1.00											
Silt	-0.89	1.00										
Clay	-0.93	**0.66**	1.00									

OC	-0.81	**0.80**	**0.70**	1.00								
Al	-0.80	**0.67**	**0.77**	**0.84**	1.00							
Fe	-0.85	**0.71**	**0.84**	**0.88**	**0.87**	1.00						
Mn	-0.25	0.17	0.27	0.39	**0.53**	**0.45**	1.00					
Ni	-0.67	**0.61**	**0.62**	**0.78**	**0.57**	**0.82**	0.22	1.00				
Zn	-0.75	**0.65**	**0.72**	**0.80**	**0.73**	**0.83**	0.25	**0.81**	1.00			
Cu	-0.79	**0.70**	**0.73**	**0.81**	**0.92**	**0.85**	**0.61**	**0.61**	**0.75**	1.00		
Co	-0.46	0.40	**0.44**	**0.48**	**0.47**	**0.54**	0.33	**0.54**	**0.46**	**0.47**	1.00	
Cr	-0.81	**0.68**	**0.80**	**0.84**	**0.82**	**0.97**	**0.45**	**0.81**	**0.76**	**0.79**	**0.42**	1.00

(d)

F8	Sand	Silt	Clay	OC	Al	Fe	Mn	Ni	Zn	Cu	Co	Cr
Sand	1.00											
Silt	-0.79	1.00										
Clay	-0.67	0.06	1.00									
OC	-0.77	**0.57**	**0.55**	1.00								
Al	-0.80	**0.58**	**0.59**	**0.95**	1.00							
Fe	-0.86	**0.68**	**0.57**	**0.88**	**0.90**	1.00						
Mn	0.12	-0.16	0.01	0.09	0.14	0.19	1.00					
Ni	-0.69	**0.61**	0.38	**0.67**	**0.63**	**0.76**	-0.15	1.00				
Zn	-0.73	**0.68**	0.37	**0.80**	**0.84**	**0.86**	0.38	**0.52**	1.00			
Cu	-0.77	**0.84**	0.23	**0.65**	**0.65**	**0.74**	0.02	**0.68**	**0.69**	1.00		
Co	-0.30	0.16	0.30	0.23	0.32	0.29	-0.37	0.44	-0.05	0.18	1.00	
Cr	-0.72	**0.50**	**0.56**	**0.79**	**0.76**	**0.86**	0.35	**0.67**	**0.80**	**0.59**	0.15	1.00

(e)

Table 3.2.6 Pearson's Correlation between sand, silt, clay, organic carbon (OC) and metals of: a) G3, (b) G4, (c) G5 and (d) G6

G3	Sand	Silt	Clay	OC	Al	Fe	Mn	Ni	Zn	Cu	Co	Cr
Sand	1.00											
Silt	-0.99	1.00										
Clay	-0.78	**0.67**	1.00									
OC	-0.97	**0.96**	**0.73**	1.00								
Al	-0.96	**0.93**	**0.79**	**0.95**	1.00							
Fe	-0.98	**0.96**	**0.78**	**0.97**	**0.95**	1.00						
Mn	-0.38	0.33	**0.48**	0.38	0.33	**0.51**	1.00					
Ni	-0.82	**0.83**	**0.60**	**0.80**	**0.80**	**0.81**	0.14	1.00				
Zn	-0.56	**0.56**	**0.41**	**0.44**	**0.53**	**0.57**	0.34	**0.47**	1.00			
Cu	-0.86	**0.83**	**0.72**	**0.81**	**0.80**	**0.84**	0.41	**0.73**	**0.59**	1.00		
Co	-0.15	0.15	0.13	0.15	0.05	0.12	-0.10	0.37	0.05	0.17	1.00	
Cr	-0.77	**0.70**	**0.81**	**0.74**	**0.76**	**0.73**	0.32	**0.64**	**0.54**	**0.78**	0.37	1.00

(a)

G4	Sand	Silt	Clay	OC	Al	Fe	Mn	Ni	Zn	Cu	Co	Cr
Sand	1.00											
Silt	-0.93	1.00										
Clay	-0.94	**0.75**	1.00									
OC	-0.76	**0.73**	**0.69**	1.00								
Al	-0.24	0.40	0.08	0.19	1.00							
Fe	-0.43	**0.58**	0.24	**0.48**	**0.81**	1.00						
Mn	-0.37	**0.45**	0.26	0.32	**0.55**	**0.49**	1.00					
Ni	-0.78	**0.80**	**0.67**	**0.66**	**0.64**	**0.71**	**0.47**	1.00				
Zn	-0.50	**0.57**	0.37	**0.58**	**0.74**	**0.91**	**0.42**	**0.73**	1.00			
Cu	-0.66	**0.59**	**0.64**	**0.68**	0.31	**0.49**	0.27	**0.68**	**0.69**	1.00		
Co	-0.39	0.30	0.41	0.13	-0.01	0.14	0.24	0.05	0.10	0.22	1.00	
Cr	-0.62	**0.63**	**0.54**	**0.75**	**0.52**	**0.75**	0.38	**0.73**	**0.85**	**0.87**	0.17	1.00

(b)

G5	Sand	Silt	Clay	OC	Al	Fe	Mn	Ni	Zn	Cu	Co	Cr
Sand	1.00											
Silt	-0.99	1.00										
Clay	-0.99	**0.97**	1.00									
OC	-0.98	**0.96**	**0.98**	1.00								
Al	-0.97	**0.96**	**0.96**	**0.96**	1.00							
Fe	-0.97	**0.95**	**0.97**	**0.99**	**0.98**	1.00						
Mn	-0.90	**0.88**	**0.91**	**0.91**	**0.85**	**0.90**	1.00					
Ni	-0.83	**0.79**	**0.86**	**0.84**	**0.84**	**0.86**	**0.66**	1.00				
Zn	-0.96	**0.94**	**0.97**	**0.96**	**0.96**	**0.97**	**0.87**	**0.89**	1.00			
Cu	-0.96	**0.94**	**0.96**	**0.96**	**0.98**	**0.98**	**0.84**	**0.90**	**0.97**	1.00		
Co	-0.96	**0.94**	**0.96**	**0.96**	**0.95**	**0.98**	**0.94**	**0.80**	**0.95**	**0.95**	1.00	
Cr	-0.92	**0.92**	**0.91**	**0.91**	**0.95**	**0.90**	**0.77**	**0.80**	**0.88**	**0.90**	**0.87**	1.00

(c)

G6	Sand	Silt	Clay	OC	Al	Fe	Mn	Ni	Zn	Cu	Co	Cr
Sand	1.00											
Silt	-0.92	1.00										
Clay	-0.96	**0.77**	1.00									
OC	-0.71	**0.66**	**0.67**	1.00								
Al	-0.79	**0.67**	**0.79**	**0.62**	1.00							
Fe	-0.44	**0.48**	0.36	0.29	**0.64**	1.00						
Mn	-0.63	**0.76**	**0.47**	**0.61**	**0.50**	**0.45**	1.00					
Ni	-0.34	0.37	0.28	0.30	**0.46**	**0.55**	**0.54**	1.00				
Zn	-0.44	**0.55**	0.30	**0.47**	**0.54**	**0.58**	**0.71**	**0.57**	1.00			
Cu	-0.61	**0.60**	**0.55**	0.40	**0.78**	**0.75**	**0.56**	**0.56**	**0.58**	1.00		

Co	-0.02	0.00	0.04	-0.17	0.24	0.30	0.20	0.39	0.23	0.28	1.00	
Cr	-0.26	0.19	0.29	-0.04	**0.44**	**0.64**	0.00	0.40	0.17	**0.61**	0.04	1.00

(d)

3.2 D Enrichment Factor (EF) and Pollution Load Index (PLI)

Table 3.2.7 Enrichment Factor (EF) and Pollution Load Index (PLI)

Core	Fe(EF)	Mn(EF)	Ni(EF)	Zn(EF)	Cu(EF)	Co(EF)	Cr(EF)	PLI
F4	0.8	0.2	1.2	0.4	1.0	0.8	1.2	0.8
F5	1.0	0.3	**2.4**	0.8	**1.6**	**2.2**	**2.6**	1.0
F6	1.0	0.2	**2.4**	0.7	1.5	1.0	**2.9**	1.1
F7	0.7	0.4	1.1	0.8	**2.8**	1.2	**1.9**	0.5
F8	0.7	0.4	1.4	0.6	**2.7**	1.1	1.4	0.5
G3	1.3	0.6	**1.9**	0.8	**1.8**	0.9	**2.6**	0.6
G4	0.9	0.2	1.0	0.8	1.4	0.7	**2.0**	0.8
G5	0.9	0.3	1.7	0.5	1.3	0.5	1.7	0.7
G6	1.2	0.2	**1.8**	0.6	**1.7**	0.8	**3.6**	0.6

Further, from Enrichment Factor and Pollution Load Index table, (Table 3.2.7) it is noticed that there is minor enrichment of Ni in core F5, F6, G3, G5 and G6, Cu in core F5, F7, F8, G3 and G6; Co in core F5, Cr in core F5, F6, F7, G3, G4 and G6. However, from PLI results, it is observed that there is no high metal loading at any of the core locations.

3.2 E Comparison between estuaries

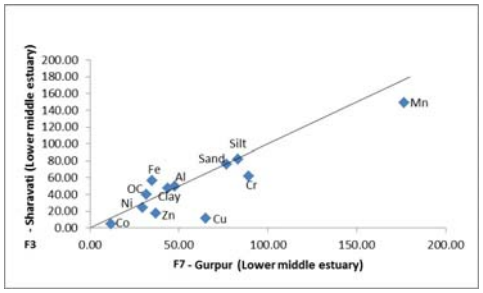

Fig. 3.2.19 Isocon plot for mudflat cores in lower middle regions

When the cores of lower middle estuaries of Gurpur and Sharavati were compared (Fig. 3.2.19), Mn along with all trace metals are noted to be higher in Gurpur estuary whereas Al, Fe along organic carbon associated with clay is found to be enriched in Sharavati estuary.

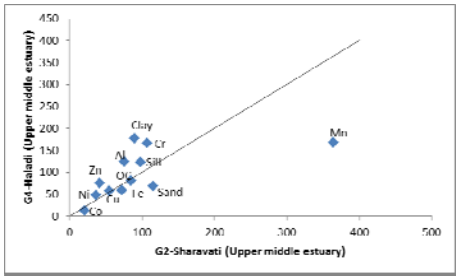

Fig. 3.2.20 Isocon plot for mangrove cores in upper middle regions

When the cores of upper middle estuaries of Sharavati and Haladi were compared (Fig. 3.2.20), sand along with, Fe, Mn and Co are noted to be higher in Sharavati, whereas, Al along organic carbon associated with silt and clay and trace metals Ni, Zn, Cu and Cr are found to be enriched in Haladi estuary. From the above observations, it is clear that, higher hydrodynamic energy conditions prevalent in larger estuaries is responsible for retaining coarser sediments, whereas, calmer hydrodynamic conditions in the smaller estuaries facilitate deposition of finer sediments, organic carbon and most of the trace metals.

3.3 Section III

Distribution of metals in sediments of different particle size (sand, medium silt and clay)

Estuarine mudflats are preferential sites for deposition of fine sediments (Singh and Nayak 2009) and adjacent mangrove sediments are generally known to retain large amount of organic matter which are from various sources viz. terrestrial, marine and atmospheric (Wu et al. 2011). Sediments constitute different size classes which act as potential binding phases for metals to accumulate in the estuarine system. The organic matter associated with the finer sediments provides favourable conditions for the accumulation of metals (Spencer et al. 2003). In addition, Fe-Mn oxide and organic matter are considered important phases which influence the metal transport and its distribution (Tribovillard et al. 2006). Metals deposited within the sediments may be later released to the overlying water column by the process of diffusion either due to diagenesis or physical disturbances (Jones and Turki 1997).

Concentration of various metals is in sediments strongly influenced by the texture of sediment particles of all sizes ranging from clay to sand. Once settled, finer sediments provide large surface area and therefore facilitate concentration of metals readily (Nobi et al. 2010). However, metals also get adsorbed on to the coarser sediment particles (Aloupi and Angelidis 2002). The ability of mobilization of metals depends on the properties of the different size fractions (sand, silt and clay) of sediments. Therefore an attempt has been made to understand the role of different sediment size fractions in the distribution and abundance of metals, and to know the level of metal accumulation leading to pollution.

The distribution of metals within sediment will depend on the property of each sediment size fraction. Thus the investigation on the metals associated with different size fractions, namely sand, silt and clay is important in understanding the role and its ability to retain the metals within the sediments. Here, an attempt has been made to understand the distribution of metals in different sediment size fractions {viz. sand (4Ø), medium silt [silt+clay] (6Ø) and clay (8Ø)} in mangrove and mudflat core sediments. When the average values of metals in different size fractions (viz. sand, medium silt

and clay) of entire core were compared (Table 3.3.1 a, b), it was noted that most of the metals were enriched in the finer sediments except Mn in core F3.

Table 3.3.1. Average value of metals in sand (4Ø), medium silt (6Ø) and clay (8Ø) fraction in: a) mudflat core (F3) and b) mangrove core (G1)

(a)

Sediment size fraction	Al (avg)	Fe (avg)	Mn (avg)	Ni (avg)	Zn (avg)	Cu (avg)	Co (avg)	Cr (avg)
Sand	3	1	123	13	5	8	3	56
Silt	8	6	56	47	133	139	11	178
Clay	12	5	69	48	368	517	10	303

(b)

Sediment size fraction	Al (avg)	Fe (avg)	Mn (avg)	Ni (avg)	Zn (avg)	Cu (avg)	Co (avg)	Cr (avg)
Sand	2	0.5	103	2	11	10	7	39
Silt	6	3	102	21	110	63	17	143
Clay	7	3	160	37	320	137	20	120

3.3.1a Distribution of metals in the sand fraction (4Ø)

In core F3 (Table 3.3.2 a), it is seen that the percentage of sand decreases i. e. from section 1 to section 3 of the core from the bottom to the surface. This is also true in the case of Mn and Cu distribution. In core G1 (Table 3.3.3 a), it is noticed that sand percentage decreases from the bottom up to the surface, similar to core F3. Similar distribution is also seen in case of Co in this core. From the correlation analysis (Tables 3.3.4a and 3.3.5a), it is noticed that sand shows poor correlation with all the components in both the cores. However, Al shows significant positive correlation with Cr; Fe is significantly positively correlated with Mn and Co; and Mn with Cu in core F3 (Table 3.3.4a) and in core G1, Al is significantly positively correlated only with Ni, Zn and Cu (Table 3.3.5a).

Table 3.3.2. Average value of metals in three different sections with depth in:
a) sand (4Ø), b) medium silt (6Ø) and c) clay (8Ø) fraction in mudflat core (F3)

(a)

section	Sand (%)	OC (%)	Al (%)	Fe (%)	Mn (ppm)	Ni (ppm)	Zn (ppm)	Cu (ppm)	Co (ppm)	Cr (ppm)
3	57	1.5	3	1	93	20	7	5	3	121
2	64	1.2	3	1	119	13	4	7	3	39
1	89	0.3	3	1	136	11	6	9	3	45

(b)

section	Silt (%)	OC (%)	Al (%)	Fe (%)	Mn (ppm)	Ni (ppm)	Zn (ppm)	Cu (ppm)	Co (ppm)	Cr (ppm)
3	20	1.5	9	7	69	57	115	133	12	309
2	13	1.2	15	8	82	57	135	145	14	274
1	1	0.3	4	4	35	37	137	137	9	71

(c)

section	Clay (%)	OC (%)	Al (%)	Fe (%)	Mn (ppm)	Ni (ppm)	Zn (ppm)	Cu (ppm)	Co (ppm)	Cr (ppm)
3	23	1.5	13	7	98	49	226	273	12	332
2	23	1.2	15	7	70	77	166	229	13	514
1	10	0.3	9	4	59	28	550	791	8	153

3.3.1b Distribution of metals in the medium silt fraction (6Ø)

This fraction delineates the metals associated with both, silt and clay fraction. It is seen from table 3.3.2b for core F3, that the percentage of silt and organic carbon is higher in the upper two sections as compared to section 1. Similar distribution is also seen in case of the metals except Zn and Cu. In section 2, it is observed that concentration of Al, Fe and Mn are higher along with Cu and Co. In core G1 (Table 3.3.3b), it is noticed that all the metals are enriched in section 2 and 3 with higher concentration in section 2. From the correlation analysis (Table 3.3.4 b), Silt shows good association with organic carbon, Al, Fe and almost all trace metals except Zn and Cu in core F3, whereas, in core G1 (Table 3.3.5 b), silt is significantly positively correlated only with Al. However, in this fraction, in core F3, Al, Fe and Mn show significant positive correlation with each other and trace metals except Ni and Cu. In core G1, Al, Fe and Mn show good association with each other. In this core, Al also shows good correlation with all trace metals except Cu; Fe is associated only with Ni and Co, whereas, Mn is associated with Ni, Cu and Co.

Table 3.3.3. Average value of metals in three different sections with depth in:
a) sand (4Ø), b) medium silt (6Ø) and c) clay (8Ø) fraction in mangrove core (G1)

(a)

section	Sand (%)	OC (%)	Al (%)	Fe (%)	Mn (ppm)	Ni (ppm)	Zn (ppm)	Cu (ppm)	Co (ppm)	Cr (ppm)
3	72	1	2	0.6	111	5	13	13	4	28
2	79	0.4	1.9	0.4	94	1.2	11	11	6	53
1	89	0.2	1.7	0.4	108	1.1	11	7	9	31

(b)

section	Silt (%)	OC (%)	Al (%)	Fe (%)	Mn (ppm)	Ni (ppm)	Zn (ppm)	Cu (ppm)	Co (ppm)	Cr (ppm)
3	6.4	1	8	4	119	29	123	50	19	120
2	6.5	0.4	10	4.3	152	33	129	78	23	266
1	0.7	0.2	1.4	0.4	43	6	85	54	10	31

(c)

section	Clay (%)	OC (%)	Al (%)	Fe (%)	Mn (ppm)	Ni (ppm)	Zn (ppm)	Cu (ppm)	Co (ppm)	Cr (ppm)
3	22	1	10	5.3	173	46	243	87	24	167
2	15	0.4	9	3	132	39	185	94	17	128
1	10	0.2	4.5	2.9	181	29	495	206	22	89

3.3.1c Distribution of metals in the clay fraction (8Ø)

In core F3 (Table 3.3.2c) and core G1 (Table 3.3.3c) higher percentage of clay and organic carbon is observed in the upper two sections as compared to section 1. Similar distribution is also seen in case of the metals except Zn and Cu in core F3. However in section 2 of core F3, it is observed that the concentration of Al, Fe, Ni, Co and Cr are higher compared to section 1 and 3. In core G1, Al and Fe along with all metals except Mn, Zn and Cu were found to be higher in section 3. In core F3 (Table 3.3.4c) clay is significantly positively correlated with organic carbon, Al and Fe, Ni, Co, Cr; however, only with organic carbon in case of core G1 (Table 3.3.5c). In this fraction of core F3, Al is strongly associated with Fe, Co and Cr; Fe is associated with Ni, Co and Cr. However, in case of core G1, Ni is found to be associated with Al and Fe.

Table 3.3.4. Pearson's correlation between organic carbon and metals in:
(a) sand (4Ø) (b) medium silt (6Ø) and (c) clay (8Ø) fraction of mudflat core (F3)
(a)

	Sand	OC	Al	Fe	Mn	Ni	Zn	Cu	Co	Cr
Sand	1.00									
OC	-0.96	1.00								
Al	0.07	-0.13	1.00							
Fe	-0.16	0.20	0.22	1.00						
Mn	0.35	-0.20	-0.28	**0.58**	1.00					
Ni	-0.55	0.47	0.32	0.38	-0.24	1.00				
Zn	0.44	-0.55	0.42	0.45	0.16	0.31	1.00			
Cu	0.39	-0.25	-0.35	0.30	**0.66**	-0.24	-0.05	1.00		
Co	0.39	-0.48	0.39	**0.60**	0.37	0.06	**0.66**	0.32	1.00	
Cr	-0.16	0.08	**0.67**	0.24	-0.27	**0.71**	0.53	-0.42	0.18	1.00

(b)

	Silt	OC	Al	Fe	Mn	Ni	Zn	Cu	Co	Cr
Silt	1.00									
OC	**0.93**	1.00								
Al	**0.90**	**0.96**	1.00							
Fe	**0.63**	**0.85**	**0.79**	1.00						
Mn	0.36	0.57	**0.62**	**0.61**	1.00					
Ni	**0.62**	**0.83**	**0.77**	**0.95**	**0.65**	1.00				
Zn	0.05	-0.10	-0.03	-0.37	-0.01	-0.38	1.00			
Cu	0.10	-0.06	0.00	-0.35	0.07	-0.33	**0.97**	1.00		
Co	**0.62**	**0.83**	**0.84**	**0.90**	**0.71**	**0.95**	-0.26	-0.24	1.00	
Cr	**0.87**	**0.90**	**0.86**	**0.72**	**0.60**	**0.81**	-0.06	0.01	**0.78**	1.00

(c)

	Clay	OC	Al	Fe	Mn	Ni	Zn	Cu	Co	Cr
Clay	1.00									
OC	**0.93**	1.00								
Al	**0.80**	**0.77**	1.00							
Fe	**0.69**	**0.81**	**0.76**	1.00						
Mn	-0.06	0.12	-0.01	0.45	1.00					
Ni	**0.76**	**0.84**	0.54	**0.61**	0.11	1.00				
Zn	-0.53	-0.42	-0.56	-0.64	-0.33	-0.34	1.00			
Cu	-0.51	-0.50	-0.64	-0.70	-0.22	-0.41	**0.64**	1.00		
Co	**0.87**	**0.90**	**0.72**	**0.84**	0.34	**0.75**	-0.57	-0.61	1.00	
Cr	**0.79**	**0.77**	**0.93**	**0.61**	-0.12	**0.59**	-0.36	-0.45	**0.66**	1.00

*In bold, correlations are significant at $p < 0.05$, n=12

Table 3.3.5. Pearson's correlation between organic carbon and metals in:
(a) sand (4Ø) (b) medium silt (6Ø) and (c) clay (8Ø) fraction of mangrove core (G1)

(a)

	Sand	OC	Al	Fe	Mn	Ni	Zn	Cu	Co	Cr
Sand	1.00									
OC	-0.82	1.00								
Al	-0.68	0.56	1.00							
Fe	-0.49	0.39	0.18	1.00						
Mn	0.08	-0.17	0.29	-0.07	1.00					
Ni	-0.73	**0.75**	**0.75**	0.31	0.32	1.00				
Zn	-0.42	0.42	**0.77**	-0.06	0.52	**0.77**	1.00			
Cu	-0.15	0.00	**0.65**	0.18	0.41	0.11	0.45	1.00		
Co	0.61	-0.39	-0.55	-0.16	0.10	-0.38	-0.17	-0.23	1.00	
Cr	-0.36	0.21	-0.09	-0.07	-0.57	-0.20	-0.16	-0.13	-0.39	1.00

(b)

	Silt	OC	Al	Fe	Mn	Ni	Zn	Cu	Co	Cr
Sand	1.00									
OC	0.59	1.00								
Al	**0.65**	0.16	1.00							
Fe	0.22	-0.02	**0.79**	1.00						
Mn	0.41	-0.02	**0.90**	**0.92**	1.00					
Ni	0.55	0.01	**0.96**	**0.78**	**0.90**	1.00				
Zn	0.04	-0.21	**0.64**	0.56	0.59	**0.71**	1.00			
Cu	0.04	-0.42	0.51	0.45	**0.65**	0.51	0.42	1.00		
Co	0.19	-0.26	**0.80**	**0.65**	**0.79**	**0.87**	**0.79**	**0.72**	1.00	
Cr	0.18	0.18	**0.68**	0.57	0.61	0.57	**0.70**	0.54	**0.69**	1.00

(c)

	Clay	OC	Al	Fe	Mn	Ni	Zn	Cu	Co	Cr
Clay	1.00									
OC	**0.80**	1.00								
Al	0.29	0.31	1.00							
Fe	0.30	0.31	0.54	1.00						
Mn	0.11	-0.23	-0.24	0.00	1.00					
Ni	0.50	0.40	**0.94**	**0.67**	-0.09	1.00				
Zn	-0.25	-0.37	-0.79	-0.08	0.36	-0.60	1.00			
Cu	-0.37	-0.33	-0.88	-0.39	0.41	-0.88	**0.68**	1.00		
Co	0.22	-0.13	0.22	0.31	0.52	0.31	0.08	0.05	1.00	
Cr	0.44	0.13	0.55	0.19	-0.01	0.51	-0.64	-0.50	0.28	1.00

*In bold, correlations are significant at $p < 0.05$, n=10

Previous studies have demonstrated that grain size is a major factor in controlling metal concentration in sediments (Lin et al. 2002; Liaghati et al. 2003; Neto et al. 2006; Aprile and Bouvy 2008; Nobi et al. 2010). In the sand fraction, decrease in sand, Mn and Cu content from bottom to surface in core F3 (Table 3.3.2a) and; sand and Co in G1 (Table 3.3.3a) indicates association of these metals with sand grains. Further, in this fraction, significant positive correlation of Al with Cr; Fe with Mn and Co; Mn with Cu in core F3 (Table 3.3.4a) and; Al with Ni, Zn, Cu; organic carbon with Ni in core G1 (Table 3.3.5a), indicates role of Al, Fe, Mn in the distribution of Cr, Co and Cu in core F3 and Al in the distribution of Ni, Zn and Cu in core G1. This further indicates detrital source to core G1 and the role of alumino-silicate with Fe-Mn cycling in case of core F3. Volvoikar and Nayak (2013b) stated that trace metals may also be associated with silt fraction along with clay fraction. In the silt fraction, organic carbon and most of the metals are highly

concentrated in section 2 and 3 compared to section 1 in both the cores (Table 3.3.2b, 3.3.3b). Further, silt and organic carbon are correlated with Al, Fe, Ni, Co and Cr whereas Zn and Cu are not showing association with any other parameters in core F3 (Table 3.3.4b). In core G1 (Table 3.3.5b), silt shows significant positive correlation with Al. However, organic carbon shows negative correlation with metals indicating no role in metal distribution. Al, Fe and Mn show significant positive correlation with each other and with trace metals. The distribution of metals in silt, therefore, is regulated by alumino-silicates of detrital origin in both the cores. However, in mudflat, organic matter association and degradation seems to play a role in distribution of metals along with Fe and Mn cycling in core F3. It is noticed that silt and organic carbon do not play a role in controlling the distribution of Zn and Cu in both the cores. In case of mangroves, no role of organic matter is noted in the silt fraction. In the clay fraction, of core F3 (Table 3.3.2c), organic carbon and metals are highly concentrated in section 2 and 3 except Zn and Cu. However Al, Fe, Ni, Co and Cr are higher in section 2. Further, clay and organic carbon are correlated with Al, Fe, Ni, Co and Cr (Table 3.3.4c). Al and Fe show significant positive correlation with Co and Cr whereas Ni is significantly correlated only with Fe. In case of core G1 (Table 3.3.3c), higher content of organic carbon and metals are observed in section 2 and 3 as compared to section 1. Al and Fe along with all trace metals, except Mn, Zn and Cu are higher in section 3. Further in this fraction Al and Fe are significantly associated only with Ni (Table 3.3.5c). Therefore alumino-silicates of detrital origin along with Fe cycling play an important role in the distribution of metals in clay fraction in both the cores. Organic carbon associated with clay fraction and its degradation governs the distribution of metals in core F3. Humic Acids released after the degradation of organic matter play important role in the metal distribution in sediments. It is dependent upon the metal concentration and pH (Anuradha et al. 2011). Some metals preferentially bind on the humic acids at specific pH. It is believed that small materials can get easily trapped inside voids within the humic acid molecules (Schulten and Schnitzer 1995). Calace et al. (2006) had studied the sorptional capacity of humic acids at varying pH from 2 to 6 and had established that the adsorption increased as the pH increased from 2 to 6. It was observed that maximum adsorption is at almost neutral pH by Anuradha et al. (2011). In case of mangroves, organic carbon does not play a role in metal distribution. High metal concentration is associated with clay fraction of section 2 in mudflat and section 3 in mangrove sediments.

From the above discussion, it is clear that the distribution of Cu is regulated by Mn coating on sand in core F3. Further, association of Al with other metals indicates lithogenic source and consists of feldspars in addition to quartz grains. Compared to silt and clay, role of sand is less in distribution of metals as particles in the size range of coarse silt to fine sand are generally composed of quartz and feldspars, which have relatively low metal concentrations (Ackerman 1980; Forstner 1982; Gibbs 1977). Silt in both the cores and clay in mudflat core along with organic carbon are responsible in retaining higher concentration of metals in section 2. Organic carbon increases along with finer fraction and decreases with increasing coarser fraction in the sediments (Kumar and Sheela 2014) due to their similarity in settling velocity. Association of organic carbon with clay fraction is of particular significance in estuarine sediments (Nair and Ramchandran 2002). Greater accumulation of organic carbon is found along with clay due to larger surface area for the adsorption of organic carbon (Rajamanickam and Setty 1973). Early diagenetic mobilization is responsible for higher concentration of metals in section 3 of mangrove sediments. However, in case of mudflat, metals are probably diffused to water column from section 3 due to higher rate of flushing compared to mangroves.

3.3.2 Enrichment Factor and Pollution Load Index (PLI)

Table 3.3.6: Enrichment Factor (EF) and Pollution Load index (PLI) of metals in bulk sediment and three different fractions of sediment of mudflat core (F3) and mangrove core (G1)

	Fe (EF)	Mn (EF)	Ni (EF)	Zn (EF)	Cu (EF)	Co (EF)	Cr (EF)	PLI
F3 (bulk)	1.0	0.3	0.8	0.3	0.4	0.4	1.1	0.3
G1 (bulk)	0.8	0.4	0.6	0.5	0.6	0.6	1.5	0.2
F3 (Sand)	0.9	0.5	0.8	0.2	0.5	0.5	1.8	0.1
F3 (medium Silt)	1.5	0.1	1.3	2.6	5.6	0.8	2.0	0.7
F3 (Clay)	0.8	0.1	0.7	5.5	15.5	0.4	2.3	1.03
G1 (Sand)	0.5	0.6	0.2	0.6	1.0	1.8	2.1	0.1
G1 (medium Silt)	0.7	0.2	0.6	2.9	4.2	2.0	2.2	0.6
G1 (Clay)	1.0	0.3	0.9	5.7	5.2	1.4	1.7	1.0

Considering metal associations, with sediment particle size, effort was made to understand their enrichment. It is known from literature that, if an EF value is between 0.5 and 1.5, it suggests natural input and if EF value is greater than 1.5, it suggest anthropogenic input of metals (Sarkar et al. 2011). In the present study, average EF

value of Cr in all the three fractions of both the cores is greater than 1.5 (Table 3.3.6) suggesting anthropogenic input. Higher EF values of Zn and Cu are observed in the silt and clay fraction of mudflat core, whereas Zn, Cu, Co and Cr are enriched in the silt and clay fraction of mangrove core. However, EF values computed for bulk sediments do not exceed 1.5.

The PLI value of > 1 is considered to be polluted, whereas <1 indicates no pollution. The average PLI for metals in the bulk sediments is less than 1 whereas, in clay fraction; it's equal to 1 in both the cores. This suggests the role of clay in the metal enrichment in sediments due to its large surface area and also the organic matter associated with it.

Table 3.3.7. Average values of metals in the bulk sediments of mudflat and mangrove environment.

Core	Fe (%)	Mn (ppm)	Ni (ppm)	Zn (ppm)	Cu (ppm)	Co (ppm)	Cr(ppm)
F3	3	149	**24**	17	11	5	**62**
G1	1.6	130	11	17	9	4	52

Table 3.3.8a Screening Quick Reference Table (SQUIRT) for metals in marine sediments (Buchman, 1999)

Elements	Threshold Effect Level (TEL)	Effects Range Low (ERL)	Probable Effects Level (PEL)	Effects Range Median (ERM)	Apparent Effects Threshold (AET)
Fe	-	-	-	-	22 % (Neanthes)
Mn	-	-	-	-	260 (Neanthes)
Ni	15.9	20.9	42.8	51.6	110 (Echinoderm Larvae)
Zn	124	150	271	410	410 (Infaunal community)
Cr	52.3	81	160.4	370	62 (Neanthes)
Cu	18.7	34	108.2	270	390 (Microtox and Oyster larvey)
Co	-	-	-	-	10 (Neanthes)

Table 3.3.8b Sediment guidelines and terms used in SQUIRT.

Sediment Guidelines	
Threshold Effect Level (TEL)	Maximum concentration at which no toxic effects are observed
Effects Range Low (ERL)	10^{th} percentile values in effects or toxicity may begin to be observed in sensitive species
Probable Effects Level (PEL)	Lower limit of concentrations at which toxic effects are observed

Efects Range Median (ERM)	50th percentile value in effects
Apparent Effects Threshold (AET)	Concentration above which adverse biological impacts are observed.

The average total metal concentration in sediments (Table 3.3.7) and metals in three fractions was compared with SQUIRT's table (Table 3.3.8). In the total metal concentration Ni value fell in the range between Effects Range Low (ERL) and Probable Effects Level (PEL), whereas Cr is between TEL and ERL value in core F3. However, values of metal concentration in core G1 are below the Threshold Effect Level (TEL) value. In the three fractions, in sand (Table 3.3.1a), Cr fell between TEL and Effects Range Low (ERL) value in core F3. Further, in silt fraction, Zn fell between TEL and Effects Range Low (ERL) whereas Ni and Cu fell between Probable Effects Level (PEL) and Effects Range Median (ERM) value which seem to be less toxic. However, Co exceeded the Apparent Effects Threshold (AET) value probably indicating harm to the biota than Ni, Zn and Cu. In clay fraction, Co is equal to the AET whereas, Cu exceeded the Apparent Effects Threshold (AET) value. In this core, Ni, Zn and Cr values fell between PEL and ERM. In core G1, in sand fraction (Table 3.3.1b), all values of metals are below the toxic levels. In silt fraction, Ni and Cu fell between ERL and PEL value; however Co exceeded AET value; Cr fell between ERL and PEL. In clay fraction, only Ni fell between ERL and PEL; Zn and Cu fall between PEL and ERM; and Co value again exceeded the AET value. Cr value fell between ERL and PEL.

Among the different sections, in core F3, in sand fraction (Table 3.3.2a), Ni value fell between TEL and ERL and; Cr between ERL and PEL in section 3. Metals attached to sand is considered to be from an anthropogenic source and hence loosely bound which can be easily mobilised. In silt fraction (Table 3.3.2b), in section 1, Zn and Cr fell between TEL and ERL; Ni fell between ERL and PEL and; Cu fall between PEL and ERM. In section 2, Zn fell between TEL and ERL; Cu and Cr between PEL and ERM; Ni exceeded the ERM value and Co exceeded AET value. In section 3, Cu and Cr fell between PEL and ERM, however, Ni exceeded ERM value whereas, Co exceeded AET value. In clay fraction (Table 3.3.2c), in section 1, Ni fell between ERL and PEL whereas, Zn and Cu exceed AET value; Cr fall between ERL and PEL. In section 2, Zn fell between ERL and PEL, Cu fell between PEL and ERM and; Ni and Cr exceeds ERM value. Co exceeds AET value. In section 3, Zn fell between ERL and PEL, Ni and

Cr fell between PEL and ERM and Cu exceeds ERM value. Co is found to exceed AET value.

In core in core G1, in sand fraction (Table 3.3.3a), Cr fell between TEL and ERL in section 2. In silt fraction (Table 3.3.3b), in section 1, Cu fell between ERL and PEL; and Co is equal to the AET value. In section 2, Zn fell between TEL and ERL; Ni and Cu between ERL and PEL; Cr fell between PEL and ERM; and Co exceeds AET value. In section 3, Ni, Cu and Cr fell between ERL and PEL, however Co exceeds AET value. In clay fraction (Table 3.3.3c), in section 1, Ni and Cr fell between ERL and PEL whereas, Cu falls between PEL and ERM; Zn and Co exceed AET value. In section 2, Ni, Zn and Cu fell between ERL and PEL. Co is found to exceed AET value. In section 3, Zn and Cu fell between ERL and PEL, Ni and Cr fell between PEL and ERM value. Co exceeds AET value. Values below ERM are considered to be less toxic as compared to those which exceed the AET values hence; Co is more toxic than other metals in both the cores.

3.4 Section IV

Speciation of metals

The study of elemental speciation in environment is a significant step in understanding the potential environmental pollution risk, mobility and bioavailability of pollutants (Tuzen 2003). Elemental speciation helps in understanding the different phases in which an element exists in the environment. Metals available in the bioavailable phases (exchangeable > carbonate > Fe-Mn oxide > organic bound fraction) are loosely attached and are easily available to the biota. To understand to know the processes governing metal bioavailability, speciation study was carried out on redox sensitive elements (Fe and Mn) together with trace metals Ni, Zn, Cu, Co and Cr.

3.4.1 Mudflats

3.4.1.1 Lower estuarine region

3.4.1.1A Iron (Fe) and Manganese (Mn)

The speciation analysis of core F1 revealed that, Fe was mainly found to be associated in the residual fraction which ranges from 92 to 97 % (avg. 95 %) (Table 3.4.1). Next to residual fraction, Fe is mainly bound to Fe-Mn oxides fraction ranging from 3 to 8 % (avg. 4 %). Fe concentration in the exchangeable, carbonate and organic bound are found to be very low ranging from 0.003 to 0.053 % (avg. 0.13 %), 0.005 to 0.013 % (avg. 0.009 %) and 0.09 to 0.59 % (avg. 0.25 %) respectively. From the vertical variation it was noted that Fe in the bioavailable fractions was relatively high at 18 cm depth (Fig. 3.4.1). Manganese concentration in the residual fraction of core F1 ranges from 58 to 81 % (avg. 75 %). Next to residual, Mn was found to be associated with Fe-Mn oxides fraction ranging from 8 to 13 % (avg. 11 %). Mn concentration in the bioavailable fractions was also found to be low. In exchangeable fraction, carbonate bound fraction and organic bound fraction it ranges from 0.19 to 30 % (avg. 8 %), 4 to 8 % (avg. 5 %) and 0.24 to 1.76 % (avg. 0.77 %). From the vertical variation it is noted that Mn in bioavailable fractions was highest at 14 cm depth.

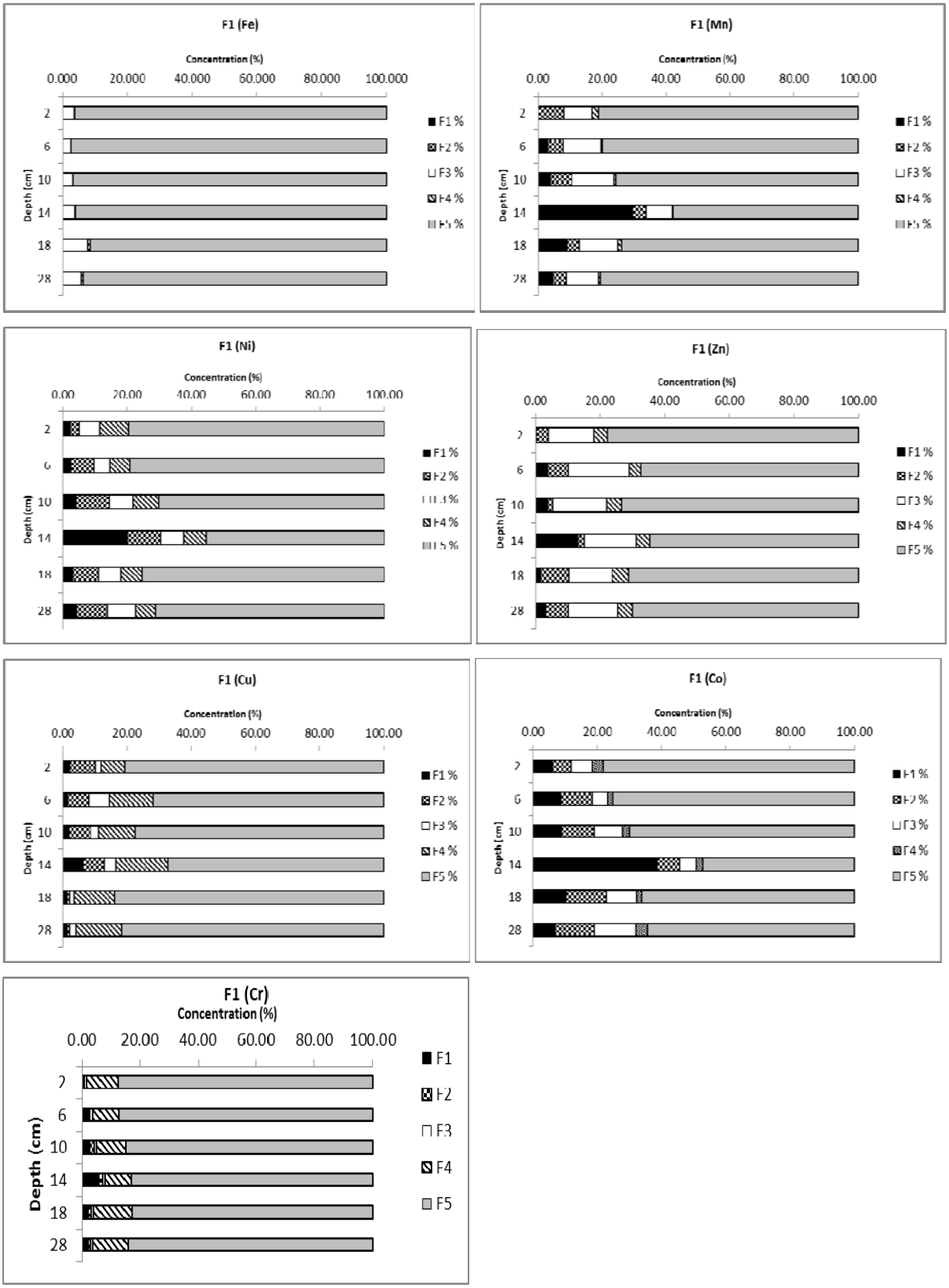

Fig. 3.4.1 Extractable contents of Fe, Mn, Ni, Zn, Cu, Co and Cr in Tessier sequential extraction protocol for core F1 F1 exchangeable fraction, F2 carbonate bound fraction, F3 Fe – Mn oxide fraction, F4 organic / sulfide bound fraction, F5 residual fraction

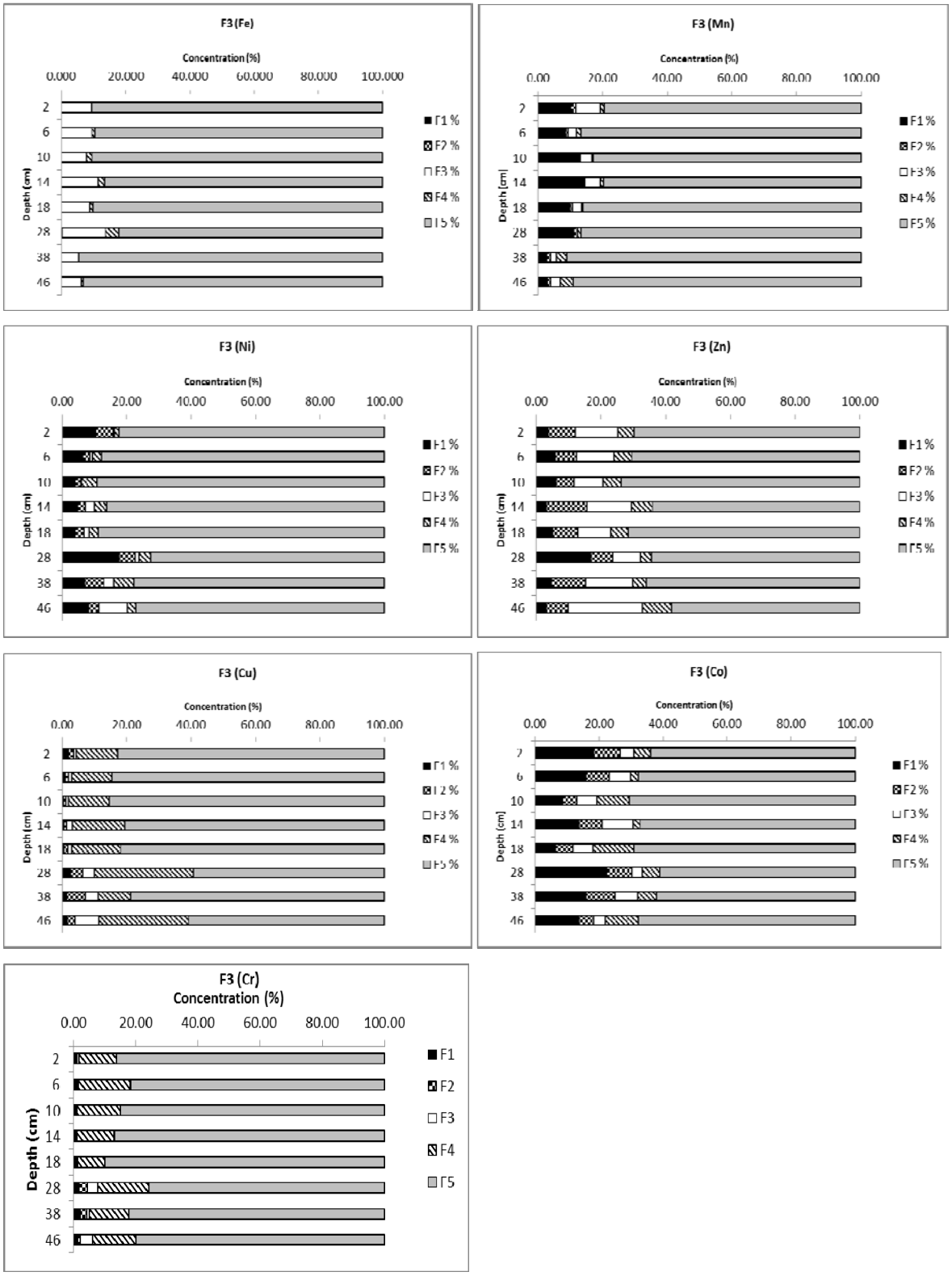

Fig. 3.4.2 Extractable contents of Fe, Mn, Ni, Zn, Cu, Co and Cr in Tessier sequential extraction protocol for core F3 F1 exchangeable fraction, F2 carbonate bound fraction, F3 Fe – Mn oxide fraction, F4 organic / sulfide bound fraction, F5 residual fraction

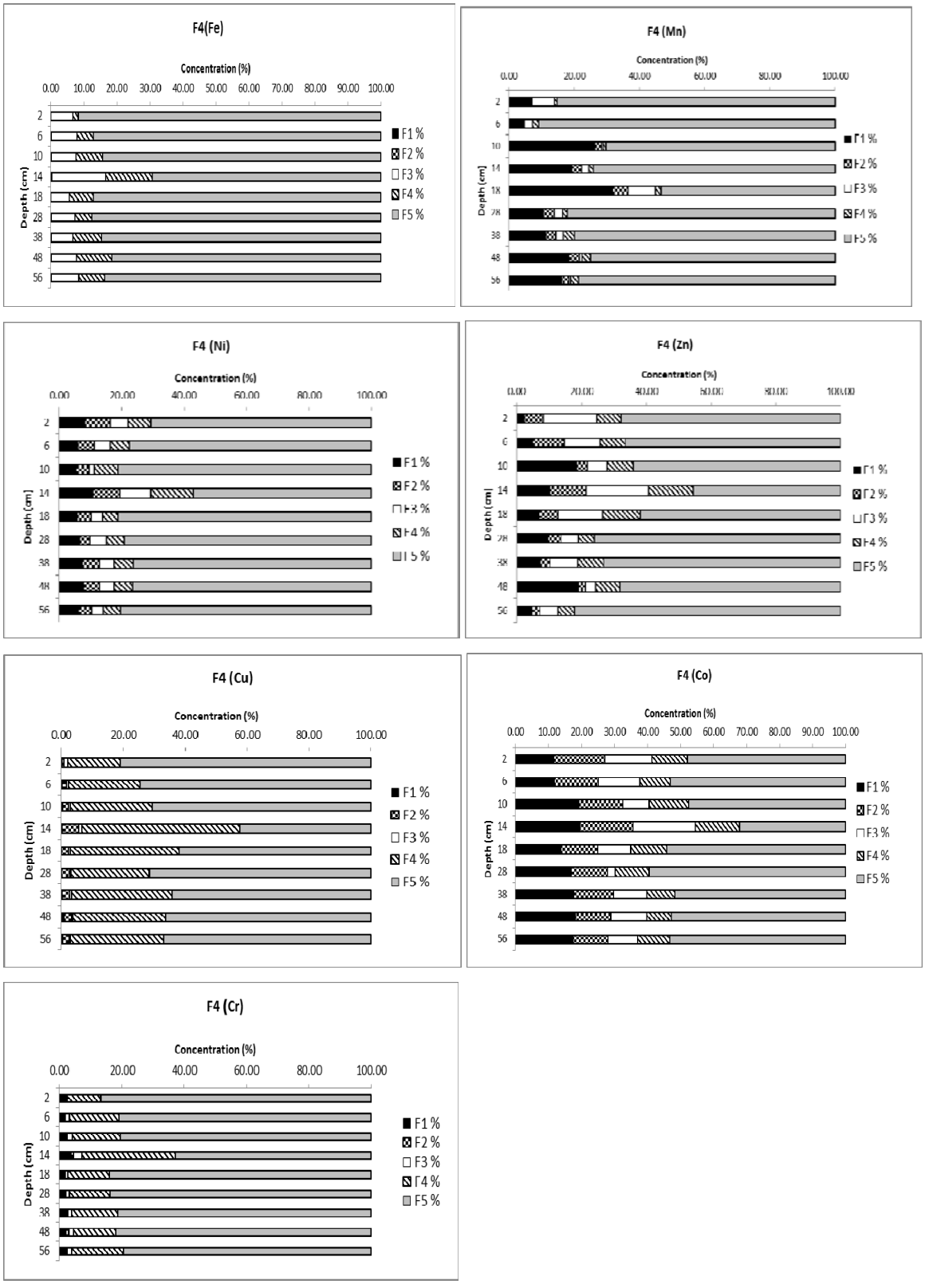

Fig. 3.4.3 Extractable contents of Fe, Mn, Ni, Zn, Cu, Co and Cr in Tessier sequential extraction protocol for core F4 F1 exchangeable fraction, F2 carbonate bound fraction, F3 Fe – Mn oxide fraction, F4 organic / sulfide bound fraction, F5 residual fraction

3.4.1.1B Trace metals

In core F1, Ni, Zn, Cu, Co and Cr concentration in the residual fraction ranges from 55 to 80 % (avg. 72 %), 65 to 78 % (avg. 71 %), 67 to 84 % (avg. 77 %), 47 to 78 % (avg. 67 %) and 83 to 87 % (avg. 85 %), respectively. Next to residual, Ni was found to be associated with carbonate bound fraction ranging from 3 to 10 % (avg. 8 %). Zn was mainly bound to the Fe-Mn oxides fraction ranging from 13 to 19 % (avg. 16 %) after residual fraction. However, Cu and Cr was associated with the organic bound fraction ranging from 7 to 16 % (avg. 13 %) and 9 to 13 % (avg. 11 %) respectively. Co concentration was found to be associated with exchangeable fraction which ranges from 6 to 39 % (avg. 13 %) next to residual fraction. Ni, Zn, Cu and Co in the bioavailable fraction was also found to be high 14 cm depth and showed decreasing concentration to towards the surface similar to that of Mn distribution.

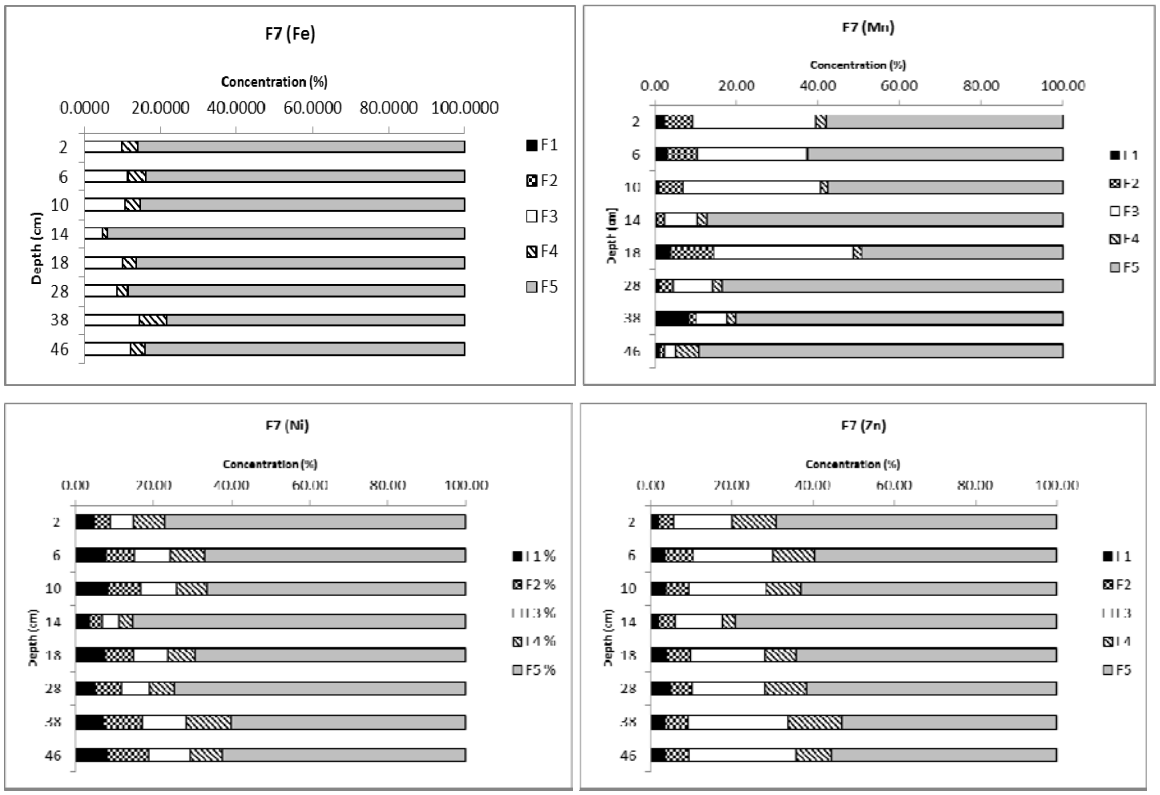

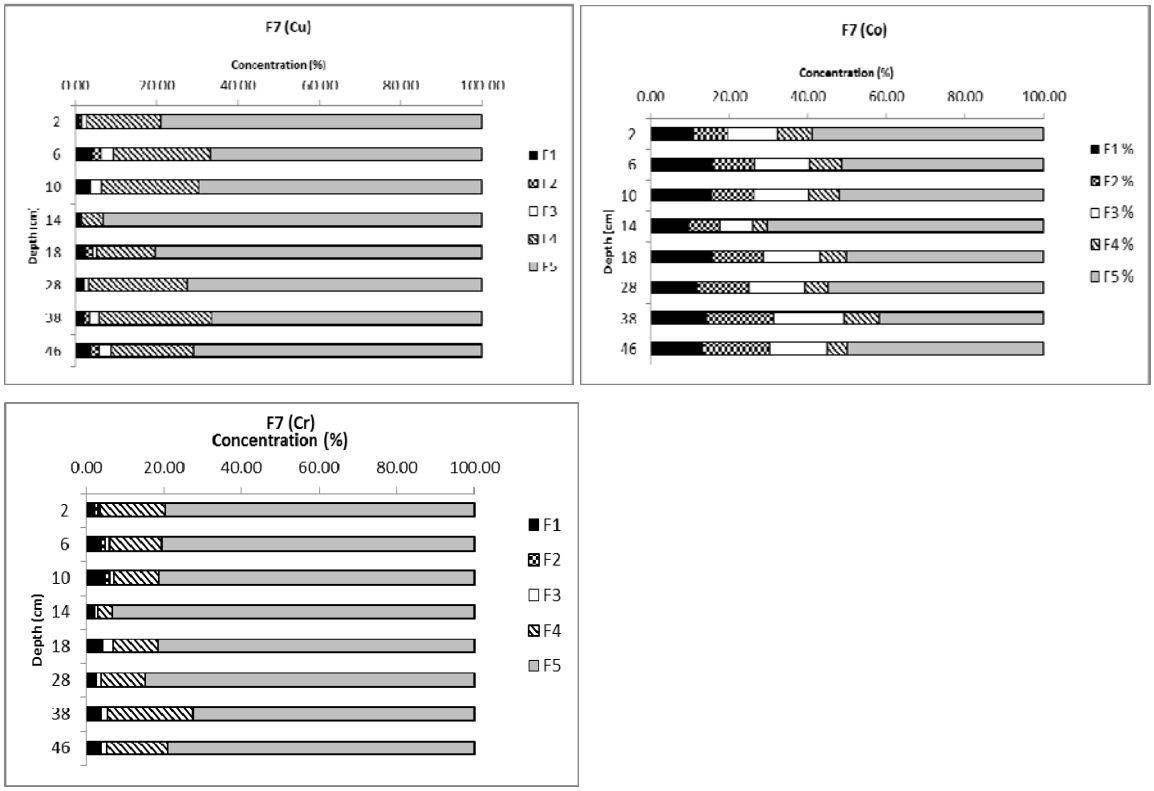

Fig. 3.4.4 Extractable contents of Fe, Mn, Ni, Zn, Cu, Co and Cr in Tessier sequential extraction protocol for core F7 F1 exchangeable fraction, F2 carbonate bound fraction, F3 Fe – Mn oxide fraction, F4 organic / sulfide bound fraction, F5 residual fraction

3.4.1.2 Lower middle estuarine regions

3.4.1.2A Iron (Fe) and Manganese (Mn)

In cores F3, Fe was mainly found to be associated in the residual fraction which ranges from 82 to 94 % (avg. 90%). Next to residual fraction Fe was associated with Fe-Mn oxide fraction ranging from 5 to 14 % with average 9 %. Fe concentration in the exchangeable, carbonate and organic bound are found to be very low which ranges from 0.002 to 0.019 % (avg. 0.008 %), 0.007 to 0.091 % (avg. 0.035 %) and 0.1 to 4.14 % (avg. 1.39 %) respectively. From the vertical variation it was noted that Fe in the bioavailable fractions was high at 28 cm depth (Fig 3.4.2) and decreased towards the surface. Mn in the residual fraction varies from 79 to 91 % (avg. 85 %). Next to residual, Mn was found to be associated with exchangeable fraction ranging from 3 to 14 % (avg. 9 %). Mn in bioavailable fraction increased towards surface in this core.

In core F7, Fe ranged from 78 to 94 % (avg. 86 %) in residual fraction. After residual fraction Fe is mainly bound to Fe-Mn oxides fraction ranging from 5 to 14 % with

average value 10 %. Fe concentration in the exchangeable, carbonate and organic bound vary from 0.003 to 0.01 % (avg. 0.008 %), 0.007 to 0.028 % (avg. 0.018 %) and 1.21 % to 7 % (avg. 4.01 %) respectively. From the vertical variation it was noted that Fe in the bioavailable fractions was high at 38 cm. Mn in the residual fraction varies from 49 to 89 % (avg. 71 %). Next to residual, Mn was found to be associated with Fe-Mn oxides ranging from 3 to 34 % (avg. 19 %) fraction. From the vertical variation it is noted that Mn in bioavailable fractions showed higher values near the surface, highest concentration noted being at 18 cm depth (Fig. 3.4.4).

3.4.1.2B Trace metals

In core F3, Ni, Zn, Cu, Co and Cr concentration in the residual fraction varied from 73 to 89 % (avg. 83 %), 58 to 74 % (avg. 67%), 59 to 85 % (avg. 77 %), 61 to 70 % (avg. 66 %) and 76 to 90 % (avg. 83 %), respectively. After residual fraction, Ni and Co were associated with exchangeable fraction which ranges from 4 to 18 % (avg. 8 %) and 7 to 22 % (avg. 14 %), respectively. Zn was mainly bound to Fe-Mn oxide fraction ranging from 8 to 23 % (avg. 13 %), after residual fraction. Cu and Cr were associated with organic bound fraction which ranges from 10 to 31 % (avg. 17 %) and 9 to 17 % (avg. 13 %), respectively, after residual fraction. In the profiles, bioavailable phases of Ni, Cu, Cr, and to some extent Zn showed higher concentration in the deeper layers. Co distribution is largely constant being highest at 28 cm depth.

In core F7, Ni, Zn, Cu, Co and Cr concentration in the residual fraction varied from 60 to 85 % (avg. 70 %), 53 to 79 % (avg. 63 %), 66 to 93 % (avg. 75 %), 42 to 70 % (avg. 54 %) and 73 to 93 % (avg. 82 %), respectively. Next to residual Ni, Zn and Co was associated with Fe-Mn oxide fraction ranging from 4.2 % to 11.1 % (avg. 8.3 %), 12 to 26 % (avg. 19 %) and 8 to 18 % (avg. 13.7 %), respectively. However, Cu and Cr were largely associated with the organic bound fraction next to residual fraction ranging from 5 to 28 % (avg. 20 %) and 4 to 22 % (avg. 13 %), respectively. Trends of all trace metal distribution in bioavailable phases are similar to that of Fe with lowest concentration at 14 m depth.

3.4.1.3 Upper middle estuarine regions

3.4.1.3A Iron (Fe) and Manganese (Mn)

In core F4, Fe was largely associated in the residual fraction which ranges between 69 and 92 % (avg. 84 %). Next to residual fraction, Fe is mainly bound to Fe-Mn oxides fraction ranging from 6 to 16 % (avg. 8.2 %). Fe concentration in the exchangeable and carbonate are found to be very low (Table 3.4.1). In organic bound phase its average concentration is 7.6 %. Manganese concentration in the residual fraction ranges between 53 and 91 % (avg. 77 %). Next to residual, Mn was found to be associated with exchangeable fraction ranging between 4 to 32 % (16 %). In the profiles, bioavailable Fe is found to be highest at 14 cm depth, whereas Mn at 18 cm depth (Fig. 3.4.3)

In core F8, Fe was largely associated in the residual fraction which ranges between 92 and 94 % (avg. 93 %). Next to residual fraction, Fe was mainly bound to Fe-Mn oxides fraction ranging from 5 to 7 % (avg. 6 %). Very low concentration of Fe was associated with exchangeable, carbonate and organic bound. Manganese concentration in the residual fraction of core F8 ranges between 78 to 94 % (avg. 90 %). Next to residual, Mn was found to be associated with Fe-Mn oxide fraction ranging between 2 to 11 % (avg. 6 %). In the profiles, bioavailable concentration of Fe was almost constant whereas Mn increased towards surface (Fig. 3.4.5)

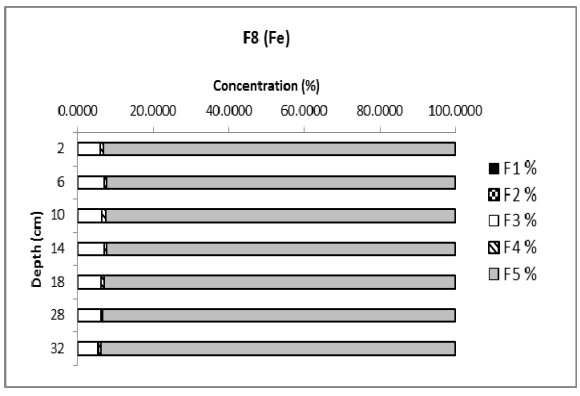

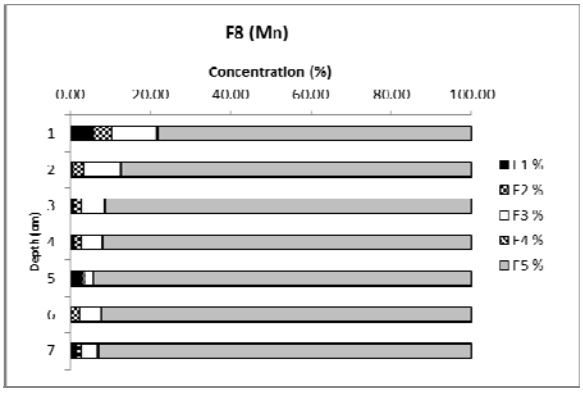

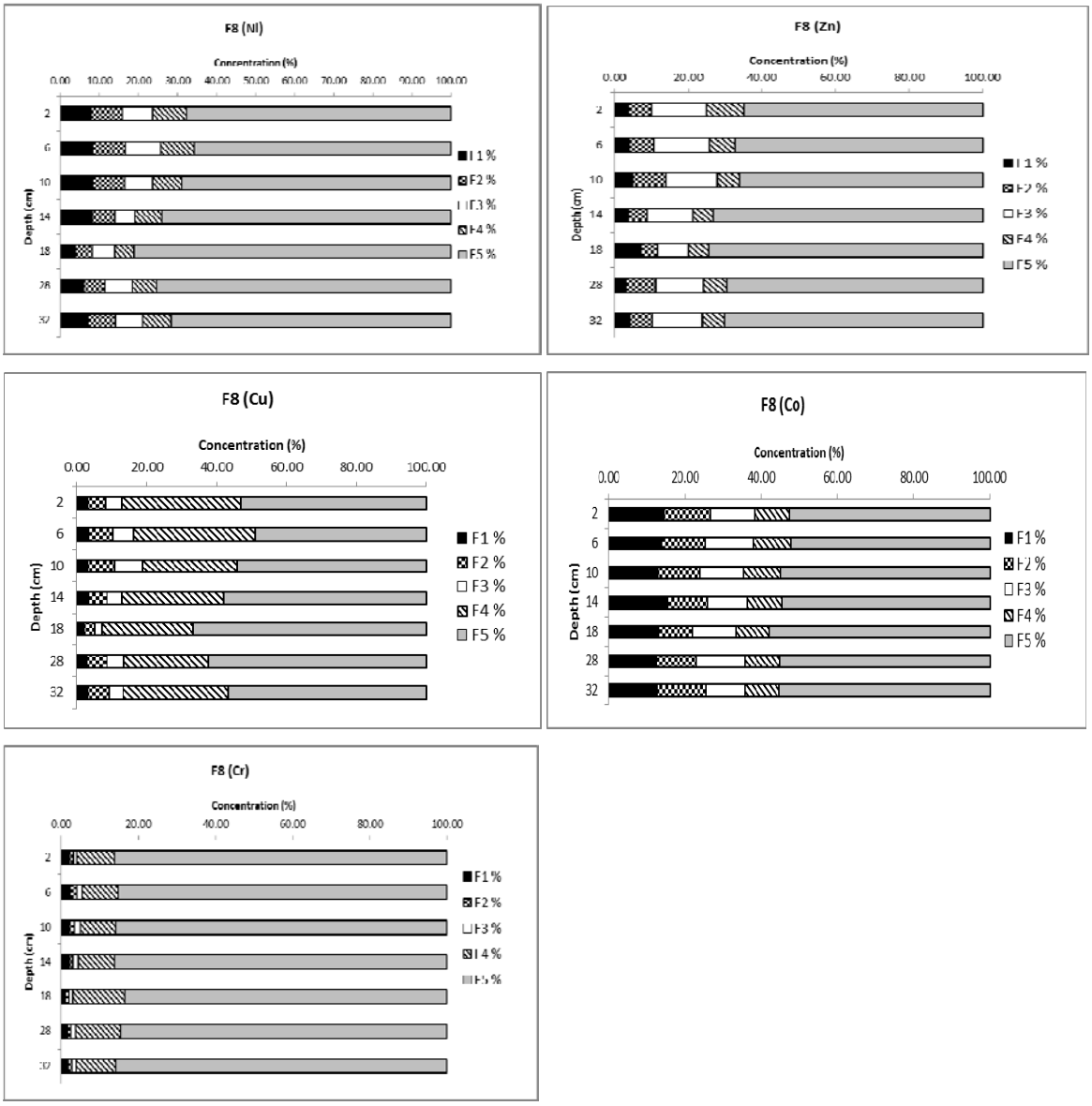

Fig. 3.4.5 Extractable contents of Fe, Mn, Ni, Zn, Cu, Co and Cr in Tessier sequential extraction protocol for core F8 F1 exchangeable fraction, F2 carbonate bound fraction, F3 Fe – Mn oxide fraction, F4 organic / sulfide bound fraction, F5 residual fraction

3.4.1.3B Trace metals

In core F4, Ni, Zn, Cu, Co and Cr concentration in the residual fraction ranges between 57 to 81 % (avg. 76 %), 46 to 82 % (avg. 67 %), 42 to 81 % (avg. 67 %), 32 to 60 % (avg. 50 %) and 63 to 87 % (avg. 80 %), respectively. After residual fraction, Ni and Co were associated with exchangeable fraction ranging from 5 to 11 % (avg. 7 %) and 12 to 19 % (avg. 16 %), respectively. Zn was mainly bound to the Fe-Mn oxides fraction after residual fraction ranging from 3 to 19 % (avg. 10 %). Cu and Cr were associated with organic bound fraction ranging from 17 to 51 % (avg. 30 %) and 11 to 30 %

(avg.16 %) after residual fraction. Along the profiles in bioavailable fractions, all the metals showed distribution similar to that of Fe with maximum concentration at 14 cm depth.

In core F8, Ni, Zn, Cu, Co and Cr concentration in the residual fraction ranges from 66 to 81 % (avg. 72 %), 65 to 74 % (avg. 69 %), 49 to 67 % (avg. 57 %), 52 to 58 % (avg. 55 %) and 84 to 86 % (avg. 85 %), respectively. After residual fraction, Co was associated with exchangeable fraction ranging from 12 to 15 % (avg. 14 %). Ni was equally associated with all four bioavailable fractions. Zn was mainly bound to the Fe-Mn oxides fraction after residual fraction ranging from 8 to 15 % (avg. 13 %). Cu and Cr were associated with organic bound fraction ranging from 24 to 35 % (avg. 29 %) and 9 to 13 % (avg.10 %) after residual fraction. In the profiles, bioavailable fraction showed enrichment for Ni, Zn, Cu and Co. Cr distribution is similar to that of Fe exhibiting constant values.

3.4.2 Mangroves

3.4.2.1 Lower middle estuarine region

3.4.2.1A Fe and Mn

In core G1, Fe was also mainly associated with the residual fraction which ranges from 82 to 96 % (avg. 89 %). Next to residual, Fe was found to be associated with Fe-Mn oxide fraction ranging from 4 to 15 % (avg. 9 %). From the vertical variation it was noted that Fe in bioavailable fractions was highest at 14 cm depth which decreased further at 10 cm and further remained almost constant up to the surface. Manganese was also mainly associated with the residual fraction which ranges from 72 to 90 % (avg. 83%). Next to residual, Mn was found to be associated with exchangeable fraction ranging from 2 to 22 % (avg. 11 %). From the vertical variation it was noted that Mn in bioavailable fractions was highest at 18 cm depth which decreased further at 14 cm, 10 cm and 6 cm depth, later increased towards the surface (Fig. 3.4.6).

3.4.2.1B Trace metals

Ni, Zn, Cu, Co and Cr concentration in the residual fraction ranges from 57 to 86 % (avg. 76 %), 65 to 70 % (avg. 67 %), 62 to 84 % (avg. 73 %), 49 to 67 % (avg. 59 %) and 83 to 91 % (avg. 86 %), respectively. Next to residual, Ni was found to be

associated with exchangeable fraction ranging from 3 to 25 % (avg. 10 %). Zn was mainly bound to the Fe-Mn oxides fraction ranging from 8 to 16 % (avg. 12 %) after residual fraction. However, Cu and Cr was associated with the organic bound fraction which ranges from 11 to 32 % (avg. 20 %) and 8 to 13 % (avg. 9 %), respectively. Co concentration was found to be associated with exchangeable fraction ranging from 9 to 32 % (avg. 19 %) next to residual fraction. Ni and Co in the bioavailable fraction was also found to be high at bottom of the core; Zn and Cr were high at 14 cm depth similar to Fe (Fig. 3.4.6) but maintained similar concentration along the core. Bioavailable fraction of Cu was high at 18 cm, which further showed gradual decrease towards the surface.

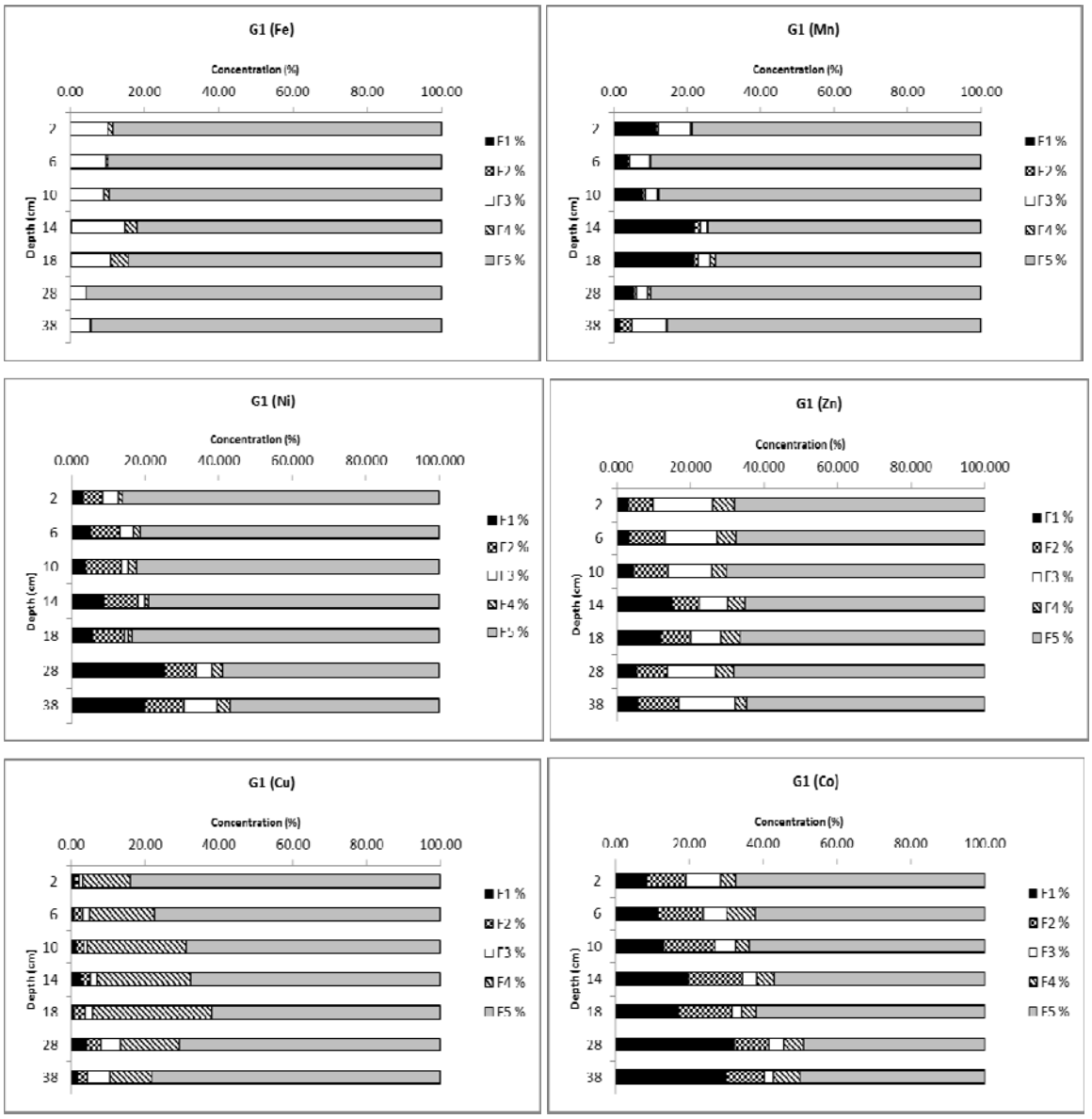

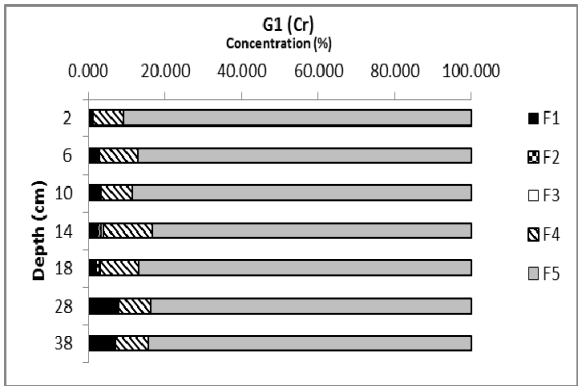

Fig. 3.4.6 Extractable contents of Fe, Mn, Ni, Zn, Cu, Co and Cr in Tessier sequential extraction protocol for core G1 F1 exchangeable fraction, F2 carbonate bound fraction, F3 Fe – Mn oxide fraction, F4 organic / sulphide bound fraction, F5 residual fraction

3.4.2.2 Upper middle estuarine region

3.4.2.2 A Fe and Mn

In core G2, Fe in residual fraction ranges from 69 to 85 % (avg. 76 %). Next to residual fraction, Fe is mainly bound to Fe-Mn oxides fraction, which ranges from 8 to 24 % (Avg. 16%). Iron concentration in exchangeable fraction ranges from 0.003 to 0.190 % % (Avg. 0.038 %). In carbonate bound fraction it varies from 0.040 to 0.153 % (avg. 0.106 %). In the organic bound fraction Fe ranges from 3 to 11 % (avg. 8 %). Mn in the residual fraction ranges from 40 to 75 % (avg. 65 %). Next to residual fraction, Mn is mainly bound to exchangeable fraction which ranges from 8 to 53 % (avg. 28 %). Mn in the carbonate fraction ranges from 0.32 % to 4 % (avg. 1.46 %) and in Fe-Mn oxide fraction it varies from 2 to 14 % (avg. 5 %). Mn concentration (%) in organic bound fraction ranges from 0.15 to 1.68 % (avg. 0.97 %). Sum of the bioavailable phases of Fe and Mn found to increase from bottom up to 6 cm depth and decrease near the surface (Fig. 3.4.7).

3.4.2.2 B Trace metals

Trace elements viz. Ni, Zn, Cu, Co and Cr in the residual fraction ranges from 70 % to 84 % (avg. 79 %), 66 % to 77 % (avg. 73 %), 60 % to 80 % (avg. 71 %), 55 % to 68 % (avg. 63 %) and 78 % to 88 % (avg. 85 %), respectively. Next to residual fraction Ni, Cu and Cr were associated with in the organic bound fraction ranging from 5 to 15 % (avg. 8 %), 16 to 33 % (avg. 23 %) and 9 to 17 % (avg. 13 %), respectively. Ni in exchangeable, carbonate bound, Fe-Mn oxide fraction, ranges from, 2 to 9 % (avg. 6

%), 3 to 5 % (avg. 4 %) and 2 to 6 % (avg. 4 %). Cu and Cr in exchangeable, carbonate and organic bound fractions are very low in concentration. Zn in Fe-Mn oxide fraction ranges from 5 to 14 % (avg. 9 %), after residual fraction. In exchangeable, carbonate bound and organic bound fraction it ranges from 1.14 to 13 % (avg. 8.6 %), 3 to 5 % (avg. 4 %), 4 to 13 % (avg. 6 %), respectively. Next to residual Co was associated with exchangeable fraction ranging from 5 to 19 % (avg. 14 %). The concentration of Co, in carbonate bound, Fe-Mn oxide fraction and organic bound fraction ranges from 5 to 9 % (avg. 8 %), 5 to 11 % (avg. 8 %), 5 to 13 % (avg. 7 %), respectively. Sum of the bioavailable phases of Ni, Zn, Cu and Cr showed decrease towards surface. Co profile showed higher concentration near the surface.

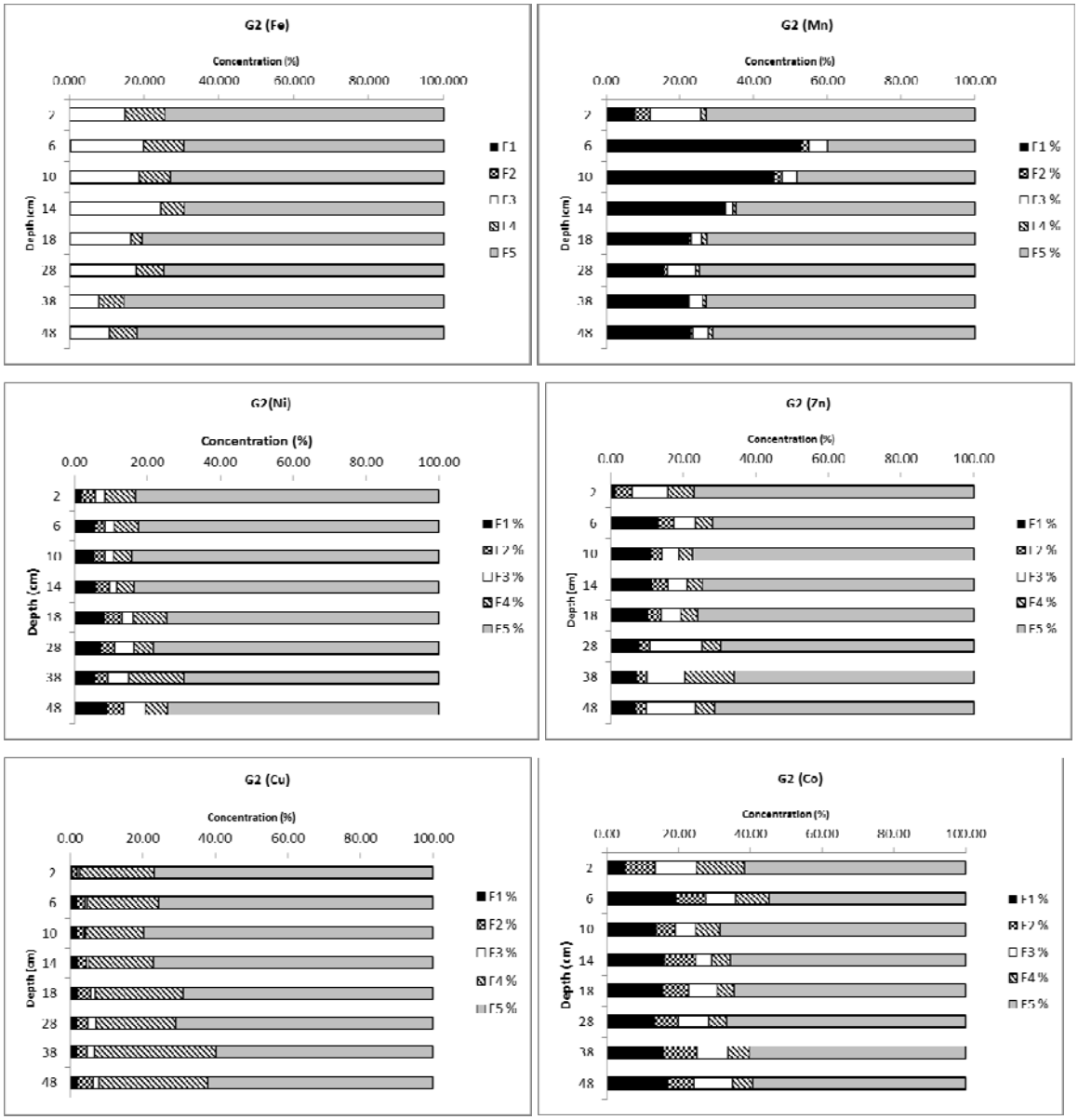

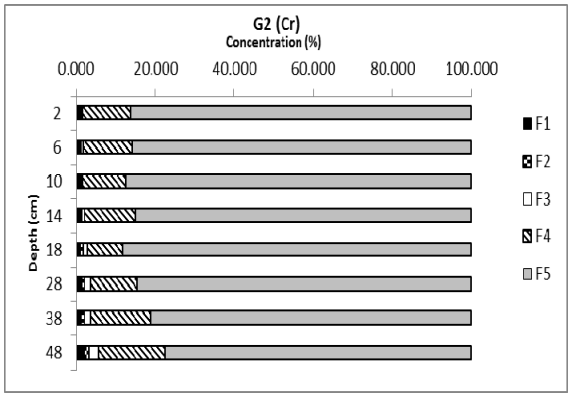

Fig. 3.4.7 Extractable contents of Fe, Mn, Ni, Zn, Cu, Co and Cr in Tessier sequential extraction protocol for core G2 F1 exchangeable fraction, F2 carbonate bound fraction, F3 Fe – Mn oxide fraction, F4 organic / sulfide bound fraction, F5 residual fraction

In core G2, Fe in bioavailable fraction increases from bottom up to 6 cm with lower values at the surface. Similar distribution is also observed in case of Mn, however with higher concentration seen in exchangeable fraction at 6 cm depth. Concentration in bioavailable fraction is found to decrease from bottom up to the surface in case of Ni, Zn, Cu and Cr. Relatively higher concentration of Co was noted in the bioavailable fraction, highest at 6 cm depth similar to Mn (Fig. 3.4.7). Slightly higher concentration at 6 cm is also noted for Zn and Cu.

3.4.3 Comparison between regions and environments

3.4.3A Mudflat environment

When cores F3 (Sharavati estuary) and F7 (Gurpur estuary), collected from lower middle estuarine regions were compared, concentration of all the studied metals was relatively higher in the residual fraction of core F3 as compared to core F7. However, Mn, Ni, Zn and Co in exchangeable fraction is higher in core F3. Further, in core F3, all the trace metals, except Zn exhibited highest concentration at 28 m depth along with Fe, and they decrease towards surface. In core F7, Ni, Zn, Cu, Co and Cr in bioavailable fractions showed lowest concentration at 14 cm and highest concentration at 38 cm similar to that of Fe distribution. From 14 cm towards the surface concentration of all the metals increased similar to Fe and Mn distribution. At the surface they showed a decrease in the bioavailable fractions and increase in the residual fraction.

When cores F4 (Swarna estuary) and F8 (Gurpur estuary), collected from upper middle estuarine regions were compared, Fe, Mn, Zn, Co and Cr, associated with the residual fraction was relatively higher in core F8. From the vertical variation it was noted that Fe in the bioavailable fractions was high at 14 cm in core F4 (Fig. 3.4.3) depth whereas no much variation with depth was noted in core F8 (Fig. 3.4.5). From the vertical variation it is noted that Mn in bioavailable fractions in core F4 showed large fluctuations with depth, highest concentration noted being at 18 cm depth whereas in core F8 it showed gradual increase from the bottom up to the surface. Ni, Zn, Cu, Co and Cr in the bioavailable fraction were also found to be high at 14 cm depth in core F4 similar to that of Fe distribution. However in core F8, Ni, Zn, Cu, Co in bioavailable fractions showed gradual increase from bottom up to the surface similar to Mn distribution.

When cores F7 (lower middle) and F8 (upper middle), collected from Gurpur estuary were compared, it was noted that, all the elements except Cu in residual fraction were relatively higher in core F8. Fe, Mn, Ni and Zn were associated with Fe-Mn oxide fraction after residual fraction in both the cores. Co in the exchangeable fraction was relatively higher core F8 as compared to core F7. In core F7 (Fig. 3.4.4), all metals (except Mn) in bioavailable fraction show decreasing trend from bottom up to the surface with lower concentration at 14 cm depth. However, in core F8, metal concentration in the bioavailable fraction show an increasing trend from bottom up to the surface, except Fe and Cr.

3.4.3B Mangrove environment

When cores G1 (lower middle) and G2 (upper middle) from Sharavati estuary were compared, it is noted that, Fe, Mn, Cu and Cr associated with residual fraction were relatively higher in core G1. Mn in the exchangeable fraction was relatively higher in core G2. Fe and Mn concentration in the bioavailable fraction showed an increasing trend from bottom up to 6 cm depth with lower values at the surface in core G2. However, trace metal (except Co in core G2) concentration in bioavailable fraction, showed decreasing trend from bottom up to the surface in both the cores.

3.4.3C Mangrove and mudflat environment

When cores F3 (mudflat) and G1 (mangrove) collected from lower middle region of Sharavati estuary were compared, it is noted that, concentration of all elements except Cr in the residual fraction was relatively higher in core F3. In the vertical distribution, Fe profile shows similar distribution in both the cores; however, in bioavailable fraction it shows high at 28 cm and 14 cm depth in core F3 (Fig. 3.4.2) and G1 (Fig. 3.4.6), respectively. Mn also shows similar distribution in both the cores; however, in bioavailable fraction is highest at 14 cm and 18 cm, in F3 and G1, respectively. Ni shows similar distribution in both the cores, i.e. high concentration at 28 cm depth and further shows sharp decrease at 18 cm depth which remains fairly constant up to the surface. Similar distribution is observed in case of Cu and Cr in core F3. However in core G1, Cu in bioavailable fraction show high concentration at 18 cm which further gradually decreases up to the surface. Bioavailable Co concentration decreases towards surface in mangroves, while it slightly fluctuates in mudflat core.

Fe concentration was found to be very low in the bioavailable phases i.e., exchangeable, carbonate bound, Fe-Mn oxide and organic bound fractions when added together. Major quantity (> 76 %) of Fe and Cr was found to be associated with the residual fraction in all the cores. Metals in this fraction are considered to be in inert phase which are stable and do not react during sedimentation and diagenesis, and therefore have less potential bioavailability as they cannot be mobilized (Tessier et al. 1979; Sarkar et al. 2014). Large amount of Fe associated with the residual fraction (F5) can thus be directly attributed to its high abundance in the earth's crust (Yuan et al. 2004; Jain et al. 2008). This is probably due relatively low mobility of this element (Caplat et al. 2005) as compared to Mn, as metals associated with this fraction cannot be remobilized under the conditions normally encountered in nature (Izquierdo et al. 1997). Considerably higher amount of Mn was present in the bioavailable phases in cores G2, F7, F1 and F4. The higher concentration of Mn in exchangeable fraction in cores G2, F4, G1, F3 and F1 indicates weakly bound Mn, which is the most unstable and reactive (Passos et al. 2010). Further, higher concentration of bioavailable Fe in all the cores in oxides and that of Mn accumulation within reducible fraction in core F1 and F7 may be related to precipitation and co-precipitation with Fe-Mn oxides (Li et al. 2001; Fernandes et al. 2014). The trace metals Ni, Cu, Co, Zn, except for Ni in core F3

and G2 are less than 76 % in residual fraction, Co concentration being lowest in all the cores. Among bioavailable fractions metals association of Cu and Cr defined to organic bound in all the cores. Co is available highest in exchangeable, though present in considerable concentration in other phases. Similarly Zn is highest in oxide phase though associated with other bioavailable phases. Ni is distributed in all the bioavailable phases, in all the cores.

In cores F1, F4 and G1 higher percentage of exchangeable bound Mn is present at greater depths whereas in cores F3, F8 and G2 the loosely bound exchangeable fraction increases towards the surface, and is probably derived from recent anthropogenic activities. Distribution of Mn in different bioavailable phases in core F1, F4, F7 and G1 indicates the diagenetic mobilization and diffusion of Mn to water column in case of core F1 and F4. In cores F3, F8 and G2, and to some extent cores F7 and G1 Mn associated with bioavailable fractions increased and that associated with residual fraction decreased from bottom to surface. Towards the surface of the cores increase of Fe and Mn in Fe-Mn oxide bound fraction is noted in cores F7, F8, G1 and G2 (except Mn). Reductive dissolution of Fe-Mn hydroxides in the suboxic zone, can release dissolved Mn (II) and Fe (II) to pore waters, potentially making them more bioavailable and mobile (Koretsky et al. 2007). These freshly formed Fe–Mn oxides are very efficient at scavenging a variety of metals (Singh et al. 1984). Similar distribution of Fe along with trace metals Ni, Zn, Cu, Co and Cr in bioavailable fractions in core F3, F4, F7 and partially G1; and that of Mn in cores F1 and F8, indicate the diagenetic mobilization of metals and decrease in their concentration at the surface reflect their diffusion to water column. Similar distribution pattern of Fe and Mn along with all the trace metals indicate the role played by Fe oxides in the distribution of Ni (except in core G1), Zn, Cu, Co and Cr in F3, F4, F7 and G1 and; similar distribution of trace metals with Mn indicate the role played by Mn oxides in case of cores F1 and F8 (except Cr), through diagenetic processes. Further, decrease in concentration near surface indicates diffusion. If sediments are further disturbed by process of bioturbation or human interference like dredging, else a change in pH, redox conditions or degradation of organic matter can lead to release of metals at the sediment water interface that is into the estuarine environment, causing a potential risk of toxicity to the organisms. Considerable amount of Zn is present in Fe-Mn oxide fraction in all the

cores (Li et al. 2001; Volvoikar and Nayak 2015). This could be due of adsorption of Zn by Fe-Mn oxides (Shuman 1985). Considerable amount of Cu and Cr are present in the organic bound although they are largely associated in the residual fraction in all the cores. Earlier studies elsewhere in marine sediments have also reported association of Cu with organic matter (Tokalioglu et al. 2000) Copper and Chromium are characterized by high stability constant with organic matter and thus it can be hypothesized that Cu and Cr are bound to labile organic matter (Avudainayagam et al. 2003). Thus, solubility and mobility of Cu and Cr is largely controlled by organic matter mineralisation (Caplat et al. 2005) and that of Zn by the redox conditions. Among the studied trace metals Co is the only metal which is largely available in the labile fractions in all the cores and therefore of concerned of its toxicity to the environment.

3.4.4 Risk assessment

3.4.4A Comparison of average total metal concentration and sum of the bioavailable fractions (first four fractions) in sediments with SQUIRT's table

Further, in order to understand the risk of metals to the sediment dwelling organisms and consequently to the human population, the data of metals in the bioavailable fractions (F1 + F2 + F3 + F4) is compared with the sediment quality values (SQV) given in the SQUIRT (Screening Quick Reference Table). SQUIRT was developed by NOAA for screening purposes. The guideline values were categorized by Buchman (1999) into five classes (Tables 3.3.8a, b) namely TEL, ERL, PEL, ERM and AET. The average total metal concentration in sediments (Table 3.4.1) was compared with SQUIRT's table (Table 3.3.8a, b). In the total metal concentration, Mn exceeded the Apparent Effects Threshold (AET) value in core G2 and F4. Ni falls in the range between Effects Range Low (ERL) and Probable Effects Level (PEL) in core F1, F3, F7, F8 and G2, whereas, exceeded the Effects Range Median (ERM) value in core F4. Cu falls in the range between Effects Range Low (ERL) and PEL in all the cores except in core F3 and G1. Co exceeded the AET value in core F4, F7, F8 and G2. Cr fell in the range between Threshold Effect Level (TEL) and ERL in core F1, F3 and F8; between ERL and PEL in core F4, F7 and G2.

In the sum of the bioavailable fractions, Co in core F4 exceeded the AET value. Cobalt in all the cores was mainly associated with exchangeable fraction and therefore

indicates anthropogenic origin. Co in bioavailable fraction (Table 3.4.2) in core F4 exceeded AET therefore suggesting a high risk of toxicity (Table 3.3.8a, b). Fe, Ni, Zn, Cu and Cr were mainly bound to the residual fraction and represented metals of natural origin. Also, the percentage of Fe and Mn along with Ni, Zn, Cu and Cr was very low compared to AET indicating no harm to the biota. However, Co associated with bioavailable fractions exceeded the AET suggesting risk of toxicity of Co to organisms associated with the sediments of Swarna estuary.

3.4.4 B Comparison of sum of average percentage of metals in F1 and F2 fraction in sediments with RAC criteria

The risk assessment code indicates the sediment which can release heavy metal in exchangeable and carbonate fractions; % of the total concentration<1: No risk, will be considered safe for the environment, 1–10: Low risk, 11–30: medium risk, 31–50 high risk, >50: very high risk, and can easily enter the food chain (Perin et al. 1985). Risk Code Assessment (RAC) values (Table 3.4.3) computed indicate no risk of Fe (Table 3.4.2) in the studied estuaries. Medium risk of Mn in core F1, F4, G1 and G2, whereas, low risk in cores F3, F7 and F8. Medium risk of Ni in all the cores is noticed except core G2 which is under low risk class. Medium risk of Zn in F3, F4, F8, G1 and G2; low risk in cores F1 and F7 are seen. Cu and Cr values show low risk in all the studied cores as they are largely bound to organic phase and not fraction 1 and fraction 2. High risk of Co is seen in core G1 and medium risk in all the other cores. Exchangeable and carbonate fractions are released in normal conditions to the environment. The studied area therefore is under high risk from Co at core G1. Medium risk by Co, Mn, Ni and Zn in many of the cores and is of environmental concern. Further, F1 and F2 fractions are high near the surface in most of the cores studied. The elements Co, Mn, Ni, and Zn can be therefore released to the water column in normal conditions and are toxic to the environment.

Table 3.4.1 Average concentration of metals in each extracted fractions

Core	Metal	F1 (%)			F2 (%)			F3 (%)			F4 (%)			F5 (%)		
		Min	Max	Avg	Min	Max	Avg	Min	Max	Avg	Min	Max	Avg	Min	Max	Avg
F1	Fe	0.003	0.053	0.013	0.005	0.013	0.009	3	8	4	0.09	0.59	0.25	92	97	95
	Mn	0.19	30	8	4	8	5	8	13	11	0.24	1.76	0.77	58	81	75
	Ni	2	20	6	3	10	8	5	9	7	6	9	7	55	80	72

	Zn	0.19	13	4	2	9	5	13	19	16	4	5	4	65	78	71
	Cu	1.33	6	2	0.69	8.12	5	2	7	3	7	16	13	67	84	77
	Co	6	39	13	6	13	10	5	13	8	2	4	2	47	78	67
	Cr	0.88	6	3	0.03	1.39	0.79	0.65	1.06	0.81	9	13	11	83	87	85
F3	Fe	0.002	0.019	0.008	0.007	0.091	0.035	5	14	9	0.10	4.14	1.39	82	94	90
	Mn	3	14	9	0.20	1.74	0.90	0.06	7.58	3.33	0.26	4.10	1.53	79	91	85
	Ni	4	18	8	2	6	4	0.27	8.92	2.43	2.57	6.08	3.44	73	89	83
	Zn	3	17	6	6	13	8	8	23	13	3	9	6	58	74	67
	Cu	0.30	2.71	1.27	0.64	6	2	1	7	3	10	31	17	59	85	77
	Co	7	22	14	5	9	7	3	10	6	2	13	7	61	70	66
	Cr	0.59	2.20	1.11	0.11	2.51	0.87	0.27	4	1.31	9	17	13	76	90	83
F4	Fe	0.004	0.050	0.015	0.019	0.280	0.119	6	16	8.2	1.6	14	7.6	69	92	84
	Mn	4	32	16	0.14	4.82	2.48	0.48	8	3	0.5	4	2	53	91	77
	Ni	5	11	7	3	9	5.5	1	10	5	5	14	6.98	57	81	76
	Zn	2	19	9	2	11	5	3	19	10	5	14	8	46	82	67
	Cu	0.08	0.92	0.30	0.79	5.28	2.25	0.46	1.22	0.70	17	51	30	42	81	67
	Co	12	19	16	11	16	13	2	19	11	7	13	10	32	60	50
	Cr	1.55	3.55	2.09	0.21	0.95	0.46	0.57	2.71	1.30	11	30	16	63	87	80
F7	Fe	0.003	0.010	0.008	0.007	0.028	0.018	5	14	10	1.21	7	4	78	94	86
	Mn	0.42	8	3	1.13	11	5	3	34	19	0.31	6	2	49	89	71
	Ni	3.6	8.4	6.5	3.5	10.5	7.2	4.2	11.1	8.3	3.4	11.6	7.7	60	85	70
	Zn	2.02	5	3	4	7	5	12	26	19	3	13	9	53	79	63
	Cu	0.91	4	2	0.17	2	1.12	0.08	3	1.81	5	28	20	66	93	75
	Co	10	16	13.3	8	17	12	8	18	13.7	4	9	7	42	70	54
	Cr	2.04	5	3	0.16	1.25	0.58	0.48	2.60	1.29	4	22	13	73	93	82
F8	Fe	0.002	0.024	0.007	0.007	0.031	0.016	5	7	6	0.57	1.02	0.78	92	94	93
	Mn	0.08	6	2	1	4	2	2	11	6	0.04	0.45	0.17	78	94	90
	Ni	4	8	7	4	8	7	5	9	7	5	9	7	66	81	72
	Zn	3	7	4	4	9	7	8	15	13	5	10	7	65	74	69
	Cu	2	3	3	3	8	6	2	8	5	24	35	29	49	67	57
	Co	12	15	14	9	13	11	10	13	12	9	10	9	52	58	55
	Cr	1.08	2.20	1.84	0.80	1.79	1.12	0.93	1.48	1.18	9	13	10	84	86	85
G1	Fe	0.002	0.187	0.034	0.008	0.098	0.040	4	15	9	0.12	5	2	82	96	89
	Mn	2	22	11	0.61	3.20	1.29	2	10	5	0.25	1.38	0.59	72	90	83
	Ni	3	25	10	5	11	9	0.99	9.01	3.72	0.90	3.38	2	57	86	76
	Zn	3	15	7	7	11	9	8	16	12	3	6	5	65	70	67
	Cu	0.70	4.31	1.78	1.19	3.73	2.54	0.96	6	3	11	32	20	62	84	73
	Co	9	32	19	10	15	12	2	9	5	4	8	5	49	67	59
	Cr	1.04	7.02	3.42	0.09	0.86	0.47	0.03	0.68	0.35	8	13	9	83	91	86

G2	Fe	0.003	0.190	0.038	0.040	0.153	0.106	8	24	16	3	11	8	69	85	76
	Mn	8	53	28	0.32	4	1.46	2	14	5	0.15	1.68	0.97	40	75	65
	Ni	2	9	6	3	5	4	2	6	4	5	15	8	70	84	79
	Zn	1.14	13	8.6	3	5	4	5	14	9	4	13	6	66	77	73
	Cu	0.61	2.18	1.83	1.60	4.41	2.71	0.50	2.36	1.21	16	33	23	60	80	71
	Co	5	19	14	5	9	8	5	11	8	5	13	7	55	68	63
	Cr	0.69	1.89	1.06	0.33	1.45	0.72	0.39	2.19	1.06	9	17	13	78	88	85

Table 3.4.2 Total concentration of metals, bioavailable fractions and sum of exchangeable (F1 %) and carbonate bound fraction (F2 %)

Core		Fe (%)	Mn	Ni	Zn	Cu	Co	Cr
F1	Total metal	2	280	27	22	53	5	54
	F1+F2+F3+F4	0.17	65	8	8	3	4	13
	F1+F2	0.021	14	14	9	7	23	4
F3	Total metal	3	149	24	17	11	5	62
	F1+F2+F3+F4	0.24	32	5	10	4	5	15
	F1+F2	0.043	10	11	14	3	21	2
F4	Total metal	4	193	77	52	54	19	134
	F1+F2+F3+F4	0.41	25	12	14	9	11	17
	F1+F2	0.134	19	13	15	3	29	3
F7	Total metal	2	177	30	37	65	12	89
	F1+F2+F3+F4	0.21	33	10	10	4	6	11
	F1+F2	0.025	8	14	9	4	26	4
F8	Total metal	2	203	39	31	65	12	68
	F1+F2+F3+F4	0.12	16	9	8	7	8	10
	F1+F2	0.023	4	14	11	9	25	3
G1	Total metal	2	130	11	17	9	4	52
	F1+F2+F3+F4	0.21	33	6	9	5	6	13
	F1+F2	0.074	12	19	16	4	31	4
G2	Total metal	2	364	36	42	55	20	107
	F1+F2+F3+F4	0.12	128	12	15	12	9	20
	F1+F2	0.023	29	10	12	5	22	2

*For total metal concentration and sum of bioavailable fraction all units are in ppm except for Fe

Table 3.4.3 Criteria for Risk Assessment Code (RAC) by Perin et al. 1985

Risk Assessment Code (RAC)	Criteria (%)
No risk	< 1
Low risk	1 - 10
Medium risk	11 - 30
High risk	31 - 50
Very high risk	> 50

Chapter 4

Summary and Conclusion

Estuaries are transition zones between terrestrial and marine ecosystem and thus acts as important environmental interfaces. Vast amount of organic matter and metals enter into the estuarine waters through river run off, in-situ primary productivity, atmospheric deposition, diagenetic remobilization and anthropogenic inputs. Source of anthropogenic material includes industrial and agricultural activities and also urban effluents that supply significant loads of toxic metals to the estuaries. The material entered into the estuaries slowly gets deposited in quiet environment of deposition in mudflats and mangroves. Thus, mudflats and mangroves sediments are considered as potential reservoir of metals. Within these environments remobilizations of trace metals are regulated by redox sensitive elements and are recycled with changing physicochemical conditions through the sediment–water interface. Therefore metals may get released into the water column of the estuary even after effluent discharge is ceased.

Along this coast Sharavati is the large estuary and; Chakra Nadi, Haladi, Sita Nadi, Swarna, Udyavara, Pavanje and Gurpur are smaller estuaries. These rivers travel through migmatite, granodiorite, granitic gneisses, charnockites and amphibolites and laterite rock types in the catchment area. Further, area receives an average rainfall of 3500 mm during June to September. Weathered material from the catchment area is brought to estuaries during these monsoon months. Along this coast tidal range is small and is less than 2m.

Estuaries in Karnataka are continuously influenced by geological processes like erosion, deposition, periodic storms and floods and changing sea level. Increasing population, industrial establishments and developments are common near the river banks along this coast. Soil erosion is the biggest problem along river banks and coasts which poses greater threats to natural habitats and agro-ecosystem with the growing pollution. Life in the rivers, estuaries and the coastal seas is under greater stress. Coastal Karnataka is emerging as an urbanized region with industrial growth. River acts as a sink to many types of pollutants due to effluent discharge by industries of different kind, port activities and dumping of fish and organic wastes. Industrial effluents with toxic chemicals enhance the level of bioavailability of metals which can pose a risk to biota. Estuaries in Karnataka have also been affected greatly due to construction of

dams on rivers. This has led to change in deposition pattern of sediments, organic matter and metals over a period of time. It has become a necessity to understand the level of metal pollution along the estuaries in Karnataka coast. Therefore an attempt has been made to

1. To study the spatial and temporal variation of sediment components within the estuaries along the Karnataka coast.
2. To understand the depositional environment and diagenetic processes using the distribution pattern of sediment components and metals.
3. To determine chemical speciation of selected metals and to understand the bioavailability of metals.

In order to achieve the objectives, fourteen sediment cores were collected representing mudflat and mangrove sedimentary environments within estuaries and were analysed for various sedimentological and geochemical parameters which include analysis of sediment components, organic matter, metals in bulk as well as in sand, silt and clay sediment fraction, metal speciation analyses in sediment core samples. Isocon plots were plotted and used to compare the parameters and to understand metal enriched areas. Statistical analyses like Pearson's correlation were used to understand the association and source of metal input in sediments. Enrichment Factor (EF) and Pollution Load Index (PLI) were computed to understand the enrichment of metal concentrations in sediments. Metal concentration in total sediment as well as in those associated with different sedimentary phases (sequential extraction procedure) was compared with sediment quality values (SQV's) using SQUIRT's table and also the sum of fraction 1 and 2 were compared with Risk Assessment Code (RAC) to understand the risk of toxicity of these studied metals to the biota.

The study of distribution of sediment components in general, indicated a decrease in deposition of coarser sediments and simultaneous increase in deposition of finer sediments from bottom to surface of cores (except core F1). Thus suggested prevalence of relatively higher and varying hydrodynamic energy conditions facilitating greater deposition of sand particles in the past, while, lower and stable hydrodynamic conditions in recent years seemed to have resulted in deposition of finer particles towards the surface. Spatial variation in distribution of sediment components was

attributed to the location of core samples from which they were collected. High average sand percentage in cores collected from lower region (core F2) and high mud content in cores collected from middle region (core G2) of Sharavati estuary was attributed to progressive sorting of sediments by tidal currents as well as decrease in the hydrodynamic energy conditions away from the mouth. Organic carbon profiles of all the cores were similar to that of finer sediments profiles indicating settling in similar hydrodynamic energy condition and their association. Along this coast systematic distribution of sediment components in mangroves and large fluctuation in case of mudflats was noted. Therefore, variation in hydrodynamics affected mudflats and less in mangroves.

Further, distribution and association of redox sensitive metals namely Fe and Mn and lithogenic element Al were studied. The result indicated association of Al with other sedimentary components such as silt and clay in all the cores. The similarity in distribution of Fe and Mn with Al at various depths further represented weathered material of terrestrial source rock and / or portion of alumina-silicate mineral bound fraction. While Mn in core F1, G1 and F8 showed dissimilar distribution pattern to that Fe and Al suggesting difference in their processes of deposition. Diagenetic enrichment of Fe and Mn was noted in all the cores. Distribution of trace metals namely Ni, Zn, Cu, Co and Cr was also studied. Large similarity in vertical distribution patterns of metals in most of the studied cores suggested that they were derived from the same source and / or had undergone similar post-depositional changes except for Mn, Ni and Co in some cores indicating its origin from a different source. Finer sediment and organic carbon was found to play a significant role in distribution of metals in all the cores. High Mn along with high sand content in core F1 and F3 indicate a coating on coarser particle indicating an anthropogenic source. Enrichment Factor indicated minor enrichment of Ni, Cu, Co and Cr in some studied cores.

The study of metals in different sediment size fractions of mudflat (F3) and mangrove (G1) cores in the middle estuary revealed that the sediments are more with coarser sediments at the bottom section and finer sediments in the upper sections. However, the average sand content was relatively higher in the mangrove core. Organic carbon showed positive correlation with finer sediments and negative correlation with sand in

both the cores. The early diagenetic mobilization of trace metals is noted in mudflat core indicating the role of Fe-Mn oxides in the distribution of trace metals in this core which is also supported by the brown colour in the upper 8 cm of the core. Significant positive correlation of metals with Al and finer sediments indicated their natural lithogenic source. Study of metal association with the bulk fraction and different sediment size fractions revealed that metals are enriched in the upper sections indicating the role of finer sediments and organic carbon in their distribution. Higher coarser sediment content in lower section seemed to dilute the metal concentration in both the cores. Correlation analysis among the different fractions revealed that organic carbon played an important role in the distribution of metals in silt and clay fraction in mudflat core. Relatively higher EF values of Zn in silt and clay fraction and; Co in sand and silt fraction are observed in the mangrove core as compared to mudflat core, whereas, Cu is enriched in the silt and clay fraction of mudflat core. However, Cr was enriched in all the fractions of both the cores. PLI indicated higher metal enrichment in the clay fraction of both the cores.

Further, speciation of metals i. e. the concentration of metals (Fe, Mn, Ni, Zn, Cu , Co and Cr) in five different fractions viz. exchangeable, carbonate bound, Fe-Mn oxide, organic matter / sulphide and residual fraction was studied in order to investigate metal sources, mobility, bioavailability, as well as the risk of toxicity to sediment dwelling organisms. Every estuary experiences two high tides and two low tides in a day and metals associated with exchangeable (fraction 1) and carbonate bound (fraction 2) are easily mobilised with change in pH conditions as there is mixing of fresh and marine water. Relatively higher amount of Mn and Co was associated with exchangeable fraction in core F4 (Swarna) and core G2 (Sharavati), indicating an anthropogenic input in recent years. Change in the pH conditions due to fresh water influx from the upper middle estuary has led to the diffusion of metals to the overlying water column. However, change in Eh conditions mobilises the metals associated with Fe-Mn oxide (fraction 3) and organic bound (fraction 4) as the conditions change from anoxic to oxic. Such post depositional changes on metal speciation was noted in mudflat cores F1, F3, F4 and F7 with precipitation of metals in Fe-Mn oxide and organic phase. Zn was largely associated with Fe-Mn oxide fraction, whereas, Cu and Cr with organic bound fraction. Cobalt showed value above Apparent Effects Threshold (AET) in Swarna

estuary, thus suggesting its risk of toxicity and high bioavailability to sediment dwelling organisms. Risk Assessment Code (RAC) criteria indicated high risk of Co in core G1 and medium risk all the studied cored.

References

Ackerman, F. 1980. A procedure for correcting the grain size effect in heavy metal analyses of estuarine and coastal sediments. Environmental Technology Letters, 1, 518-527.

Ahlf, W., Drost, W. and Heise, S. 2009. Incorporation of metal bioavailability into regulatory frameworks-metal exposure in water and sediment. Journal of Soils and Sediments, 9, 411–419.

Alongi, D. M. 1998. Coastal Ecosystem Processes. CRC Press, Boca Raton, FL, USA. pp. 419.

Aloupi, M. and Angelidis, M. O. 2002. The significance of coarse sediments in metal pollution studies in the coastal zone. Water Air and Soil Pollution, 133,121–131.

Anithamary, I., Ramkumar, T. and Venkatramanan, S. 2012. Distribution and Accumulation of Metals in the Surface Sediments of Coleroon River Estuary, East Coast of India. Bulletin of Environmentalal Contamination and Toxicology, 88, 413–417. DOI 10.1007/s00128-011-0504-8

Anuradha, V., Nair, S. M. and Kumar, N. C. 2011. Humic acids from the sediments of three ecologically different estuarine systems-a comparison. International Journal of Environmental Sciences, 2(1), 174-184.

Aprile, F. M. and Bouvy, M. 2008. Distribution and enrichment of heavy metals in sediments at the Tapacurá river basin, northeastern Brazil. Brazilian Journal of Aquatic Science and Technology, 12(1), 1-8.

Avinash, K., Jayappa, K. S. and Vethamony, P. 2012. Evolution of Swarna estuary and its impact on braided islands and estuarine banks, Southwest coast of India. Environmental Earth Sciences, 65, 835–848. DOI 10.1007/s12665-011-1128-3.

Avudainayagam, S., Megharaj, M., Owens, G., Kookana, R. S., Chittleborough, D. and Naidu, R. 2003. Chemistry of Chromium in Soils with Emphasis on Tannery Waste Sites. Reviews of Environmental Contamination and Toxicology, 178, 53–91.

Badr, N. B., El-Fiky, A. A., Mostafa, A. R. and Al-Mur, B. A. 2009. Metal pollution records in core sediments of some Red Sea coastal areas, Kingdom of Saudi Arabia. Environmental Monitoring and Assessment, 155, 509–526.

Bai, J., Cui, B., Chen, B., Zhang, K., Deng, W., Gao, H. and Xiao, R. 2011. Spatial distribution and ecological risk assessment of heavy metals in surface sediments from a typical plateau lake wetland, China. Ecological Modelling, 222, 301–306.

Balasubramanyan, M. N. 1978. Geochronology and geochemistry of Archean tonalitic gneisses and granites of South Kanara district, Karnataka State, India. In: Windley BF, Naqvi SM (eds) The origin and evolution of Archean continental crust. Elsevier, Amsterdam, pp 59–77.

Bartoli, G., Papa, S., Sagnella, E. and Fioretto, A. 2011. Heavy metal content in sediments along the Calore river: relationships with physical–chemical characteristics. Journal of Environmental Management, 1–6.

Bates, R. l. and Jackson, J. A. 1987. (Eds.). Glossary of Geology, 3rd edn. American Geological Institute.

Buchman, M. F. 1999. NOAA screening quick reference tables. NOAA HAZMAT Report 99-1, Seattle, WA, Coastal protection and restoration division, national oceanic and atmospheric administration, p.12.

Caetano, M., Prego, R., Vale, C., de Pablo, H. and Marmolejo-Rodrguez, J. 2009. Record of diagenesis of rare earth elements and other metals in a transitional sedimentary environment. Marine Chemistry, 116, 36–46.

Calace, N., Cardellicchio, N., Petronio, B. M., Pietrantonio, M. and Pietroletti, M. 2006. Sedimentary humic substances in the northern Adriatic sea (Mediterranean sea). Marine environmental research, 61, 40-58.

Caplat, C., Texier, H., Barillier, D., Lelievre, C., 2005. Heavy metals mobility in harbour contaminated sediments: the case of Port-en-Bessin. Marine Pollution Bulletin, 50, 504–511.

Carman, C.M., Li, X.D., Zhang, G., Wai, O.W.H. and Li, Y.S. 2007. Trace metal distribution in sediments of the Pearl River Estuary and the surrounding coastal area, South China. Environmental Pollution, 147, 311–323.

Cat, N. N., Tien, P. H., Sam, D. D. and Bien, N. N. 2006. Status of coastal erosion of Viet Nam and proposed measures for protection. http://www.fao.org/forestry/11286-08d0cd86bc02ef85da8f5b6249401b52f.pdf.

Clough, B., Tan, D. T., Phuong, D. X., Buu, D. C. 2000. Canopy leaf area index and litter fall in stands of the Mangrove *Rhizophora apiculata* of different age in the Mekong Delta, Vietnam. Aquatic Botany, 66, 311- 320.

Deng, H. G., Zhang, J., Wang, D. Q., Chen, Z. L. and Xu, S. Y. 2010. Heavy metal pollution and assessment of the tidal flat sediments near the coastal sewage outfalls of shanghai, China. Environmental Earth Sciences, 60, 57–63.

Dessai, D. V., Nayak, G. N. and Basavaiah, N. 2009. Grain size, geochemistry, magnetic susceptibility: Proxies in identifying sources. Estuarine, Coastal and Shelf Science, 85, 307–318.

Díaz-de Alba, M., Galindo-Riano, M.D., Casanueva-Marenco, M.J., García-Vargas, M. and Kosore, C.M. 2011. Assessment of the metal pollution, potential toxicity and speciation of sediment from Algeciras Bay (South of Spain) using chemometric tools. Journal of Hazardous Materials, 190, 177–187.

Dolch, T. and Hass, H. C. 2008. Long-term changes of intertidal and subtidal sediment compositions in a tidal basin in the northern Wadden Sea (SE North Sea). Helgoland Marine Research, 62, 3-11.

Esen, E., Kucuksezgin, F. and Uluturhan. E. 2010. Assessment of trace metal pollution in surface sediments of Nemrut Bay, Aegean Sea. Environmental Monitoring and Assessment, 160, 257–266. DOI 10.1007/s10661-008-0692-9

Fairbridge, R.W. 1980. The Estuary: its definition and geodynamic cycle. In: Olausson, E., Cato, I. (Eds.), Chemistry and Biogeochemistry of Estuaries. Wiley, New York, 1-35.

Falco, G. H., Magni, P., Teräsvuori, L. M. H. and Matteucci, G. 2004. Sediment grain size and organic carbon distribution in the Cabras lagoon (Sardinia, Western Mediterranean). Chemistry and Ecology, 20, 367-377. DOI:10.1080/02757540310001629189.

Fernandes, L., Nayak, G. N., Ilangovan, D. and Borole, D. V. 2011. Accumulation of sediment, organic matter and trace metals with space and time, in a creek along Mumbai coast, India. Estuarine, Coastal and Shelf Science, 91, 388-399.

Fernandes, M. C. and Nayak, G. N. 2015. Speciation of metals and their distribution in tropical estuarine mudflat sediments,southwest coast of India. Ecotoxicology and Environmental Safety, 122, 68-75.

Fernandes, M. C., Nayak, G. N., Pande, A., Volvoikar, S. P. and Dessai, D. R. G. 2014. Depositional environment of mudflats and mangroves and bioavailability of selected metals within mudflats in a tropical estuary. Environmental Earth Sciences, 72(6), 1861–1875.

Filho, E. V., Jonathan, M. P., Chatterjee, M., Sarkar, S. K., Sella, S. M., Bhattacharya, A. and Satpathy, K. K. 2011. Ecological consideration of trace element

contamination in sediment cores from Sundarban wetland, India. Environmental Earth Sciences, 63, 1213–1225.

Folk, R. L. 1968. Petrology of Sedimentary rocks. Hemphills: Austin, p 177.

Forstner, U. 1982. Cumulative phases for heavy metals in limnic systems. Hydrobiologia, 91, 299-313.

Gibbs, R. J. 1977. Transport phases of transition metals in the Amazon and Yukon rivers. GSA Bulletin, 88, 829-843.

Grant, J. A. 1986. The isocon diagram—a simple solution to Gresen's equation for metasomatic alteration. Economic Geology, 81, 1976 – 1982.

Harikumar, P. S. and. Nasir, U.P. 2010. Ecotoxicological impact assessment of heavy metals in core sediments of a tropical estuary. Ecotoxicology and Environmental Safety, 73, 1742–1747.

Hejabi, A. T., Basavarajappa, H. T., Karbassi, A. R. and Monavari, S. M. 2011. Heavy metal pollution in water and sediments in the Kabini River, Karnataka, India. Environmnetal Monitoring and Assessment, 182, 1–13. DOI 10.1007/s10661-010-1854-0

Heltai, G., Percsich, K., Halasz, G., Jung, K. and Fekete, I. 2005. Estimation of ecotoxicological potential of contaminated sediments based on a sequential extraction procedure with supercritical CO2 and subcritical H2O solvents. Microchemical Journal, 79, 231–237.

Ho, H. H., Swennen, R., and Damme, A. V. 2010. Distribution and contamination status of heavy metals in estuarine sediments near Cua Ong harbor, Ha Long bay, Vietnam. Geologica Belgica, 13 (1-2), 37-47.

Howe, P. D., Malcolm, H. M. and Dobson, S. 2005. Manganese and its compounds: environmental aspects. Concise International Chemical Assessment Document 63.

Huaiyang, Z., Xiaotong, P. and Jianming, P. 2004. Geochemical characteristics and sources of some chemical components in sediments of Zhujiang (Pearl) river estuary. Chinese Journal of Oceanology and Limnology, 22 (1), 34-43.

Idriss, A. A. and Ahmad, A. K. 2012. Heavy metal contamination (Cu, Cd and Pb) in sediments in the Juru river, Penang, Malaysia. Journal of Biological Sciences, 12 (7), 376-384.

Izquierdo, C., Usero, J., Gracia, I., 1997. Speciation of heavy metals in sediments from salt marshes on the southern Atlantic coast of Spain. Marine Pollution Bullettin, 34 (2), 123–128.

Jackson, M. L. 1958. Soil chemical analysis. New York: Prentice Hall.

Jain, C.K., Gupta, H., Chakrapani, G.J., 2008. Enrichment and fractionation of heavy metals in bed sediments of River Narmada, India. Environmental Monitoring and Assessment, 141, 35–47.

Jarvis, I. J. and Jarvis, K. 1985. Rare earth element geochemistry of standard sediments: a study using inductively coupled plasma spectrometry. Chemical Geology 53, 335 - 344.

Jonathan, M. P., Ram-Mohan, V. and Srinivasalu, S. 2004. Geochemical variations of major and trace elements in recent sediments, off the Gulf of Mannar, the southeast coast of India. Environmental Geology, 45, 466–480. doi:10.1007/s00254-003-0898-7.

Jones, B. and Turki, A. 1997. Distribution and speciation of heavy metals in surfacial sediments from the Tees Estuary, north-east England. Marine Pollution Bulletin, 34(10), 768-779.

Kathiresan K. 2003. How do mangrove forests induce sedimentation? Rev. Biol. Trop. 51: 355-360.

Klein, G. deVries 1985. Intertidal flats and intertidal sand bodies. In: Davis, R. A. (Ed.), Coast. Sed. Environ. Springer, New York, 187- 224.

Klinkhammer, G. P., Heggie, D. T. and Graham, D. W. 1982. Metal diagenesis in oxic marine sediments. Earth and Planetary Science Letters, 61, 211–219.

Koretsky, C. M., Haveman, M., Beuving, L., Cuellar, A., Shattuck, T. and Wagner, M. 2007. Spatial variation of redox and trace metal geochemistry in a minerotrophic fen. Biogeochemistry, 86, 33-62. doi: 10.1007/s10533-007-9143-x

Kumar, S. P. and Edward, J. K. P. 2009. Assessment of metal concentration in the sediment cores of Manakudy estuary, south west coast of India. Indian Journal of Marine Sciences, 38(2), 235 – 248.

Kumar, S. P. and Sheela, M. S. 2014. Comparative study of textural and chemical characteristics of riverine and estuarine sediments of a bar built estuary in Tamil Nadu, India. Research Journal of Chemical Sciences, 4(3), 27-31.

Law, B. A. Milligan, T. G., Hill, P. S., Newgard, J., Wheatcroft, R. A.and Wiberg, P. L. 2012. Flocculation on a muddy intertidal flat in Willapa Bay, Washington, Part I: A regional survey of the grain size of surficial sediments. Continental Shelf Research, 60, S136-S144.

Lee, S.V. and Cundy, A.B. 2001. Heavy metal contamination and mixing processes in sediments from the Humber estuary, eastern England. Estuarine Coastal and Shelf Science, 53, 619–636.

Leorri, E., Cearreta, A., García-Artola, A., Irabien, M. J. and Blake, W. H. 2013. Relative sea-level rise in the Basque coast (N Spain): Different environmental consequences on the coastal area. Ocean & Coastal Management, 77, 3-13.

Li, X., Shen, Z., Wai, O. W. H. and Li, Y-S. 2001. Chemical forms of Pb, Zn and Cu in the sediment profiles of the Pearl River estuary. Marine Pollution Bulletin, 42(3), 215–223.

Liaghati, T., Preda M. and Cox M. 2003. Heavy metal distribution and controlling factors within coastal plain sediments, Bells Creek catchment, southeast Queensland, Australia. Environment International, 935 – 948.

Lin, S., Hsieh, I. J., Huang, K. M. and Wang, C. H. 2002. Influence of the Yangtze River and grain size on the spatial variations of heavy metals and organic carbon in the East China Sea continental shelf sediments. Chemical Geology, 182, 377–394.

Liu, B., Hu, K., Jiang, Z., Yang, J., Luo, X. and Liu, A. 2011. Distribution and enrichment of heavy metals in a sediment core from the Pearl River Estuary. Environmental Earth Sciences, 62, 265–275. DOI 10.1007/s12665-010-0520-8

Luo, W., Lu, Y., Wang, T., Hu, W., Jiao, W., Naile, J. E., Khim, J. S. and Giesy, J. P. 2010. Ecological risk assessment of arsenic and metals in sediments of coastal areas of northern Bohai and Yellow Seas, China. Ambio, 39, 367–375. DOI 10.1007/s13280-010-0077-5

Luo, X. X., Yang, S.L. and Zhang, J. 2012. The impact of the Three Gorges Dam on the downstream distribution and texture of sediments along the middle and lower Yangtze River (Changjiang) and its estuary, and subsequent sediment dispersal in the East China Sea. Geomorphology, 179, 126–140.

Mayer, L. M. and Xing, B. S. 2001. Organic matter - surface area relationships in acid soils. Soil Science Society of America Journal, 65, 250-258.

McCann, S. B. 1980. Classification of tidal environments. In: McCann, S.B. (Ed.), Sedimentary Processes and Animal-Sediment Relationships in Tidal Environments, Short Course Notes, V. 1. Geological Association Canada, St. Johns, Newfoundland, 1 - 24.

Mikhailov, V. N. and Gorin, S. L. 2012. New Definitions, regionalization and typification of river mouth areas and estuaries as their parts. Water Resources, 39 (3), 247-260.

Mikulic, N., Orescanin, V., Elez, L., Pavicic, L., Pezelj, D., Lovrencic, I. and Lulic, S. 2008. Distribution of trace elements in the coastal sea sediments of Maslinica Bay, Croatia. Environmental Geology. 53, 1413-1419. 10.1007/s00254-007-0750-6.

Mohamed, I. F. 2012. Environmental geochemistry of El Temsah Lake sediments, Suez Canal district, Egypt. Arabian Journal of Geosciences, DOI 10.1007/s12517-012-0669-4

Mohiuddin, K. M., Zakir, H. M., Otomo, K., Sharmin, S. and Shikazono, N. 2010. Geochemical distribution of trace metal pollutants in water and sediments of downstream of an urban river. Internaational Journal of Environmental Science and Technology, 7 (1), 17-28.

Muzuka, A. N. and Shaghude, Y. W. 2000. Grain size distribution along the Msasani Beach, North of Dar es Salaam Harbour. Journal of African Earth Sciences, 30, 417–426.

Nair, M. M. N. and Ramchandran, K. K. 2002. Textural and trace elemental distribution in sediments of Beypore estuary (SW coast of India) and adjoining innershelf. Indian Journal of Marine Sciences, 31(4), 295-304.

Nasnodkar, M. R. and Nayak, G. N. 2015. Processes and factors regulating the distribution of metals in mudflat sedimentary environment within tropical estuaries, India. Arabian Journal of Geosciences 8, 9389-9405.

Nasrabadi, T., Bidhendi, G. N., Karbassi, A. and Mehrdadi, N. 2010. Evaluating the efficiency of sediment metal pollution indices in interpreting the pollution of Haraz River sediments, southern Caspian Sea basin. Environmental Monitorin and Assessment, 171, 395–410. DOI 10.1007/s10661-009-1286-x

Natesan, U. and Seshan, B. R. R. 2010. Vertical profile of heavy metal concentration in core sediments of Buckingham cannal, Ennore. Indian Journal of Geo-Marine Sciences, 40 (1), 83-97.

Nemati, K., Abu Bakar, N.K., Abas, M.R. and Sobhanzadeh, E. 2011. Speciation of heavy metals by modified BCR sequential extraction procedure in different depths of sediments from Sungai Buloh, Selangor, Malaysia. Journal of Hazardous Materials, 192, 402–410.

Neto, J. A. B., Gingele, F. X., Leipe, T. and Brehme, I. 2006. Spatial distribution of heavy metals in surficial sediments from Guana-bara Bay, Rio de Janeiro, Brazil. Environmental Geology, 49, 1051–1063.

Nguyen, H.L., Braun, M., Szaloki, I., Baeyens, W., Van Grieken, R. and Leermakers, M. 2009. Tracing the metal pollution history of the Tisza River through the analysis of a sediment depth profile. Water, Air and Soil Pollution, 200, 119–132.

Nobi, E. P., Dilipan, E., Thangaradjou, T., Sivakumar, K. and Kannan, L. 2010. Geochemical and geo-statistical assessment of heavy metal concentration in the sediments of different coastal ecosystems of Andaman islands, India. Estuarine, Coastal and Shelf Science, 87, 253–264.

Pande, A. and Nayak, G. N. 2013. Understanding distribution and abundance of metals with space and time in estuarine mudflat sedimentary environment. Environmnetal Earth Sciences. DOI 10.1007/s12665-013-2298-y.

Pande, A. and Nayak, G. N. 2013a. Depositional environment and elemental distribution with time in mudflats of Dharamtar creek, west coast if India. Indian Journal of Geo-Marine Sciences, 42 (3), 360-369.

Passos, E. A., Alves, J. C., Santos, I. S., Alves, J. P. H., Garcia, C. A. B. and Costa, A. C. S. 2010. Assessment of trace metals contamination in estuarine sediments using a sequential extraction technique and principal component analysis. Microchemical Journal, 96, 50–57.

Patersion, D. M., Crawford, R. M. and Little, C. 1990. Subaerial exposure and changes in the stability of intertidal estuarine sediments. Estuarine Coastal and Shelf Science, 30, 541 – 556.

Perin, G., Craboledda, L., Lucchese, M., Cirillo, R., Dotta, L., Zanetta, M. L., et al. 1985. Heavy metal speciation in the sediments of northern Adriatic sea. A new approach

for environmental toxicity determination. In Lakkas TD (Ed). Heavy metals in the environment, CEP consultants, Edinburg. Environmental Pollution, 110, 3-9.

Pritchard, D. W. 1955. Estuarine circulation pattern. American Society of Civil Engineers, 81, 717, 7 –11.

Pritchard, D. W. 1967. What is an estuary: Physical view point. In: Lauff, G. H. (Ed.), Estuaries. American Association for the Advancement of Science, 83, 3 – 5.

Qiao, Y., Yang, Y., Gu, J. and Zhao, J. 2012. Distribution and geochemical speciation of heavy metals in sediments from coastal area suffered rapid urbanization, a case study of Shantou Bay, China. Marine Pollution Bulletin, http://dx.doi.org/10.1016/j.marpolbul.2012.12.003

Rajamanickam, G. V. and Setty, M. G. A. P. 1973. Distribution of phosphorus and organic carbon in the nearshore sediments of Goa. Indian Journal of Marine Sciences, 2, 84-89.

Raju, K. V., Somashekar, R. K. and Prakash, K. L. 2012. Heavy metal status of sediment in river Cauvery, Karnataka. Environmental Monitoring and Assessment, 184, 361–373. DOI 10.1007/s10661-011-1973-2

Reddy, M. P. M., Hariharan, V. and Kurian, N. P. 1979. Sediment movement and siltation in the navigational channel of Old Mangalore Port. Proceedings of the Indian Academy of Sciences,88 (Part II), 121-130.

Reineek, H. E. 1972. Tidal flats. In: Rigby, J. K. and Hamblin, W. K. (Eds.), Recognition of Ancient Sedimantary Environments, Tulsa, Okla. Soc. Econ. Paleontol. Mineral. Spec. Publ., 16, 146 – 159.

Rogers, J. J. W., Callahan, E. J., Dennen, K. O., Fullagar, P. D., Stroh, P. T. and Wood, L. F. 1986. Chemical evolution of Peninsular Gneiss in the western Dharwar Craton, Southern India. Geological Journal, 94(2), 233–246.

Rosales- Hoz, L., Cundy, A. B. and Bahena – Manjarrez, J. L. 2003. Heavy metals in sediment cores from a tropical estuary affected by anthropogenic discharges: Coatzacoalcos estuary, Mexico. Estuarine, Coastal and Shelf Science, 58, 117 – 126.

Ruiz, J. M. and Saiz-Salinas, J. I. 2000. Extreme variation in the concentration of trace metals in sediments and bivalves from the Bilbao estuary (Spain) caused by the 1989-1990 drought. Marine Environmental Research, 49, 307-317.

Saleem, M., Iqbal, J. and Shah, M. H. 2015. Geochemical speciation, anthropogenic contamination, risk assessment and source identification of selected metals in freshwater sediments—A case study from Mangla Lake, Pakistan. Environmental Nanotechnology, Monitoring & Management, 4, 27–36.

Sarkar, S. K., Favas, P. J. C., Rakshit, D. and Satpathy, K. K. 2014. Geochemical Speciation and Risk Assessment of Heavy Metals in Soils and Sediments. Environmental Risk Assessment of Soil Contamination, edited by Maria C. Hernandez-Soriano, 918 pp, Publisher: InTech, http://dx.doi.org/10.5772/57295

Sarkar, S., Ghosh, P. B., Sil, A. K and Saha, T. 2011. Heavy metal pollution assessment through comparison of different indices in sewagefed fishery pond sediments at East Kolkata Wetland, India. Environmental Earth Sciences, 63, 915–924.

Schulten, H. R. and Schniter, M. 1995. Three dimensional models for humic acids and soil organic matter. Naturwissenschaften, 82, 487-498.

Selvaraj, K., Parthiban, G., Chen, C. T. A. and Lou, J. Y. 2010. Anthropogenic effects on sediment quality offshore southwestern Taiwan: assessing the sediment core geochemical record. Continental Shelf Research, 30, 1200-1210.

Shi, Z. and Chen, J. Y. 1996. Morphodynamics and sediment dynamics on intertidal mudflats in China 1961-1994). Continental Shelf Research, 16, 1909 - 1926.

Shuman, L. M. 1985. Fractionation method for soil microelements. Soil Science, 140 (1), 11-22.

Singh, K. T. and Nayak, G. N. 2009. Sedimentary and Geochemical signatures of depositional environment of sediments in mudflats from a microtidal Kalinadi estuary, central west coast of Inida. Journal of Coastal Research, 25 (3), 641-650.

Singh, K. T. Nayak, G. N., Fernandes, L., Borole, D. V. and Basaviah, N. 2013a. Changing environmental conditions in recent past — Reading through the study of geochemical characteristics, magnetic parameters and sedimentation rate of mudflats, central west coast of India. Palaeogeography, Palaeoclimatology, Palaeoecology, http://dx.doi.org/10.1016/j.palaeo.2013.04.008

Singh, K. T. Nayak, G. N. and Fernandes, L. 2013b. Geochemical Evidence of Anthropogenic Impacts in Sediment Cores from Mudflats of a Tropical Estuary, Central West Coast of India. Soil and Sediment Contamination, 22(3), 256-272, DOI: 10.1080/15320383.2013.726291

Singh, S. K., Subramanian, V. and Gibbs, R. J. 1984. Hydrous FE and MN oxides – scavengers of heavy metals in the aquatic environment. Critical Reviews in Environmental Science and Technology, 14, 33–90.

Siraswar, R. and Nayak, G. N. 2011. Mudflats in lower middle estuary as a favourable location for concentration of metals, west coast of India. Indian Journal of Geo-Marine Science, 40 (3), 372-385.

Spalding, M.D, Blasco, E and Field, CD. (Eds). 1997. World Mangrove Atlas. The International Society for Mangrove Ecosystems, Okinawa, Japan, pp 178.

Spencer, K. L., Cundy, A. B. and Croudace, I. W. 2003. Heavy metal distribution and early diagenesis in salt marsh sediments from the Medway Estuary, Kent, UK. Estuarine, Coastal and Shelf Sciences, 57, 43 -54.

Tessier, A., Campbell, P. G. C. and Bisson, M. 1979. Sequential extraction procedure for the speciation of particulate trace metals. Analytical Chemistry, 51(7), 844 – 851.

Thomson, J., Dyer, F. M. and Croudace, I. W. 2002. Records of radionuclide deposition in two salt marshes in the United Kingdom with contrasting redox and accumulation conditions. Geochimica et Cosmochimica Acta, 16, 577-588.

Tokalioglu, S¶ ., Kartal, S¶ ., Elçi, L., 2000. Determination of heavy metals and their speciation in lake sediments by flame atomic absorption spectrometry after a four-stage sequential extraction procedure. Analytica Chimica Acta, 413, 33–40.

Tomlinson, D. C., Wilson, J.G., Harris, C. R. and Jeffery, D. W. 1980. Problems in the assessment of heavy metals levels in estuaries and the formation of a pollution index. Helgoländer Meeresuntersuchungen, 33 (1-4), 566-575.

Tribovillard, N., Algeo, T., Lyons, T. and Riboulleau, A. 2006. Trace metals as paleoredox and paleoproductivity proxies: an update. Chemical Geology, 232, 12–32.

Tripti, M., Gurumurthy, G. P., Balakrishna, K. and Chadaga, M. D. 2013. Dissolved trace element biogeochemistry of a tropical river, Southwestern India. Environmental Science and Pollution Research, 20, 4067-4077. DOI 10.1007/s11356-012-1341-y.

Turekian, K. K. and Wedepohl, K. H. 1961. Distribution of the elements in some major units of the earth's crust. Geological Society of America Bulletin, 72, 175 –192.

Tuzen, M. 2003. Determination of heavy metals in soil, mushroom and plant samples by atomic absorption spectrometry. Microchemcal Journal, 74, 289-297.

Vink, J. P. M. 2009. The origin of speciation: trace metal kinetics over natural water/sediment interfaces and the consequences for bioaccumulation. Environmental Pollution, 157, 519–527.

Voilvoikar, S. P. and Nayak, G. N. 2014. Reading source and processes with time from mangrove sedimentary environment of Vaitarna estuary, west coast of India. Indian Journal of Geo-Marine Sciences, 43 (6), 1063-1075.

Volvoikar, P. S. and Nayak, G. N. 2013. Factors controlling the distribution of metals in intertidal mudflat sediments of Vaitarna estuary, North Maharashtra coast, India. Arabian Journal of Geosciences, DOI 10.1007/s12517-013-1162-4.

Volvoikar, S. P. and Nayak, G. N. 2013. Depositional environment and geochemical response of mangrove sediments. Marine Pollution Bulletin 69, 223–227.

Volvoikar, S. P. and Nayak, G. N. 2013a. Evaluation of impact of industrial effluents on intertidal sediments of a creek. International Journal of Environmental Science and Technology, 10, 941–954. DOI 10.1007/s13762-013-0231-2

Volvoikar, S. P. and Nayak, G. N. 2015. Impact of industrial effluents on geochemical association of metals within intertidal sediments of a creek. Marine Pollution Bulletin, (In press).

Volvoikar, S. P. and Nayak, G. N. 2013b. Factors controlling the distribution of metals in intertidal mudflat sediments of Vaitarna estuary, North Maharashtra coast, India. Arabian Journal of Geosciences, DOI 10.1007/s12517-013-1162-4.

Walkley, A. 1947. A critical examination of a rapid method for determining organic carbon in soil: effect of variations in digestion conditions and of inorganic soils constituents. Soil Science 63, 251–263.

Williams, T. P., Bubb J. M. and Lester J. N. 1994. Metal accumulation within salt marsh environments: A review. Marine Pollution Bulletin, 28, 277 – 290.

Wu, Z., He, M., Lin, C. and Fan, Y. 2011. Distribution and speciation of four heavy metals (Cd, Cr, Mn and Ni) in the surficial sediments from estuary in daliao river and yingkou bay. Environmental Earth Sciences, 63, 163–175.

Yallop, K. M., De Winter, B., Paterson, D. M. and Stal, L. J. 1994. Comparative structure, primary production and biogenic stabilization on cohesive and non-

cohesive marine sediments inhabited by micro-phytobenthos. Estuarine Coastal and Shelf Science, 39, 565 – 582.

Yang, S. L., Li, H., Ysebaert, T., Bouma, T. J., Zhang, W. X., Wang, Y. Y., Li, P., Li, M. and Ding, P. X. 2008. Spatial and temporal variation in sediment grain size in tidal wetlands, Yangtze Delta: On the role of physical and biotic controls. Estuarine, Coastal and Shelf Science, 77, 657-671.

Yuan, C., Shi, J., He, B., Liu, J., Liang, L. and Jiang, G. 2004. Speciation of heavy metals in marine sediments from the East China Sea by ICP-MS with sequential extraction. Environmental International, 30, 769–783.

Zhang, J. and Liu, C. L. 2002. Riverine composition and estuarine geochemistry of particulate metals in China-weathering features, anthropogenic impact and chemical fluxes. Estuarine Coastal and Shelf Sciences 54, 1051–1070.

Zhou, Y., Zhao, B., Peng, Y. and Chen, G. 2010. Influence of mangrove reforestation on heavy metal accumulation and speciation in intertidal sediments. Marine Pollution Bulletin, 60, 1319-1324.

Zourarah, B., Maanan, M., Robin, M. and Carruesco, C. 2009. Sedimentary records of anthropogenic contribution to heavy metal content in Oum Er Bia estuary (Morocco). Environmental Chemistry Letters, 7, 67–78. doi:10.1007/s10311-008-0138-1.

Zwolsman, J. J. G., Berger, G. W. and Van Eck, G. T. M. 1993. Sediment accumulation rates, historical input, post- depositional mobility and retention of major elements and trace elements in salt marsh sediments of the Scheldt estuary, SW Netherlands. Marine Chemistry, 44, 73–94.

List of publications

M. C. Fernandes, G. N. Nayak, A. Pande, S. P. Volvoikar and D. R. G. Dessai. (2014) Depositional environment of mudflats and mangroves and bioavailability of selected metals within mudflats in a tropical estuary. Environmental Earth Sciences, V. 72 (6), pp 1861-1875.

Maria C. Fernandes and G. N. Nayak. (2015) Speciation of metals and their distribution in tropical estuarine mudflat sediments, south central west coast of India. Ecotoxicology and Environmental Safety, V. 122, pp 68-75.

Maria C. Fernandes and G. N. Nayak. (2015) Role of sediment size in the distribution and abundance of metals in a tropical**.** Arabian Journal of Geosciences, DOI 10.1007/s12517-015-2127-6.